

# Cyclic diacyl thioureas enhance activity of corrector Lumacaftor on F508del-CFTR

Andrea Spallarossa,<sup>\*,[a]</sup> Nicoletta Pedemonte,<sup>[b]</sup> Emanuela Pesce,<sup>[b]</sup> Enrico Millo,<sup>[c]</sup> Elena Cichero,<sup>[a]</sup> Camillo Rosano,<sup>[d]</sup> Matteo Lusardi,<sup>[a]</sup> Erika Iervasi,<sup>[d]</sup> and Marco Ponassi<sup>[d]</sup>

Cystic fibrosis is a genetic disease caused by mutations in the cystic fibrosis transmembrane conductance regulator (CFTR) protein. In the search of novel series of CFTR modulators, a library of mono and diacyl thioureas were prepared by sequential synthesis. When tested alone, the obtained compounds **5** and **6** poorly affected F508del-CFTR conductance but, in combination with Lumacaftor, selected derivatives showed the ability to increase the activity of the approved modulator.

Analogue **6i** displayed the most marked enhancing effect and acylthioureas **6d** and **6f** were also able to improve efficacy of Lumacaftor. All compounds proved to be non-cytotoxic against different cancer cell lines. Good pharmacokinetic properties were predicted for derivatives **5** and **6**, thus supporting the value of these compounds for the development of novel modulators potentially useful for cystic fibrosis.

## Introduction

Cystic fibrosis (CF) is a genetic disease with a prevalence of one case per 2500 live births.<sup>[1]</sup> CF is caused by a mutation in the cystic fibrosis transmembrane conductance regulator (CFTR) gene leading to a dysregulation of chloride transport across epithelial cells in different organs (e.g., lungs, pancreas, intestines, sweat glands and male reproductive tract).<sup>[2]</sup> The build up of sticky mucous in the different body districts induces chronic airway inflammation and infection, exocrine pancreatic insufficiency with nutrient malabsorption, hepatobiliary dysfunction and male infertility. Furthermore, CF patients have increased risk to develop digestive tract neoplasms, lymphoid leukemia and testicular cancer.<sup>[3,4]</sup> Death usually occurs from respiratory failure, secondary to chronic airway inflammation and infection.<sup>[5,6]</sup> So far, more than 2000 CFTR mutations have

been identified and classified in seven classes based on the type of DNA alteration.<sup>[7]</sup> In particular, class I mutations induce a block of protein synthesis whereas class II mutations (including the common F508del variant) cause the synthesis of a misfolded CFTR protein, leading to the failure of maturation and trafficking to the cell surface. Mutations of class III inactivate the ion transport function, and class IV modifications reduce the number of chloride ions transported through the pore. Class V mutations diminish the quantities of CFTR protein and class VI alterations produce unstable channels with a short half-life. Finally, class VII mutations, recently introduced, lead to the absence of full-length mature RNA interfering with mRNA splicing so that CFTR protein is totally absent.<sup>[8–11]</sup>

Traditionally, CF treatment was oriented on symptom control and prevention of complications.<sup>[5,6]</sup> Recently, novel drugs able to modulate CFTR activity have been identified and effectively introduced in the treatment of CF patients.<sup>[12]</sup> CFTR modulators are small molecules that target either abnormal channel gating (potentiators) or protein folding and cellular trafficking (correctors).<sup>[13]</sup> Ivacaftor (IVA, Figure 1A) represents the first potentiator receiving approval in 2012, yielding clinical benefits in CF patients.<sup>[14–17]</sup> Approved correctors lumacaftor (LUM), tezacaftor (TEZ) and elexacaftor (ELX) (Figure 1A) proved to improve CFTR protein folding in the endoplasmic reticulum and subsequent trafficking to the cell surface. The therapeutic approach of CF is usually based on a combination of IVA and correctors (e.g., IVA/LUM, Orkambi®; ELX/TEZ/IVA, Trikafta®) to address coexistent folding and gating abnormalities. However, the nature of corrector/potentiator and the CFTR genotype deeply affect CFTR functional restoration, thus supporting the research for novel modulators.<sup>[12]</sup>

Thiourea derivatives represent valuable compounds in medicinal chemistry as they showed significant biological properties including antibacterial,<sup>[18]</sup> antioxidant,<sup>[19]</sup> antidiabetic<sup>[20]</sup> and anticancer<sup>[21]</sup> activities. Moreover, thiourea derivatives I and II (Figure 1B) were studied as CFTR modulators. In particular, cyanoquinoline I was identified as a strong

[a] Prof. A. Spallarossa, Prof. E. Cichero, Dr. M. Lusardi  
Department of Pharmacy  
Università degli Studi di Genova  
Viale Benedetto XV 3, 16132 Genova, Italy  
E-mail: andrea.spallarossa@unige.it

[b] Dr. N. Pedemonte, Dr. E. Pesce  
UOC Genetica Medica  
IRCCS Istituto Giannina Gaslini  
Via Gerolamo Gaslini, 5, 16147 Genova, Italy

[c] Prof. E. Millo  
Department of Experimental Medicine, Section of Biochemistry,  
Università degli Studi di Genova  
Viale Benedetto XV 1, 16132 Genova, Italy

[d] Dr. C. Rosano, Dr. E. Iervasi, Dr. M. Ponassi  
Proteomics and Mass Spectrometry Unit  
IRCCS Ospedale Policlinico San Martino  
Largo R. Benzi, 10, 16132 Genova, Italy

Supporting information for this article is available on the WWW under <https://doi.org/10.1002/cmdc.202300391>

© 2023 The Authors. ChemMedChem published by Wiley-VCH GmbH. This is an open access article under the terms of the Creative Commons Attribution License, which permits use, distribution and reproduction in any medium, provided the original work is properly cited.

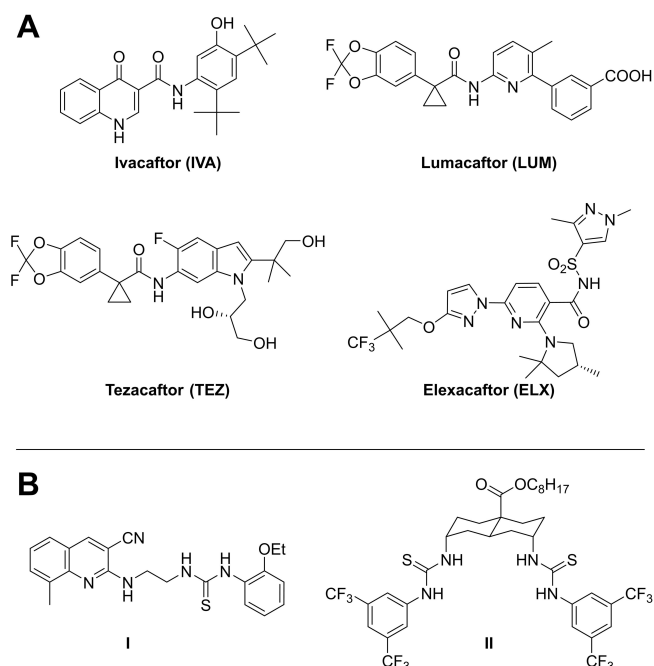


**Figure 1.** A) Approved CFTR modulators. B) Thioureas derivatives previously studied as CFTR modulators.

potentiator of F508del-CFTR devoid of any corrector activity.<sup>[22]</sup> Trans-decalin II showed relevant anionophores activity and proved to efficiently transport chloride anions in vesicles; this compound was therefore indicated as a potential lead for channel replacement therapy in CF.<sup>[23]</sup>

Recently, we reported an efficient, robust and versatile synthetic protocol for the preparation of monoacyl thioureas **2** (Figure 2),<sup>[24]</sup> Our synthetic strategy involved the condensation of imidazolidine-2-thione **1** and the acyloximinium salts, generated in situ by the reaction between dimethylacetamide (DMA) and acyl chlorides. The developed procedure represented an innovative synthetic method for the preparation of monoacylated thiourea, otherwise difficult to obtain. In fact, the formation of the diacylated compounds is favoured also when acyl chlorides were used as limiting reagents.<sup>[25]</sup> Moreover, compounds **2** proved to be useful intermediates for the preparation of non-cytotoxic asymmetric diacylthioureas **3**.<sup>[24]</sup>

To further exploit the chemical versatility of the identified protocol, tetrahydropyrimidine-2(1*H*)-thione **4** (a higher homo-

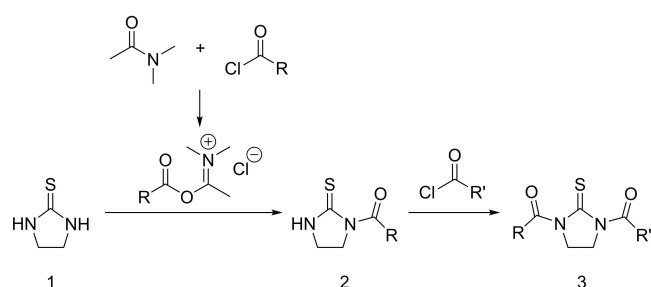


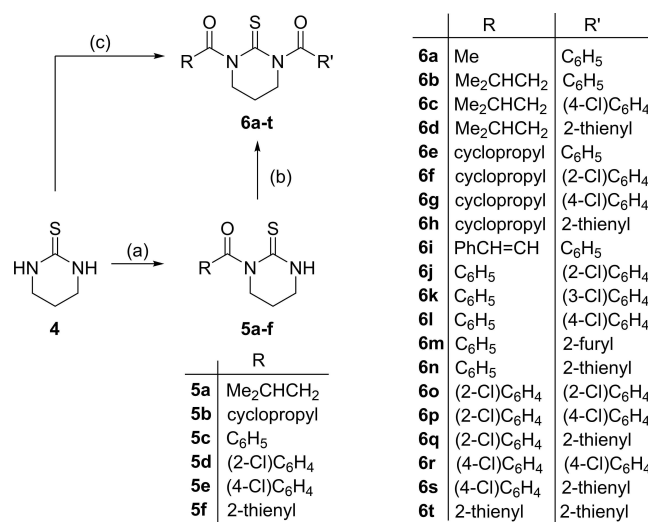
**Figure 2.** Developed synthetic procedure for the preparation of asymmetric diacylthioureas **3**.

logue of **1**) was selected as starting material for the preparation of a library of mono- and di-acylthioureas (compounds **5** and **6**; Scheme 1). To assess the robustness of the preparative procedure acyl chlorides with different steric and electronic properties were selected. Thus AC<sub>1-10</sub> building blocks (Figure 3) included (cyclo)alkyl, arylalkenyl, benzyl and heteroaryl substructures. The new thiourea series were evaluated as CFTR-modulating agents with the halide-sensitive yellow fluorescent protein (HS-YFP) assay in F508del-CFTR-expressing CFBE41o-cells. Furthermore, derivatives **5** and **6** were tested for their cytotoxic activity against a panel of tumor cell lines.

## Results and Discussion

### Chemistry

The synthesis of the asymmetric diacylthioureas **6** was carried out as previously reported.<sup>[24]</sup> Thus, the condensation of cyclic thiourea **4** (Scheme 1) with the proper acyl chloride in DMA led to the formation of the mono-acyl derivatives **5 a-f** in yields of 32–53%. The isolated mono-acyl thioureas (MAT) were converted into the desired asymmetric diacyl thioureas by the reaction with one equivalent of the suitable acyl chloride.



**Scheme 1.** Synthesis of monoacyl thioureas **5** and diacylthioureas **6**. Reaction conditions: (a) DMA, AC<sub>2,3,5,6,8,10</sub> (1 equiv), 90 °C, 30 min. (b) DMF or Py, acyl chlorides AC<sub>1-10</sub> (1 equiv), various time and temperature (see Table 1). (c) Py, AC<sub>6,8,10</sub> (2 equivs), 90 °C, 30 min. The chemical structures of AC<sub>1-10</sub> are reported in Figure 3.

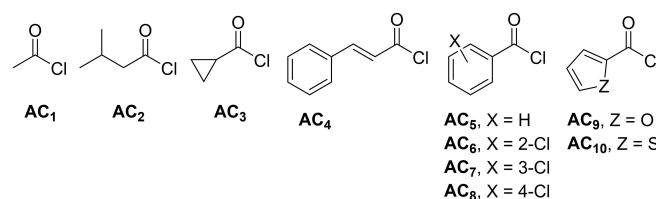


**Figure 3.** Chemical structures of acyl chlorides AC<sub>1-10</sub>.

As detailed in Table 1, different reaction conditions were adopted to compensate the different reactivity of the acylating agents toward the parent mono-acylated substrates. In particular, derivatives **6a–d**, **6f–i**, **6q**, **6s** were prepared using DMF as solvent and *N,N,N',N'*-tetramethylethylenediamine (TMEDA) or triethylamine (TEA) as HCl scavengers. Differently, the other asymmetric thioureas derivatives (namely, **6e**, **6j–n**, **6p**) were obtained by condensing the proper mono acylated precursor **5** in pyridine, as previously reported.<sup>[26]</sup> The symmetric thioureas **6o**, **6r**, **6t** were prepared by reacting the tetrahydropyrimidine-2(1*H*)-thione **4** with two equivalents of acyl chloride in pyridine.

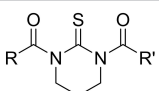
## Biology

Monoacyl thioureas **5** and diacyl thioureas **6** were tested in a CFTR corrector assay carried out on CFBE41o- cells expressing F508del-CFTR and the halide-sensitive yellow fluorescent protein (HS-YFP). CFTR-dependent iodide influx causes fluorescence quenching at a rate proportional to the amount of CFTR channels in the membrane; therefore, the quenching rate (QR) value reflects the efficacy of modulators in rescuing mutant CFTR from intracellular compartments. To evaluate possible synergistic effects, cells were incubated for 24 h with thiourea derivatives (10  $\mu$ M) alone and in combination with the reference drug Lumacaftor (1  $\mu$ M). After treatment, cells were further

stimulated with forskolin and genistein to fully activate CFTR in the plasma membrane and promote anion transport. As reported in Figure 4A, monoacyl thioureas **5** and diacyl thioureas **6** (10  $\mu$ M) poorly affected mutant CFTR trafficking without significative improvement over the control DMSO.

Noteworthy, in cells treated with thiourea compounds the initial YFP fluorescence did not decrease, thus evidencing the lack of cytotoxic effects. All tested derivatives proved to be inactive as CFTR modulator, showing QR values not significantly higher than the control. However, when tested in combination with the clinically used modulator, compounds **6d** (+5%;  $p < 0.05$ ), **6f** (+8%;  $p < 0.05$ ) and **6i** (+16%;  $p < 0.05$ ) significantly enhanced the activity of LUM. The additive effects of diacylthioureas appear to be related to the properties of both acyl substituents. Thus, the replacement of **6i** *trans*-cinnamic group with linear, branched or cyclic alkyl chains (compounds **6a**, **6b**, **6e**), chloro-substituted phenyl rings (compounds **6j–l**) and heteroaryl moieties (compounds **6m**, **6n**) or its removal (compounds **5c**) led to a decrease of the additive effect. Among cyclopropancarbonyl thioureas **5b** and **6e–h**, only compound **6d** positively affected LUM efficacy highlighting the relevant role of the 2-chlorobenzoyl substructure for the activity of this series. The thenoyl/isovaleryl analogue **6d** showed significant additive effect whereas other thenoyl substituted molecules (i.e., **5f**, **6h**, **n**, **q**, **s**, **t**) marginally influenced LUM activity. Noteworthy, the different effects of derivatives **5** and **6** on F508del-

**Table 1.** Reaction conditions of diacyl-thioureas **6**.

Cpd	MAT	R	R'	Reaction conditions
				
<b>6a</b>	5c	Me	Ph	DMF/TEA, 60 °C, 2 h
<b>6b</b>	5c	Me <sub>2</sub> CHCH <sub>2</sub>	Ph	DMF/TMEDA, 80 °C, 2 h
<b>6c</b>	5e	Me <sub>2</sub> CHCH <sub>2</sub>	(4-Cl)C <sub>6</sub> H <sub>4</sub>	DMF/TMEDA, 100 °C, 1.5 h
<b>6d</b>	5a	Me <sub>2</sub> CHCH <sub>2</sub>	2-thienyl	DMF/TMEDA, 120 °C, 0.5 h
<b>6e</b>	5c	Cyclopropyl	Ph	Py, 90 °C, 0.5 h
<b>6f</b>	5b	Cyclopropyl	(2-Cl)C <sub>6</sub> H <sub>4</sub>	DMF/TMEDA, 120 °C, 0.5 h
<b>6g</b>	5e	Cyclopropyl	(4-Cl)C <sub>6</sub> H <sub>4</sub>	DMF/TMEDA, 100 °C, 1.5 h
<b>6h</b>	5f	Cyclopropyl	2-thienyl	DMF/TMEDA, 120 °C, 0.5 h
<b>6i</b>	5c	PhCH=CH	Ph	DMF/TEA; 60 °C, 2 h
<b>6j</b>	5c	Ph	(2-Cl)C <sub>6</sub> H <sub>4</sub>	Py, 90 °C, 0.5 h
<b>6k</b>	5c	Ph	(3-Cl)C <sub>6</sub> H <sub>4</sub>	Py, 90 °C, 0.5 h
<b>6l</b>	5c	Ph	(4-Cl)C <sub>6</sub> H <sub>4</sub>	Py, 90 °C, 0.5 h
<b>6m</b>	5c	Ph	2-furyl	Py, 90 °C, 0.5 h
<b>6n</b>	5c	Ph	2-thienyl	Py, 90 °C, 0.5 h
<b>6o</b>	4	(2-Cl)C <sub>6</sub> H <sub>4</sub>	(2-Cl)C <sub>6</sub> H <sub>4</sub>	Py, 90 °C, 0.5 h
<b>6p</b>	5d	(2-Cl)C <sub>6</sub> H <sub>4</sub>	(4-Cl)C <sub>6</sub> H <sub>4</sub>	Py, 90 °C, 1 h
<b>6q</b>	5d	(2-Cl)C <sub>6</sub> H <sub>4</sub>	2-thienyl	DMF/TMEDA, 120 °C, 0.5 h
<b>6r</b>	4	(4-Cl)C <sub>6</sub> H <sub>4</sub>	(4-Cl)C <sub>6</sub> H <sub>4</sub>	Py, 90 °C, 0.5 h
<b>6s</b>	5f	(4-Cl)C <sub>6</sub> H <sub>4</sub>	2-thienyl	DMF/TMEDA, 120 °C, 0.5 h
<b>6t</b>	4	2-thienyl	2-thienyl	Py, 90 °C, 0.5 h

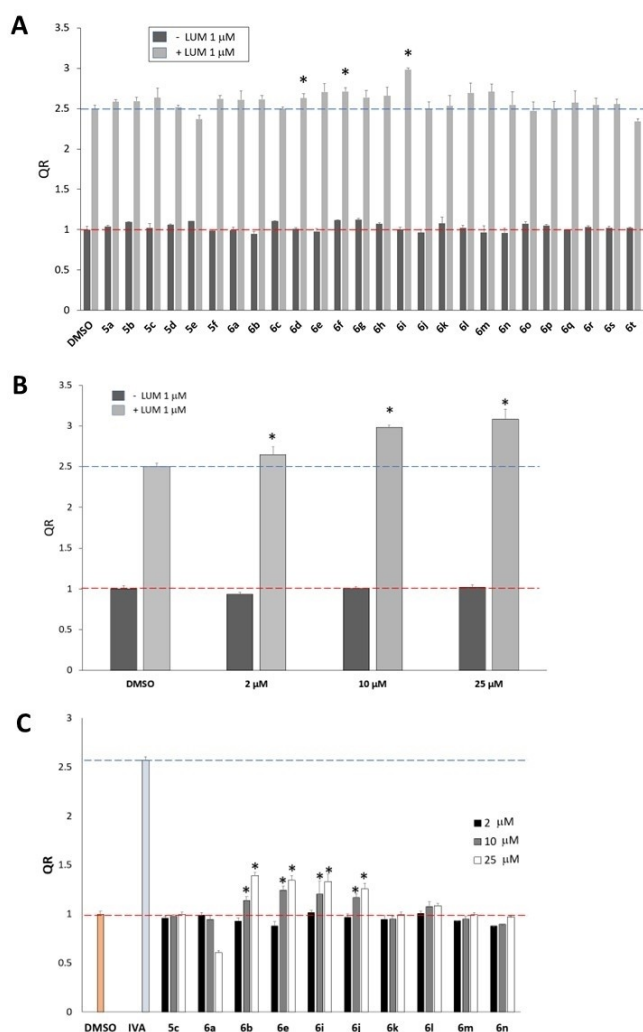


**Figure 4.** A) Functional evaluation of CFTR modulator activity of **5** and **6** series tested as neat compounds (10 μM, dark gray bars) or with LUM (1 μM, light grey bars). QR value for DMSO and LUM are indicated as red and blue dashed line, respectively. B) CFTR modulator activity of **6i** tested as neat compound or in combination with LUM (1 μM) at different concentrations. QR value for DMSO and LUM are indicated as red and blue dashed lines, respectively. C) CFTR potentiating activity of **5c** and **6a, b, e, i–n**. QR values for DMSO and IVA are indicated as red and blue dashed lines, respectively. Each bar reports the average and SD from three experiments. Significant differences ( $p \leq 0.05$ ) are indicated by an asterisk.

CFTR conductance in the absence or in the presence of LUM ruled out any intrinsic anionophore activity for the tested compounds. In fact, if the compounds would be able to carry anions, as demonstrated for compounds **II** (Figure 1B), similar extent of increase in the QR values would have been observed in the absence or in the presence of LUM.

Acylthiourea **6i** (endowed with the most relevant additive effect) was further tested at different concentrations (2, 10 and 25 μM) alone and in association with LUM (1 μM). As reported in Figure 4B, the neat compound proved to be ineffective as CFTR modulator up to 25 μM concentration. Conversely, the association of LUM with **6i** induced a dose-depending enhancement, with a maximum effect observed at 25 μM concentration (+19%;  $p < 0.05$ ). Moreover, to assess if the

observed additive effect of acylthioureas can be ascribable to a potentiating effect on CFTR rescued by LUM, selected derivatives (namely, **5c**, **6a, b, e, i–n**) were tested at different concentrations using IVA as reference drug (Figure 4C). Acylthioureas **5c**, **6a**, **6k–n** did not show any effect as CFTR potentiators at the different concentrations considered (namely, 2, 10 and 25 μM). Compounds **6b**, **6e**, **6i** and **6j** (at 10 μM and 25 μM) displayed QR values significantly higher than those of the vehicle DMSO, still resulting 2-to-4 fold less active than the clinically used CFTR potentiator IVA. These data indicated that the observed additive effect of acylthioureas/LUM association cannot be related to a potentiating effect of derivatives **5** and **6** on CFTR rescued by LUM.

As thiourea group could act as a pharmacophore for cytotoxic activity,<sup>[27]</sup> compounds **5** and **6** were evaluated for their cytotoxicity against a panel of tumor cell lines (namely, breast cancer: MCF7, SKBr3; melanoma: SKMEL28; ovarian cancer: SKOV3; liver cancer: HepG2; cervical cancer: HeLa) and normal human fibroblast GM6114. The mean growth percentage values were determined at the fixed concentration of 10 μM. The results showed in Table 2 demonstrated that all tested compounds did not exhibit any significant cytotoxic activity (grow inhibition percentage ranges higher than 56%) against the considered cancer cell lines. Additionally, all derivatives proved to be non-cytotoxic against normal human fibroblasts GM6114.

To further characterize the pharmaceutical properties of the prepared derivatives, the pharmacokinetic profile as well as the drug-likeness of compounds **5** and **6** were calculated by SwissADME.<sup>[28]</sup> As detailed in Table S1 (Supporting information), the calculated physicochemical parameters of derivatives **5** (i.e., LogP range:  $-0.7$ – $+5$ ; MW range: 150–500 g/mol; TPSA range: 20–130 Å<sup>2</sup>; Fraction  $C_{sp3}$  greater than 0.25; number of rotatable bonds: 0–9) were suitable for oral bioavailability. Furthermore, the predicted gastrointestinal (GI) absorption for the mono acylthioureas is high and only the chlorobenzoyl compounds **5d** and **5e** were predicted to penetrate the blood-brain barrier (BBB). According to the calculations, all derivatives **5** would not inhibit cytochrome (CYP) isoforms 2C9, 2D6 and 3A4, whereas CYP1A2 would be blocked by (hetero)aroyl derivatives **5c–f** but not by the (cyclo)alkylcarbonyl compounds **5a, 5b**.

Furthermore, the chlorine substitution of the benzoyl substructure or the presence of a thenoyl moiety would be related to the inhibition of CYP2C19 enzyme. All derivatives **5** did not show any violations of the Lipinski rules, thus confirming their good drug-like properties. Monoacyl thioureas **5** did not showed any pan assay interference compound (PAINS) alerts whereas the presence of the thiocarbonyl functionality was spotted as problematic portion according to the Brenk filters.<sup>[29]</sup> A molecular weight (MW) lower than 250 g/mol has been estimated to be a limitation of the lead-likeness (i.e., a suitability for optimization) of derivatives **5a–c**, **5f**, as implemented by Teague and coworkers.<sup>[30]</sup>

The physicochemical parameters (i.e. LogP; MW; TPSA; fraction  $C_{sp3}$  and number of rotatable bonds) calculated for diacylthioureas **6** (Supporting information, Table S2) would indicate a good oral bioavailability for derivatives **6a–h** while

**Table 2.** Mean growth percentage values of compounds **5** and **6**.

Cpd	< ?Mean growth percentage (%) <sup>[a]</sup>						
	MCF7	SkBr3	SkMel28	SKOV3	HepG2	HeLa	GM6114
<b>5a</b>	103	101	111	104	91	106	93
<b>5b</b>	105	98	107	100	81	99	89
<b>5c</b>	85	88	83	117	86	59	104
<b>5d</b>	102	103	110	106	90	108	94
<b>5e</b>	106	105	124	104	104	119	82
<b>5f</b>	92	98	104	90	77	103	76
<b>6a</b>	104	99	90	91	69	92	98
<b>6b</b>	86	100	95	117	93	82	108
<b>6c</b>	101	100	117	104	136	129	106
<b>6d</b>	76	87	91	76	86	86	68
<b>6e</b>	86	101	90	111	81	93	97
<b>6f</b>	101	105	108	106	89	104	97
<b>6g</b>	96	98	112	103	126	119	102
<b>6h</b>	86	99	97	87	71	92	76
<b>6i</b>	90	99	98	103	94	91	103
<b>6j</b>	95	97	91	103	91	92	99
<b>6k</b>	84	95	94	116	79	82	93
<b>6l</b>	86	82	88	112	77	58	90
<b>6m</b>	81	101	98	107	96	90	99
<b>6n</b>	87	83	92	111	61	78	80
<b>6o</b>	97	93	96	104	102	104	104
<b>6p</b>	101	102	107	105	88	102	92
<b>6q</b>	101	99	107	103	86	99	95
<b>6r</b>	90	97	99	102	109	92	98
<b>6s</b>	64	92	111	77	86	96	58
<b>6t</b>	87	98	99	91	75	79	56

[a] Data mean values for three separate experiments. Variation among triplicate samples was less than 10%.

the elevated degree of instauration (fraction  $C_{sp3}$  lower than 0.25) would negatively affect the oral absorption of derivatives **6i–t**. The penetration of the BBB would be mostly related to the absence of furoyl or thenoyl substructures even though compounds **6a** and **6e** (lacking any heteroaroyl substituent) were predicted not to enter the central nervous system. All compounds would be endowed with high GI absorption and would not inhibit the catalytic action of CYP2D6. Conversely, compounds **6** would act as inhibitors of different CYP enzymes (Table S2) being the 2C9 and 2C19 enzymes the most affected isoforms. Likewise their monoacylated precursors **5**, derivatives **6** displayed good drug-like properties as indicated by the absence of Lipinski violations. Furthermore, the lack of PAINS alerts and leadlikeness violations would support the value of derivatives **6** as hit compounds. The logP values greater than 3.5 and/or a MW value exceeding the 350 g/mol were predicted as obstacles for the chemical optimization of derivatives **6c**, **6i–l**, **6o–s**. The presence of the thiocarbonyl functionality (and of a Michael acceptor group for **6i**) would represent a druglike limitation, as highlighted by the Brenk alert value.

To identify similarities among the predicted pharmacokinetic profiles of derivatives **5** and **6**, a Principal Component Analysis (PCA) was conducted on 26 compounds, considering 17 variables (Table S3). The Chemometric Agile Tool (CAT) software was used.<sup>[31]</sup> The PCA identified two principal components explaining 61.5% of the total variance (98.82%) with 47.4% and 14.2% of variance, respectively (Scree Plot, Figure 5).

The two series of compounds (namely monoacylthioureas **5** and diacylthioureas **6**) are clearly separated in the biplot (Figure 4), thus indicating the different pharmacokinetic properties of the two classes of derivatives. In detail, the monoacyl compounds **5a** and **5b** were characterized by positive scores for PC1 and PC2 (right-hand of the biplot) showing as the polar character of the molecules positive influenced the ESOL solubility and provided a higher number of H bond donors. On the other hand, compounds **6f**, **6g** and **6i** in the left-hand side of the biplot were still characterized by positive scores for PC2 but displayed negative scores for PC1, thus indicating as the enhancement of lipophilic characteristics increase BBB permeability and LogP values but decreased the H bond donor groups

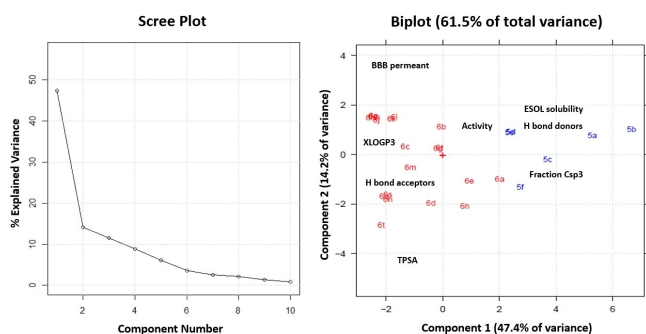


**Figure 5.** Principal component analysis of the data matrix (26 compounds, 17 variables): Scree Plot on the left and Biplot on the right.

and ESOL solubility. Interestingly, compound **6t** was characterized by the worst negative scores in both PC1 and PC2 (bottom left-hand side), showing as the thenoyl group negatively influenced the pharmacokinetic characteristics of the derivatives (see also **5f** and **6s**).

## Conclusions

The previously developed protocol for the preparation of mono-acyl imidazolidine-2-thiones<sup>[24]</sup> proved to be versatile, allowing the synthesis of the unreported mono-acylated tetrahydropyrimidin-2(1H)-thione derivatives **5**. The chemical accessibility to these compounds prompted us to prepare a library of unreported symmetric and asymmetric diacylthioureas **6** characterized by different electronic, steric and lipophilic properties. Acylthioureas **5** and **6** did not highlight any significant modulator activity in phenotypic test on CFBE410-cells expressing mutated F508del-CFTR channel. However, when used in combination with LUM (1  $\mu$ M), selected derivatives emerged to enhance the activity of the marketed drug. In particular, derivatives **6d** (+5%), **6f** (+8%) and **6i** (+16%) showed significative additive effect. In addition, the same thioureas proved to be non-cytotoxic in cell based assays against a panel of tumour and normal cell lines. Derivative **6i** emerged as the most active compound of the series and represents the first example reported in the literature of diacyl thiourea able to potentiate the effect of LUM. Overall, the improved rescue of CFTR activity, the lack of cytotoxic effect and the good predicted pharmacokinetic properties support further studies on mono- and di-acyl thioureas as novel CFTR modulator potentially useful in CF treatment.

## Experimental Section

### Chemistry

#### General

Thiourea **4** and acyl chlorides **AC**<sub>1–10</sub> were purchased by Alfa-Aesar and Sigma-Aldrich. DMF, DMA and pyridine were reagent grade

and dried on molecular sieves (5 Å 1/16" inch pellets). Unless otherwise stated, all commercially available reagents were used without further purification. Organic solutions were dried over anhydrous sodium sulphate. Aluminium-backed silica gel thin layer chromatography (TLC) plates (Merck DC-Alufolien Kieselgel 60 F254) were used to monitor the course of reactions and confirm the purity of analytical samples employed. Neat DCM or DCM/methanol (9:1) mixture were used as a developing solvent and detection of spots was made by UV light and/or by iodine vapours. Melting points were determined on a Fisher-Johns apparatus and are uncorrected. <sup>1</sup>H NMR and <sup>13</sup>C NMR spectra were recorded on a Varian Gemini (200 MHz), Bruker DPX-300 (300 MHz) or JEOL JNM-ECZR (400 MHz) instruments; chemical shifts were reported in  $\delta$  (ppm) units relative to the internal reference tetramethylsilane, and the splitting patterns were described as follows: s (singlet), bs (broad singlet), d (doublet), t (triplet), q (quartet) and m (multiplet). The first order values reported for coupling constants *J* were given in Hz. Elemental analyses were performed by an EA1110 Analyzer, Fison Instruments (Milan).

#### General procedure for the synthesis of compounds **5**

A dry DMA (8 mL) solution of **4** (1.16 g, 10 mmol) and the proper acyl chloride (10 mmol) was stirred at 90 °C for 30 min. After cooling at rt, water (30 mL) and 1 M K<sub>2</sub>CO<sub>3</sub> (pH=8) were sequentially added and the mixture was extracted with DCM (2×15 mL). The pooled organic phases were washed with water (1×10 mL), dried with anhydrous Na<sub>2</sub>SO<sub>4</sub> and concentrated under reduced pressure. The crude material was purified by crystallization from the proper solvent or solvent mixture.

**3-methyl-1-(2-thioxotetrahydropyrimidin-1(2H)-yl)butan-1-one (5a).** White solid; yield: 35%; mp: 98–100 °C (DCM/MeOH). <sup>1</sup>H NMR (200 MHz, CDCl<sub>3</sub>)  $\delta$  0.89–0.97 (m, 6H, 2 x CH<sub>3</sub>); 2.02–2.18 (m, 2H, C–CH<sub>2</sub>–C); 2.13–2.3 (m, 1H, CH) 3.10–3.21 (m, 2H, CH<sub>2</sub>–CO); 3.30–3.35 (m, 2H, CH<sub>2</sub>N); 3.75–3.81 (m, 2H, CH<sub>2</sub>N); 7.82 (bs, 1H, NH). <sup>13</sup>C NMR (50 MHz, CDCl<sub>3</sub>)  $\delta$  22.36, 23.04, 26.79, 40.47, 42.95, 43.88, 174.91, 178.44. Anal. Calcd for C<sub>9</sub>H<sub>16</sub>N<sub>2</sub>OS: C, 53.97; H, 8.05; N, 13.99; S, 16.01. Found: C, 53.87; H, 7.97; N, 14.05; S, 16.32.

**Cyclopropyl(2-thioxotetrahydropyrimidin-1(2H)-yl)methanone (5b).** White solid; yield: 37%; mp: 102–104 °C (DCM/acetone). <sup>1</sup>H NMR (200 MHz, CDCl<sub>3</sub>)  $\delta$  0.99–1.05 (m, 2H, CH<sub>2</sub>-cycloprop); 1.06–1.22 (m, 2H, CH<sub>2</sub>-cycloprop); 2.02–2.18 (m, 2H, C–CH<sub>2</sub>–C); 3.10–3.25 (m, 1H, CH-CO); 3.34–3.42 (m, 2H, CH<sub>2</sub>N); 3.74–3.80 (m, 2H, CH<sub>2</sub>N); 7.83 (bs, 1H, NH). <sup>13</sup>C NMR (50 MHz, CDCl<sub>3</sub>)  $\delta$  11.82, 14.41, 22.12, 44.87, 48.93, 172.20, 179.26. Anal. Calcd for C<sub>8</sub>H<sub>12</sub>N<sub>2</sub>OS: C, 52.15; H, 6.56; N, 15.20; S, 17.40. Found: C, 52.29; H, 6.32; N, 14.94; S, 17.63.

**Phenyl(2-thioxotetrahydropyrimidin-1(2H)-yl)methanone (5c).** White solid; yield: 38%; mp: 167–170 °C (DCM). IR (KBr) cm<sup>-1</sup> 3219 (N–H), 1694 (C=O). <sup>1</sup>H NMR (200 MHz, CDCl<sub>3</sub>)  $\delta$  2.08–2.26 (m, 2H, C–CH<sub>2</sub>–C); 3.28–3.48 (m, 2H, CH<sub>2</sub>N); 3.82 (t, 2H, J = 7.4 Hz, CH<sub>2</sub>N); 7.25–8.08 (m, 6H, arom H and NH). <sup>13</sup>C NMR (50 MHz, CDCl<sub>3</sub>)  $\delta$  22.01, 43.52, 46.52, 127.99, 128.70, 132.04, 135.48, 174.38, 178.98. Anal. Calcd for C<sub>11</sub>H<sub>12</sub>N<sub>2</sub>OS: C, 59.97; H, 5.49; N, 12.72; S, 14.56. Found: C, 59.76; H, 5.38; N, 12.72; S, 14.78.

**(2-Chlorophenyl)(2-thioxotetrahydropyrimidin-1(2H)-yl)methanone (5d).** White solid; yield: 53%; mp: 125–130 °C (DCM/MeOH). <sup>1</sup>H NMR (400 MHz, CDCl<sub>3</sub>)  $\delta$  2.15–2.26 (m, 2H, C–CH<sub>2</sub>–C); 3.36–3.45 (m, 2H, CH<sub>2</sub>N); 3.94–4.02 (m, 2H, CH<sub>2</sub>N); 7.24–7.36 (m, 3H, arom H); 7.42 (bs, 1H, NH); 7.44–7.49 (m, 1H, arom H). <sup>13</sup>C NMR (101 MHz, CDCl<sub>3</sub>)  $\delta$  21.68, 42.33, 43.88, 126.86, 129.56, 130.30, 130.51, 130.98, 137.18, 171.10, 181.75. Anal. Calcd for C<sub>11</sub>H<sub>11</sub>ClN<sub>2</sub>OS: C, 51.85; H, 4.35; N, 11.00; S, 12.59. Found: C, 52.05; H, 4.27; N, 10.81; S, 12.34.

(4-Chlorophenyl)(2-thioxotetrahydropyrimidin-1(2H)-yl)methanone (**5e**). Yellow solid; yield: 36%; mp: 125–127 °C (DCM/acetone). <sup>1</sup>H NMR (400 MHz, CDCl<sub>3</sub>) δ 2.16–2.27 (m, 2H, C–CH<sub>2</sub>–C); 3.41–3.51 (m, 2H, CH<sub>2</sub>N); 3.78–3.85 (m, 2H, CH<sub>2</sub>N); 7.33–7.39 and 7.61–7.68 (m, 4H, arom H); 8.01 (bs, 1H, NH). <sup>13</sup>C NMR (101 MHz, CDCl<sub>3</sub>) δ 21.60, 42.11, 44.63, 128.76, 130.33, 134.58, 138.41, 173.45, 181.53. Anal. Calcd for C<sub>11</sub>H<sub>11</sub>ClN<sub>2</sub>O<sub>2</sub>S: C, 51.86; H, 4.35; N, 11.00; S, 12.59. Found: C, 51.48; H, 4.33; N, 11.12; S, 12.79.

Thiophen-2-yl(2-thioxotetrahydropyrimidin-1(2H)-yl)methanone (**5f**). Pale brown solid; yield: 32%; mp: 132–135 °C (DCM/acetone). <sup>1</sup>H NMR (200 MHz, CDCl<sub>3</sub>) δ 2.04–2.24 (m, 2H, C–CH<sub>2</sub>–C); 3.40–3.48 (m, 2H, CH<sub>2</sub>N); 3.72–3.79 (m, 2H, CH<sub>2</sub>N); 7.08–7.13 and 7.62–7.74 (m, 4H, arom H + NH). <sup>13</sup>C NMR (50 MHz, CDCl<sub>3</sub>) δ 22.94, 43.82, 45.93, 127.74, 134.80, 135.62, 139.15, 166.79, 183.57. Anal. Calcd for C<sub>9</sub>H<sub>10</sub>N<sub>2</sub>O<sub>2</sub>S<sub>2</sub>: C, 47.77; H, 4.45; N, 12.38; S, 28.33. Found: C, 47.80; H, 4.36; N, 12.25; S, 28.63.

### General procedure for the synthesis of compounds 6a and 6i

To a dry DMF (10 mL) solution of **5c** (0.44 g, 2.0 mmol), TEA (308 μL, 2.2 mmol) and the proper acyl chloride (2.2 mmol) were sequentially added. The reaction mixture was stirred at 60 °C for 2 h and then stirring was prolonged at rt for 16 h. After dilution with water (20 mL), a solid precipitated. The crude solid was collected by filtration and crystallized from the suitable solvent.

1-(3-Benzoyl-2-thioxotetrahydropyrimidin-1(2H)-yl)ethan-1-one (**6a**). White solid; yield: 69%; mp: 138–140 °C (MeOH). IR (KBr) cm<sup>-1</sup> 1703 (C=O), 1687 (C=O). <sup>1</sup>H NMR (200 MHz, CDCl<sub>3</sub>) δ 2.19–2.4 (m, 2H, C–CH<sub>2</sub>–C); 2.68 (s, 3H, CH<sub>3</sub>); 3.70–3.88 (m, 2H, CH<sub>2</sub>N) 3.96–4.18 (m, 2H, CH<sub>2</sub>N); 7.22–7.81 (m, 5H, arom H). <sup>13</sup>C NMR (50 MHz, CDCl<sub>3</sub>) δ 20.65, 24.00, 43.52, 45.17, 128.02, 128.70, 133.45, 135.62, 169.50, 173.03, 178.14. Anal. Calcd for C<sub>13</sub>H<sub>14</sub>N<sub>2</sub>O<sub>2</sub>S: C, 59.52; H, 5.38; N, 10.68; S, 12.22. Found: C, 59.72; H, 5.55; N, 10.98; S, 12.04.

(E)-1-(3-Benzoyl-2-thioxotetrahydropyrimidin-1(2H)-yl)-3-phenylprop-2-en-1-one (**6i**). Yellow solid; yield: 51%; mp: 132–136 °C (MeOH). IR (KBr) cm<sup>-1</sup> 2926 (C<sub>sp3</sub>–H), 1687 (C=O), 1631 (C=O). <sup>1</sup>H NMR (200 MHz, CDCl<sub>3</sub>) δ 2.36–2.59 (m, 2H, C–CH<sub>2</sub>–C); 3.82–4.16 (m, 4H, 2 x CH<sub>2</sub>N); 7.24–7.6 (m, 10H, arom H); 7.65–7.82 (m, 2H, CH=CH). <sup>13</sup>C NMR (50 MHz, CDCl<sub>3</sub>) δ 20.53, 47.06, 49.23, 121.27, 127.99, 128.42, 128.70, 128.95, 129.92, 132.04, 135.62, 137.27, 141.56, 168.14, 171.08, 175.14. Anal. Calcd for C<sub>20</sub>H<sub>18</sub>N<sub>2</sub>O<sub>2</sub>S<sub>2</sub>: C, 68.55; H, 5.18; N, 7.99; S, 9.15. Found: C, 68.62; H, 5.41; N, 7.81; S, 8.94.

### General procedure for the synthesis of compounds 6b-d, 6f-h, 6q, 6s

To a dry DMF (10 mL) solution of the suitable monoacyl precursor **5** (2.0 mmol; see Table 1), TMEDA (335 μL, 2.2 mmol) and the proper acyl chloride (2.2 mmol) were sequentially added. The reaction mixture was stirred at different temperature for variable times (see Table 1). After dilution with water (30 mL), a solid precipitated. For compounds **6b** and **6h**, the oily residue was extracted with DCM (2x10 mL) and the pooled organic phases were washed with water (5x10 mL), dried with Na<sub>2</sub>SO<sub>4</sub> and concentrated under reduced pressure. The crude material was purified by crystallization from the suitable solvent or solvent mixture.

1-(3-Benzoyl-2-thioxotetrahydropyrimidin-1(2H)-yl)-3-methylbutan-1-one (**6b**). Yellow solid; yield: 39%; mp: 102–104 °C (DCM/MeOH). IR (KBr) cm<sup>-1</sup> 2955 (C<sub>sp3</sub>–H), 1691 (C=O). <sup>1</sup>H NMR (200 MHz, CDCl<sub>3</sub>) δ 0.92–1.10 (m, 6H, 2 x CH<sub>3</sub>); 2.18–2.39 (m, 3H, CH and C–CH<sub>2</sub>–C); 2.94–3.07 (m, 2H, CH<sub>2</sub>–CO); 3.76–3.92 (m, 2H, CH<sub>2</sub>N); 4.00–4.18 (m, 2H, CH<sub>2</sub>N); 7.40–7.64 (m, 3H, arom H); 7.68–7.84 (m, 2H, arom H). <sup>13</sup>C NMR (101 MHz, CDCl<sub>3</sub>) δ 19.36, 22.51, 25.66, 39.74, 40.75, 43.26,

128.57, 129.69, 130.25, 133.71, 171.33, 176.42, 178.67. Anal. Calcd for C<sub>16</sub>H<sub>20</sub>N<sub>2</sub>O<sub>2</sub>S<sub>2</sub>: C, 63.13; H, 6.62; N, 9.20; S, 10.53. Found: C, 63.03; H, 6.33; N, 9.32; S, 10.29.

1-(3-(4-Chlorobenzoyl)-2-thioxotetrahydropyrimidin-1(2H)-yl)-3-methylbutan-1-one (**6c**). Yellow solid; yield: 40%; mp: 103–105 °C (DCM/MeOH). <sup>1</sup>H NMR (200 MHz, CDCl<sub>3</sub>) δ 0.88–1.04 (m, 6H, 2 x CH<sub>3</sub>); 2.13–2.40 (m, 3H, C–CH<sub>2</sub>–C and CH); 2.98 (d, 2H, J = 7.0 Hz, CH<sub>2</sub>–CO); 3.81 (t, 2H, J = 7.2 Hz, CH<sub>2</sub>N); 4.04 (t, 2H, J = 6.8 Hz, CH<sub>2</sub>N); 7.37–7.45 and 7.64–7.72 (m, 4H, arom H). <sup>13</sup>C NMR (50 MHz, CDCl<sub>3</sub>) δ 20.62, 22.54, 25.61, 42.17, 44.34, 46.23, 129.39, 129.55, 133.80, 136.87, 170.03, 171.20, 177.61. Anal. Calcd for C<sub>16</sub>H<sub>15</sub>ClN<sub>2</sub>O<sub>2</sub>S<sub>2</sub>: C, 56.71; H, 5.65; N, 8.27; S, 9.46. Found: C, 56.72; H, 5.62; N, 8.50; S, 9.14.

3-Methyl-1-(3-(thiophene-2-carbonyl)-2-thioxotetrahydropyrimidin-1(2H)-yl)butan-1-one (**6d**). White solid; yield: 9%; mp: 165–168 °C (DCM/MeOH). <sup>1</sup>H NMR (200 MHz, CDCl<sub>3</sub>) δ 0.83–1.07 (m, 6H, 2 x CH<sub>3</sub>); 2.17–2.54 (m, 3H, C–CH<sub>2</sub>–C + CH); 3.06 (d, 2H, J = 7.0 Hz, CH<sub>2</sub>CO); 3.67–4.06 (m, 4H, 2 x CH<sub>2</sub>N); 7.07–7.20 (m, 1H, H-thiophene); 7.40–7.60 (m, 2H, H-thiophene). <sup>13</sup>C NMR (50 MHz, CDCl<sub>3</sub>) δ 21.29, 24.00, 27.29, 40.29, 47.58, 48.40, 128.03, 134.56, 135.33, 141.03, 164.32, 171.20, 175.98. Anal. Calcd for C<sub>14</sub>H<sub>18</sub>N<sub>2</sub>O<sub>2</sub>S<sub>2</sub>: C, 54.17; H, 5.84; N, 9.02; S, 20.66. Found: C, 54.07; H, 5.93; N, 8.98; S, 20.54.

(3-(2-Chlorobenzoyl)-2-thioxotetrahydropyrimidin-1(2H)-yl)(cyclopropyl)methanone (**6f**). Yellow solid; yield: 54%; mp: 108–110 °C (DCM/MeOH). <sup>1</sup>H NMR (200 MHz, CDCl<sub>3</sub>) δ 0.93–1.03 (m, 2H, CH<sub>2</sub>-cycloprop); 1.16–1.25 (m, 2H, CH<sub>2</sub>-cycloprop); 2.26–2.43 (m, 2H, C–CH<sub>2</sub>–C); 2.57–2.74 (m, 1H, CH); 3.92 (t, 2H, J = 7.0 Hz, CH<sub>2</sub>N); 4.05 (t, 2H, J = 7.2 Hz, CH<sub>2</sub>N); 7.23–7.54 (m, 4H, arom H). <sup>13</sup>C NMR (101 MHz, CDCl<sub>3</sub>) δ 9.32, 12.88, 19.33, 40.81, 126.79, 129.13, 131.47, 132.36, 133.34, 134.50, 169.60, 175.85, 180.56. Anal. Calcd for C<sub>14</sub>H<sub>13</sub>ClN<sub>2</sub>O<sub>2</sub>S<sub>2</sub>: calc. C, 54.46; H, 4.24; N, 9.07; S, 10.38. Found: C, 54.37; H, 4.19; N, 8.98; S, 10.24.

(3-(4-Chlorobenzoyl)-2-thioxotetrahydropyrimidin-1(2H)-yl)(cyclopropyl)methanone (**6g**). White solid; yield: 51%; mp: 159–161 °C (DCM/MeOH). <sup>1</sup>H NMR (200 MHz, CDCl<sub>3</sub>) δ 0.90–1.04 (m, 2H, CH<sub>2</sub>-cycloprop); 1.17–1.26 (m, 2H, CH<sub>2</sub>-cycloprop); 2.19–2.45 (m, 2H, C–CH<sub>2</sub>–C); 2.71–2.84 (m, 1H, CH); 3.86 (t, 2H, J = 7.2 Hz, CH<sub>2</sub>N); 4.00 (t, 2H, J = 6.6 Hz, CH<sub>2</sub>N); 7.36–7.45 and 7.63–7.73 (m, 4H, arom H). <sup>13</sup>C NMR (50 MHz, CDCl<sub>3</sub>) δ 9.65, 14.35, 20.66, 44.41, 44.89, 129.47, 130.51, 134.14, 136.98, 168.97, 170.56, 178.59. Anal. Calcd for C<sub>15</sub>H<sub>15</sub>ClN<sub>2</sub>O<sub>2</sub>S<sub>2</sub>: C, 55.81; H, 4.68; N, 8.68; S, 9.96. Found: C, 55.61; H, 4.59; N, 8.94; S, 9.77.

(3-(Cyclopropanecarbonyl)-2-thioxotetrahydropyrimidin-1(2H)-yl)(thiophen-2-yl)methanone (**6h**). Yellow solid; yield: 35%; mp: 130–135 °C (MeOH). <sup>1</sup>H NMR (200 MHz, CDCl<sub>3</sub>) δ 0.96–1.07 (m, 2H, CH<sub>2</sub>-cycloprop); 1.16–1.31 (m, 2H, CH<sub>2</sub>-cycloprop); 2.23–2.40 (m, 2H, C–CH<sub>2</sub>–C); 2.83–2.98 (m, 1H, CH-CO); 3.79 (t, 2H, J = 6.8 Hz, CH<sub>2</sub>N); 3.98 (t, 2H, J = 6.6 Hz, CH<sub>2</sub>N); 7.09–7.17 (m, 1H, H(4)-thiophene); 7.63–7.80 (m, 2H, H(3) and H(5)-thiophene). <sup>13</sup>C NMR (50 MHz, CDCl<sub>3</sub>) δ 12.12, 16.41, 21.06, 43.82, 45.93, 128.03, 133.45, 135.09, 141.03, 163.79, 168.14, 177.10. Anal. Calcd for C<sub>13</sub>H<sub>14</sub>N<sub>2</sub>O<sub>2</sub>S<sub>2</sub>: C, 53.04; H, 4.79; N, 9.52; S, 21.78. Found: C, 52.83; H, 4.79; N, 9.58; S, 21.51

(3-(2-Chlorobenzoyl)-2-thioxotetrahydropyrimidin-1(2H)-yl)(thiophen-2-yl)methanone (**6q**). Yellow solid; yield: 66%; mp: 170–175 °C (DCM/EtOH). <sup>1</sup>H NMR (200 MHz, CDCl<sub>3</sub>) δ 2.40–2.56 (m, 2H, C–CH<sub>2</sub>–C); 3.85 (t, 2H, J = 7.0 Hz, CH<sub>2</sub>N); 4.12–4.27 (m, 2H, CH<sub>2</sub>N); 7.07–7.12 and 7.20–7.37 and 7.43–7.53 and 7.61–7.78 (m, 7H, arom H). <sup>13</sup>C NMR (101 MHz, CDCl<sub>3</sub>) δ 19.41, 40.95, 126.80, 128.18, 128.97, 131.51, 132.42, 133.44, 133.91, 134.92, 166.93, 169.96. Anal. Calcd for C<sub>16</sub>H<sub>13</sub>ClN<sub>2</sub>O<sub>2</sub>S<sub>2</sub>: C, 52.67; H, 3.59; N, 7.68; S, 17.57. Found: C, 52.44; H, 3.57; N, 7.83; S, 17.51.

(3-(4-Chlorobenzoyl)-2-thioxotetrahydropyrimidin-1(2H)-yl)(thiophen-2-yl)methanone (**6s**). White solid; yield: 49%; mp: 175–178 °C (DCM/MeOH). <sup>1</sup>H NMR (200 MHz, CDCl<sub>3</sub>) δ 2.40–2.57 (m, 2H, C–CH<sub>2</sub>–C); 3.84–4.07 (m, 4H, 2 x CH<sub>2</sub>N); 7.06–7.14 (m, 1H, H-thiophene); 7.34–7.43 (m, 2H, H-thiophene); 7.60–7.77 (m, 4H, arom H). <sup>13</sup>C NMR (50 MHz, CDCl<sub>3</sub>) δ 21.59, 47.35, 48.11, 127.15, 129.97, 130.50, 133.80, 134.56, 135.09, 135.92, 138.62, 162.15, 173.55, 178.14. Anal. Calcd for C<sub>16</sub>H<sub>13</sub>ClN<sub>2</sub>O<sub>2</sub>S<sub>2</sub>: C, 52.67; H, 3.59; N, 7.68; S, 17.42. Found: C, 52.43; H, 3.53; N, 7.76; S, 17.42.

#### General procedure for the synthesis of compounds 6e, 6j–n, 6p

The proper mono-acyl derivative **5** (2 mmol, Table 1) and the suitable acyl chloride (2.2 mmol) were dissolved in anhydrous pyridine (10 mL) and heated at 90 °C for 0.5 h. After dilution with water (40 mL) the mixture was kept at 4 °C for 2 h and the precipitated solid was filtered. The crude material was purified by crystallization from DCM/MeOH mixture.

(3-Benzoyl-2-thioxotetrahydropyrimidin-1(2H)-yl)(cyclopropyl)methanone (**6e**). Yellow solid; yield: 15%; mp: 113–117 °C. IR (KBr) cm<sup>-1</sup> 1691 (C=O). <sup>1</sup>H NMR (200 MHz, CDCl<sub>3</sub>) δ 0.89–1.08 (m, 2H, CH<sub>2</sub>-cycloprop.); 1.2–1.32 (m, 2H, CH<sub>2</sub>-cycloprop.); 2.24–2.44 (m, 2H, C–CH<sub>2</sub>–C); 2.68–2.88 (m, 1H, CHCO); 3.74–3.96 (m, 2H, CH<sub>2</sub>N); 3.97–4.12 (m, 2H, CH<sub>2</sub>N); 7.30–7.82 (m, 5H, arom H). <sup>13</sup>C NMR (101 MHz, CDCl<sub>3</sub>) δ 9.53, 12.53, 19.35, 41.40, 127.33, 129.05, 129.33, 133.77, 168.03, 169.44, 176.85. Anal. Calcd for C<sub>15</sub>H<sub>16</sub>N<sub>2</sub>O<sub>2</sub>S: C, 62.48; H, 5.59; N, 9.71; S, 11.12. Found: C, 62.58; H, 5.37; N, 10.03; S, 10.91.

(3-Benzoyl-2-thioxotetrahydropyrimidin-1(2H)-yl)(2-chlorophenyl)methanone (**6j**). Yellow solid; yield: 39%; mp: 150–152 °C. IR (KBr) cm<sup>-1</sup> 2928 (C<sub>sp3</sub>–H), 1703 (C=O), 1672 (C=O). <sup>1</sup>H NMR (200 MHz, CDCl<sub>3</sub>) δ 2.42–2.59 (m, 2H, C–CH<sub>2</sub>–C); 3.88–4.25 (m, 4H, 2 x CH<sub>2</sub> N); 7.21–7.78 (m, 9H, arom H). <sup>13</sup>C NMR (101 MHz, CDCl<sub>3</sub>) δ 19.37, 40.93, 126.79, 128.59, 129.18, 129.58, 130.28, 131.46, 132.36, 133.32, 133.77, 134.50, 135.44, 169.68, 171.31. Anal. Calcd for C<sub>18</sub>H<sub>15</sub>ClN<sub>2</sub>O<sub>2</sub>S: C, 60.25; H, 4.21; N, 7.81; S, 8.94. Found: C, 60.10; H, 4.18; N, 7.85; S, 8.60.

(3-Benzoyl-2-thioxotetrahydropyrimidin-1(2H)-yl)(3-chlorophenyl)methanone (**6k**). White solid; yield: 34%; mp: 104–105 °C. IR (KBr) cm<sup>-1</sup> 2963 (C<sub>sp3</sub>–H), 1712 (C=O). <sup>1</sup>H NMR (200 MHz, CDCl<sub>3</sub>) δ 2.41–2.59 (m, 2H, C–CH<sub>2</sub>–C); 3.94–4.10 (m, 4H, 2 x CH<sub>2</sub>N); 7.29–7.76 (m, 9H, arom H). <sup>13</sup>C NMR (50 MHz, CDCl<sub>3</sub>) δ 21.29, 44.41, 45.17, 126.66, 127.90, 127.99, 128.70, 130.66, 130.76, 132.04, 133.93, 134.54, 134.93, 168.67, 168.97, 174.61. Anal. Calcd for C<sub>18</sub>H<sub>15</sub>ClN<sub>2</sub>O<sub>2</sub>S: C, 60.25; H, 4.21; N, 7.81; S, 8.94. Found: C, 60.06; H, 4.46; N, 8.02; S, 8.68.

(3-Benzoyl-2-thioxotetrahydropyrimidin-1(2H)-yl)(4-chlorophenyl)methanone (**6l**). White solid; yield: 26%; mp: 170–172 °C. IR (KBr) cm<sup>-1</sup> 3057 (C<sub>sp2</sub>–H), 2964 (–H), 1708 (C=O). <sup>1</sup>H NMR (300 MHz, CDCl<sub>3</sub>) δ 2.43–2.53 (m, 2H, C–CH<sub>2</sub>–C); 3.96–4.04 (m, 4H, 2 x CH<sub>2</sub>N); 7.32–7.71 (m, 9H, arom H). <sup>13</sup>C NMR (101 MHz, CDCl<sub>3</sub>) δ 21.59, 44.46, 44.64, 128.45, 128.62, 129.04, 129.14, 130.32, 131.66, 132.02, 132.27, 132.48, 173.88, 174.42, 181.47. Anal. Calcd for C<sub>18</sub>H<sub>15</sub>ClN<sub>2</sub>O<sub>2</sub>S: C, 60.25; H, 4.21; N, 7.81; S, 8.94. Found: C, 60.21; H, 4.15; N, 7.86; S, 8.60.

(3-Benzoyl-2-thioxotetrahydropyrimidin-1(2H)-yl)(furan-2-yl)methanone (**6m**). White solid; yield: 34%; mp: 111–112 °C. IR (KBr) cm<sup>-1</sup> 3226 (C<sub>sp2</sub>–H), 2961 (C<sub>sp3</sub>–H), 1694 (C=O). <sup>1</sup>H NMR (200 MHz, CDCl<sub>3</sub>) δ 2.38–2.58 (m, 2H, C–CH<sub>2</sub>–C); 3.86–4.1 (m, 4H, 2 x CH<sub>2</sub>N); 6.48–6.58 and 7.18–7.29 and 7.32–7.64 and 7.68–7.82 (m, 8H, arom H). <sup>13</sup>C NMR (50 MHz, CDCl<sub>3</sub>) δ 21.59, 44.41, 44.48, 114.51, 118.27, 127.75, 128.65, 132.92, 135.62, 145.74, 146.99, 158.91, 168.14, 174.38. Anal. Calcd for C<sub>16</sub>H<sub>14</sub>N<sub>2</sub>O<sub>3</sub>S: C, 61.13; H, 4.49; N, 8.91; S, 10.20. Found: C, 61.06; H, 4.35; N, 9.03; S, 10.02.

(3-Benzoyl-2-thioxotetrahydropyrimidin-1(2H)-yl)(thiophen-2-yl)methanone (**6n**). White solid; yield: 31%; mp: 209–211 °C. IR (KBr) cm<sup>-1</sup> 3089 (C<sub>sp2</sub>–H), 2961 (C<sub>sp3</sub>–H), 1703 (C=O), 1690 (C=O). <sup>1</sup>H NMR (200 MHz, CDCl<sub>3</sub>) δ 2.39–2.58 (m, 2H, C–CH<sub>2</sub>–C); 3.86–4.09 (m, 4H, 2 x CH<sub>2</sub>N); 7.07–7.14 and 7.32–7.80 (m, 8H, arom H). <sup>13</sup>C NMR (101 MHz, CDCl<sub>3</sub>) δ 21.57, 44.61, 45.04, 128.41, 128.58, 129.00, 130.25, 130.68, 132.23, 132.45, 133.73, 134.67, 173.84, 174.39, 180.24. Anal. Calcd for C<sub>16</sub>H<sub>14</sub>N<sub>2</sub>O<sub>2</sub>S<sub>2</sub>: C, 58.16; H, 4.27; N, 8.48; S, 19.41. Found: C, 57.90; H, 4.61; N, 8.72; S, 19.05.

(3-(2-Chlorobenzoyl)-2-thioxotetrahydropyrimidin-1(2H)-yl)(4-chlorophenyl)methanone (**6p**). White solid; yield: 7%; mp: 157–160 °C. <sup>1</sup>H NMR (200 MHz, CDCl<sub>3</sub>) δ 2.43–2.60 (m, 2H, C–CH<sub>2</sub>–C); 3.89–4.36 (m, 4H, 2 x CH<sub>2</sub>N); 7.12–7.54 (m, 8H, arom H). <sup>13</sup>C NMR (101 MHz, CDCl<sub>3</sub>) δ 19.28, 40.91, 126.81, 129.00, 131.50, 131.69, 132.42, 133.41, 134.58, 135.48, 169.64, 170.32. Anal. Calcd for C<sub>18</sub>H<sub>14</sub>Cl<sub>2</sub>N<sub>2</sub>O<sub>2</sub>S: C, 54.97; H, 3.59; N, 7.12; S, 8.15. Found: C, 54.35; H, 3.57; N, 7.09; S, 8.48.

#### General procedure for the synthesis of compounds 6o, 6r, 6t

The suitable acyl chloride (22 mmol) was added to a stirred anhydrous pyridine (20 mL) solution of thiourea **4** (10 mmol, 1.17 g). The resulting mixture was heated for 30 min at 90 °C. After cooling at rt, water (50 mL) was added and the obtained precipitate was filtered and washed with water. The crude material was purified by crystallization from the suitable solvents or solvent mixtures.

(2-Thioxodihydropyrimidine-1,3(2H,4H)-diyl)bis((2-chlorophenyl)methanone) (**6o**). Yellow solid; yield: 61%; mp: 196–198 °C (DCM/acetone). <sup>1</sup>H NMR (200 MHz, CDCl<sub>3</sub>) δ 2.41–2.59 (m, 2H, C–CH<sub>2</sub>–C); 4.17 (t, 4H, J = 6.6 Hz, CH<sub>2</sub>N); 7.16–7.45 (m, 8H, arom H). <sup>13</sup>C NMR (101 MHz, CDCl<sub>3</sub>) δ 21.69, 42.90, 126.82, 126.85, 131.51, 132.43, 133.45, 169.40, 181.71. Anal. Calcd for C<sub>18</sub>H<sub>14</sub>Cl<sub>2</sub>N<sub>2</sub>O<sub>2</sub>S: calc. C: 54.97, H: 3.59, N: 7.12, S: 8.15. Found: C: 54.95, H: 3.67, N: 7.02, S: 8.23.

(2-Thioxodihydropyrimidine-1,3(2H,4H)-diyl)bis((4-chlorophenyl)methanone) (**6r**). White solid; yield: 14%; mp: 118–120 °C (DCM/MeOH). <sup>1</sup>H NMR (200 MHz, CDCl<sub>3</sub>) δ 2.22–2.38 (m, 2H, C–CH<sub>2</sub>–C); 3.94–4.08 (m, 2H, 4H, 2 x CH<sub>2</sub>N); 7.30–7.74 (m, 8H, arom H). <sup>13</sup>C NMR (101 MHz, CDCl<sub>3</sub>) δ 23.59, 44.51, 129.03, 130.42, 133.01, 138.87, 172.80, 184.07. Anal. Calcd for C<sub>18</sub>H<sub>14</sub>Cl<sub>2</sub>N<sub>2</sub>O<sub>2</sub>S: calc. C: 54.97, H: 3.59, N: 7.12, S: 8.15. Found: C: 55.07, H: 3.39, N: 6.95, S: 8.02.

(2-Thioxodihydropyrimidine-1,3(2H,4H)-diyl)bis(thiophen-2-ylmethanone) (**6t**). White solid; yield: 39%; mp: 229–231 °C (DCM/acetone). <sup>1</sup>H NMR (200 MHz, CDCl<sub>3</sub>) δ 2.38–2.56 (m, 2H, C–CH<sub>2</sub>–C); 3.84–3.97 (m, 2H, 4H, 2 x CH<sub>2</sub>N); 7.08–7.14 and 7.61–7.80 (m, 6H, arom H). <sup>13</sup>C NMR (50 MHz, CDCl<sub>3</sub>) δ 22.94, 44.54, 129.10, 133.82, 134.19, 138.33, 162.26, 175.73. Anal. Calcd for C<sub>14</sub>H<sub>12</sub>N<sub>2</sub>O<sub>3</sub>S<sub>2</sub>: calc. C: 49.98, H: 3.59, N: 8.33, S: 28.59. Found: C: 49.56, H: 3.66, N: 8.79, S: 28.66.

#### Pharmacological/biological assays

##### Evaluation of CFTR modulator activity

Immortalized bronchial epithelial CFBE41o- cells stably co-expressing the halide-sensitive yellow fluorescent protein (HS-YFP) YFP-H148Q/1152L/F46L and mutant F508del-CFTR were grown in MEM (Euroclone, Milano, Italy) supplemented with 10% FBS, 2 mM L-glutamine, 100 U/mL penicillin, and 100 µg/mL streptomycin (Euroclone). CFBE41o- cells were plated (50,000 cells/well) on clear-bottom 96-well black microplates (Corning Life Sciences, Corning, NY, USA) suitable for fluorometric assays. As for CFTR corrector activity, one day after plating cells were treated with test



compounds (10  $\mu$ M final concentration) or vehicle alone (DMSO) in the absence or presence of the approved drug Lumacaftor (1  $\mu$ M). After 24 h, CFTR activity was determined by the HS-YFP microfluorimetric assay. Briefly, prior to the assay, cells were washed with PBS (137 mM NaCl, 2.7 mM KCl, 8.1 mM Na<sub>2</sub>HPO<sub>4</sub>, 1.5 mM KH<sub>2</sub>PO<sub>4</sub>, 1 mM CaCl<sub>2</sub>, and 0.5 mM MgCl<sub>2</sub>) and then incubated at 37 °C for 25 min with 60  $\mu$ L of PBS containing forskolin (20  $\mu$ M) and genistein (50  $\mu$ M), to maximally stimulate the F508del-CFTR channel. As for CFTR potentiator activity, cells were treated the day after plating with Lumacaftor (1  $\mu$ M) to rescue the trafficking defect. After 24 h, CFTR activity was determined by the HS-YFP microfluorimetric assay. In this case, cells were washed with PBS and then incubated at 37 °C for 25 min with 60  $\mu$ L of PBS containing forskolin (20  $\mu$ M) alone or in combination with test compounds (at the indicated concentration), while Ivacaftor (1  $\mu$ M) was used as positive control. Cells were then transferred to a microplate reader (Fluostar Optima; BMG Labtech, Offenburg, Germany), equipped with high-quality excitation (HQ500/20X: 500  $\pm$  10 nm) and emission (HQ535/30 M: 535  $\pm$  15 nm) filters for YFP (Chroma Technology, Bellows Falls, VT, USA). During each assay YFP fluorescence was recorded for 14 s, 2 s before and 12 s after injection of 165  $\mu$ L of an iodide-containing solution (PBS with Cl<sup>-</sup> replaced by I<sup>-</sup>; final I<sup>-</sup> concentration 100 mM). Data were normalized to the initial background-subtracted fluorescence. The I<sup>-</sup> influx rate was calculated by fitting the final 11 s of the data for each well with an exponential function to extrapolate the initial slope (dF/dt). The I<sup>-</sup> influx rate was used to estimate CFTR activity under the different experimental conditions.

### Cytotoxicity evaluation

MTT assay was carried out on a panel of neoplastic and normal cell lines. In particular, SKOV3 (ovarian adenocarcinoma, ATCC, Manassas, VA), MCF7 (breast adenocarcinoma, Biologic Bank and Cell Factory, IRCCS Policlinico San Martino, Genoa, Italy), HepG2 (hepatocellular carcinoma, ATCC, Manassas, VA), SKMel28 (skin melanoma, Biologic Bank and Cell Factory, IRCCS Policlinico San Martino, Genoa, Italy), HeLa (cervical adenocarcinoma, Biologic Bank and Cell Factory, IRCCS Policlinico San Martino, Genoa, Italy), SK-BR3 (breast adenocarcinoma, Biologic Bank and Cell Factory, IRCCS Policlinico San Martino, Genoa, Italy) and GM6114 (human embryonic fibroblasts, IRCCS Policlinico San Martino, Genoa, Italy) cell lines were cultured in DMEM (10% FBS, 2 mM Glutamine and 1% penstrep) and incubated in a humidified compartment at 37 °C with 5% CO<sub>2</sub>. Tested compounds were dissolved in DMSO to have a 10 mM stock solution. Then, once diluted with growth medium, they were added to the cultured cells to a final working concentration of 10  $\mu$ M and incubated for 48 hours. At the end of the incubation, 30  $\mu$ L of a 2 mg/mL MTT (3-(4,5-dimethyl-2-thiazolyl)-2,5-diphenyl-2H-tetrazolium bromide) PBS solution were added in each well and incubated 4 hours. Finally, the supernatant was removed and 100  $\mu$ L/well of DMSO were added to dissolve the Formazan precipitate. After 20 min, the results were read at 570 nm. Results are expressed as percentage of the control samples (considered 100% of cell growth, where cells have been treated with the same amount of DMSO but without any compound). The assay was repeated three times and a single compound was tested six times. Means and standard deviations were calculated. All cell culture reagents were acquired from EuroClone, Milan, Italy.

### Acknowledgements

This research was funded by Università degli Studi di Genova, grant Fondi di Ricerca di Ateneo (FRA) and by Fondazione Ricerca Italiana Fibrosi Cistica FFC#9/2021 to E.M. and E.C. The

authors acknowledge Dr. Silvia Sillano and Dr. Douae Meziane for helpful discussions and support.

### Conflict of Interests

The authors declare no conflict of interest.

### Data Availability Statement

The data that support the findings of this study are available from the corresponding author upon reasonable request.

**Keywords:** Acylthioureas · Cystic fibrosis · CFTR modulator · cytotoxic activity · tumor cell lines

- [1] P. R. Burgel, G. Bellis, H. V. Olesen, L. Viviani, A. Zolin, F. Blasi, J. S. Elborn, *Eur. Respir. J.* **2015**, *46*, 133.
- [2] S. Manti, G. F. Parisi, M. Papale, G. L. Marseglia, A. Licari, S. Leonardi, *Pediatr. Allergy Immunol.* **2022**, *33*, 15.
- [3] J. P. Neglia, S. C. Fitzsimmons, P. Maisonneuve, M. H. Schöni, F. Schöni-Affolter, M. Corey, A. B. Lowenfels, *N. Engl. J. Med.* **1995**, *332*, 494.
- [4] P. Maisonneuve, B. C. Marshall, E. A. Knapp, A. B. Lowenfels, *J. Natl. Cancer Inst.* **2013**, *105*, 122.
- [5] S. C. Bell, M. A. Mall, H. Gutierrez, M. Macek, S. Madge, J. C. Davies, P. R. Burgel, E. Tullis, C. Castañes, C. Castellani, C. A. Byrnes, F. Cathcart, S. H. Chotirmall, R. Cosgriff, I. Eichler, I. Fajac, C. H. Goss, P. Drevinek, P. M. Farrell, A. M. Gravelle, T. Havermans, N. Mayer-Hamblett, N. Kashirskaya, E. Kerem, J. L. Mathew, E. F. McKone, L. Naehrlich, S. Z. Nasr, G. R. Oates, C. O'Neill, U. Pypops, K. S. Raraigh, S. M. Rowe, K. W. Southern, S. Sivam, A. L. Stephenson, M. Zampoli, F. Ratjen, *Lancet Respir. Med.* **2020**, *8*, 65.
- [6] J. S. Elborn, *Lancet* **2016**, *388*, 2519.
- [7] The Clinical and Functional Translation of CFTR (CFTR2). <https://www.cftr2.org/>.
- [8] K. De Boeck, *Acta Paediatr.* **2020**, *109*, 893.
- [9] M. Shteinberg, I. J. Haq, D. Polineni, J. C. Davies, *Lancet* **2021**, *397*, 2195.
- [10] C. M. Farinha, I. Callebaut, *Biosci. Rep.* **2022**, *42*, BSR20212006.
- [11] G. F. Parisi, S. Cutello, G. Di Dio, N. Rotolo, M. La Rosa, S. Leonardi, *BMC Res. Notes* **2013**, *6*, 461.
- [12] K. A. Despotos, S. H. Donaldson, *Curr. Opin. Pharmacol.* **2022**, *65*, 102239.
- [13] J. P. Clancy, C. U. Cotton, S. H. Donaldson, G. M. Solomon, D. R. VanDevanter, M. P. Boyle, M. D. Gentzsch, J. A. Nick, B. Illek, J. C. Wallenburg, E. J. Sorscher, M. D. Amaral, J. M. Beekman, A. P. Naren, R. J. Bridges, P. J. Thomas, G. Cutting, S. Rowe, A. G. Durmowicz, M. Mense, K. D. Boeck, W. Skach, C. Penland, E. Joseloff, H. Bihler, J. Mahoney, D. Borowitz, K. L. Tuggle, *J. Cystic Fibrosis* **2019**, *18*, 22.
- [14] B. W. Ramsey, J. Davies, N. G. McElvaney, E. Tullis, S. C. Bell, P. Drevinek, M. Griese, E. F. McKone, C. E. Wainwright, M. W. Konstan, R. Moss, F. Ratjen, I. Sermet-Gaudelus, S. M. Rowe, Q. Dong, S. Rodriguez, K. Yen, C. Ordoñez, J. S. Elborn, *N. Engl. J. Med.* **2011**, *365*, 1663.
- [15] F. Van Goor, S. Hadida, P. D. J. Grootenhuis, B. Burton, D. Cao, T. Neuberger, A. Turnbull, A. Singh, J. Joubran, A. Hazlewood, J. Zhou, J. McCartney, V. Arumugam, C. Decker, J. Yang, C. Young, E. R. Olson, J. J. Wine, R. A. Frizzell, M. Ashlock, P. Negulescu, *Proc. Natl. Acad. Sci. USA* **2009**, *106*, 18825.
- [16] D. M. Goetz, A. P. Savant, *Pediatr. Pulmonol.* **2021**, *56*, 3595.
- [17] A. G. Durmowicz, R. Lim, H. Rogers, C. J. Rosebraugh, B. A. Chowdhury, *Annals Am. Thorac Soc.* **2018**, *15*, 1.
- [18] A. Maalik, H. Rahim, M. Saleem, N. Fatima, A. Rauf, A. Wadood, M. I. Malik, A. Ahmed, H. Rafique, M. N. Zafar, M. Riaz, L. Rasheed, A. Mumtaz, *Bioorg. Chem.* **2019**, *88*, 102946.
- [19] U. Zahra, A. Saeed, T. Abdul Fattah, U. Flörke, M. F. Erben, *RSC Adv.* **2022**, *12*, 12710.
- [20] M. Khan, J. Patujo, I. Mushtaq, A. Ishtiaq, M. N. Tahir, S. Bibi, M. S. Khan, N. Ullah, G. Mustafa, B. Mirza, A. Badshah, I. Murtaza, *J. Mol. Struct.* **2022**, *1253*, 132207.
- [21] W. Bai, J. Ji, Q. Huang, W. Wei, *Tetrahedron Lett.* **2020**, *61*, 152366.

- [22] P. W. Phuan, B. Yang, J. M. Knapp, A. B. Wood, G. L. Lukacs, M. J. Kurth, A. S. Verkman, *Mol. Pharmacol.* **2011**, *80*, 683–693.
- [23] H. Valkenier, L. W. Judd, H. Li, S. Hussain, D. N. Sheppard, A. P. Davis, *J. Am. Chem. Soc.* **2014**, *136*, 12507.
- [24] A. Scarsi, M. Ponassi, C. Brullo, C. Rosano, A. Spallarossa, *Mol. Diversity* **2022**.
- [25] N. P. Peet, J. Malecha, M. E. Letourneau, S. Sunder, *J. Heterocycl. Chem.* **1989**, *26*, 257.
- [26] S. Cesarini, A. Spallarossa, A. Ranise, S. Schenone, C. Rosano, P. La Colla, G. Sanna, B. Busonera, R. Loddo, *Eur. J. Med. Chem.* **2009**, *44*, 1106.
- [27] V. Kumar, S. Chimni, *Anti-Cancer Agents Med. Chem.* **2015**, *15*, 163.
- [28] A. Daina, O. Michielin, V. Zoete, *Sci. Rep.* **2017**, *7*, 42717.
- [29] R. Brenk, A. Schipani, D. James, A. Krasowski, I. H. Gilbert, J. Frearson, P. G. Wyatt, *ChemMedChem* **2008**, *3*, 435.
- [30] S. J. Teague, A. M. Davis, P. D. Leeson, T. Oprea, *Angew. Chem. Int. Ed. Engl.* **1999**, *38*, 3743.
- [31] R. Leardi, C. Melzi, G. Polotti, CAT (Chemometric Agile Tool) <http://gruppochemiometria.it/index.php/software>.

---

Manuscript received: July 26, 2023

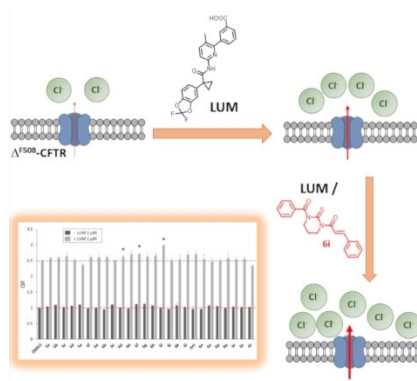
Revised manuscript received: November 30, 2023

Accepted manuscript online: December 17, 2023

Version of record online: ■ ■ ■

## RESEARCH ARTICLE

A series of mono- and di-acylthioureas was synthesised and tested as CFTR modulators. Despite the lack of any intrinsic potentiating effect, selected compounds enhanced the rescue activity of Lumacaftor, as observed in phenotypic assays. The lack of cytotoxic effects and the promising pharmacokinetic properties support the pharmacological relevance of this class of compounds as novel hits for cystic fibrosis treatment.



Prof. A. Spallarossa\*, Dr. N. Pedemonte, Dr. E. Pesce, Prof. E. Millo, Prof. E. Cichero, Dr. C. Rosano, Dr. M. Lusardi, Dr. E. Iervasi, Dr. M. Ponassi

1 – 11

**Cyclic diacyl thioureas enhance activity of corrector Lumacaftor on F508del-CFTR**



# ChemMedChem

Supporting Information

## **Cyclic diacyl thioureas enhance activity of corrector Lumacaftor on F508del-CFTR**

Andrea Spallarossa,\* Nicoletta Pedemonte, Emanuela Pesce, Enrico Millo, Elena Cichero, Camillo Rosano, Matteo Lusardi, Erika Iervasi, and Marco Ponassi

## **Cyclic diacyl thioureas enhance activity of corrector Lumacaftor on F508del-CFTR**

Andrea Spallarossa,<sup>\*[a]</sup> Nicoletta Pedemonte,<sup>[b]</sup> Emanuela Pesce,<sup>[b]</sup> Enrico Millo,<sup>[c]</sup> Elena Cichero,<sup>[a]</sup> Camillo Rosano,<sup>[d]</sup> Matteo Lusardi,<sup>[a]</sup> Erika Iervasi,<sup>[d]</sup> and Marco Ponassi<sup>[d]</sup>

- [a] Department of Pharmacy, University of Genova, Viale Benedetto XV 3, 16132 Genova, Italy
- [b] IRCCS Istituto Giannina Gaslini, UOC Genetica Medica, Via Gerolamo Gaslini, 5, 16147 Genova, Italy
- [c] Department of Experimental Medicine, Section of Biochemistry, University of Genoa, Viale Benedetto XV 1, 16132, Genova, Italy
- [d] IRCCS Ospedale Policlinico San Martino, Proteomics and Mass Spectrometry Unit, Largo R. Benzi, 10, 16132 Genova, Italy

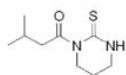
\*Correspondence: [andrea.spallarossa@unige.it](mailto:andrea.spallarossa@unige.it)

## Table of contents

- Figure S1.**  $^1\text{H}$  NMR (200 MHz,  $\text{CDCl}_3$ ) of compound **5a**  
**Figure S2.**  $^{13}\text{C}$  NMR (50 MHz,  $\text{CDCl}_3$ ) of compound **5a**  
**Figure S3.**  $^1\text{H}$  NMR (200 MHz,  $\text{CDCl}_3$ ) of compound **5b**  
**Figure S4.**  $^{13}\text{C}$  NMR (50 MHz,  $\text{CDCl}_3$ ) of compound **5b**  
**Figure S5.** IR (KBr) of compound **5c**  
**Figure S6.**  $^1\text{H}$  NMR (200 MHz,  $\text{CDCl}_3$ ) of compound **5c**  
**Figure S7.**  $^{13}\text{C}$  NMR (50 MHz,  $\text{CDCl}_3$ ) of compound **5c**  
**Figure S8.**  $^1\text{H}$  NMR (400 MHz,  $\text{CDCl}_3$ ) of compound **5d**  
**Figure S9.**  $^{13}\text{C}$  NMR (101 MHz,  $\text{CDCl}_3$ ) of compound **5d**  
**Figure S10.**  $^1\text{H}$  NMR (400 MHz,  $\text{CDCl}_3$ ) of compound **5e**  
**Figure S11.**  $^{13}\text{C}$  NMR (101 MHz,  $\text{CDCl}_3$ ) of compound **5e**  
**Figure S12.**  $^1\text{H}$  NMR (200 MHz,  $\text{CDCl}_3$ ) of compound **5f**  
**Figure S13.**  $^{13}\text{C}$  NMR (50 MHz,  $\text{CDCl}_3$ ) of compound **5f**  
**Figure S14.** IR (KBr) of compound **6a**  
**Figure S15.**  $^1\text{H}$  NMR (200 MHz,  $\text{CDCl}_3$ ) of compound **6a**  
**Figure S16.**  $^{13}\text{C}$  NMR (50 MHz,  $\text{CDCl}_3$ ) of compound **6a**  
**Figure S17.** IR (KBr) of compound **6b**  
**Figure S18.**  $^1\text{H}$  NMR (200 MHz,  $\text{CDCl}_3$ ) of compound **6b**  
**Figure S19.**  $^{13}\text{C}$  NMR (400 MHz,  $\text{CDCl}_3$ ) of compound **6b**  
**Figure S20.**  $^1\text{H}$  NMR (200 MHz,  $\text{CDCl}_3$ ) of compound **6c**  
**Figure S21.**  $^{13}\text{C}$  NMR (50 MHz,  $\text{CDCl}_3$ ) of compound **6c**  
**Figure S22.**  $^1\text{H}$  NMR (200 MHz,  $\text{CDCl}_3$ ) of compound **6d**  
**Figure S23.**  $^{13}\text{C}$  NMR (50 MHz,  $\text{CDCl}_3$ ) of compound **6d**  
**Figure S24.** IR (KBr) of compound **6e**  
**Figure S25.**  $^1\text{H}$  NMR (200 MHz,  $\text{CDCl}_3$ ) of compound **6e**  
**Figure S26.**  $^{13}\text{C}$  NMR (101 MHz,  $\text{CDCl}_3$ ) of compound **6e**  
**Figure S27.**  $^1\text{H}$  NMR (200 MHz,  $\text{CDCl}_3$ ) of compound **6f**  
**Figure S28.**  $^{13}\text{C}$  NMR (101 MHz,  $\text{CDCl}_3$ ) of compound **6f**  
**Figure S29.**  $^1\text{H}$  NMR (200 MHz,  $\text{CDCl}_3$ ) of compound **6g**  
**Figure S30.**  $^{13}\text{C}$  NMR (50 MHz,  $\text{CDCl}_3$ ) of compound **6g**  
**Figure S31.**  $^1\text{H}$  NMR (200 MHz,  $\text{CDCl}_3$ ) of compound **6h**  
**Figure S32.**  $^{13}\text{C}$  NMR (50 MHz,  $\text{CDCl}_3$ ) of compound **6h**  
**Figure S33.** IR (KBr) of compound **6i**  
**Figure S34.**  $^1\text{H}$  NMR (200 MHz,  $\text{CDCl}_3$ ) of compound **6i**  
**Figure S35.**  $^{13}\text{C}$  NMR (50 MHz,  $\text{CDCl}_3$ ) of compound **6i**  
**Figure S36.** IR (KBr) of compound **6j**  
**Figure S37.**  $^1\text{H}$  NMR (200 MHz,  $\text{CDCl}_3$ ) of compound **6j**  
**Figure S38.**  $^{13}\text{C}$  NMR (101 MHz,  $\text{CDCl}_3$ ) of compound **6j**  
**Figure S39.** IR (KBr) of compound **6k**  
**Figure S40.**  $^1\text{H}$  NMR (200 MHz,  $\text{CDCl}_3$ ) of compound **6k**  
**Figure S41.**  $^{13}\text{C}$  NMR (50 MHz,  $\text{CDCl}_3$ ) of compound **6k**  
**Figure S42.** IR (KBr) of compound **6l**  
**Figure S43.**  $^1\text{H}$  NMR (300 MHz,  $\text{CDCl}_3$ ) of compound **6l**  
**Figure S44.**  $^{13}\text{C}$  NMR (101 MHz,  $\text{CDCl}_3$ ) of compound **6l**  
**Figure S45.** IR (KBr) of compound **6m**  
**Figure S46.**  $^1\text{H}$  NMR (200 MHz,  $\text{CDCl}_3$ ) of compound **6m**  
**Figure S47.**  $^{13}\text{C}$  NMR (50 MHz,  $\text{CDCl}_3$ ) of compound **6m**  
**Figure S48.** IR (KBr) of compound **6n**  
**Figure S49.**  $^1\text{H}$  NMR (200 MHz,  $\text{CDCl}_3$ ) of compound **6n**

**Figure S50.**  $^{13}\text{C}$  NMR (101 MHz,  $\text{CDCl}_3$ ) of compound **6n**  
**Figure S51.**  $^1\text{H}$  NMR (200 MHz,  $\text{CDCl}_3$ ) of compound **6o**  
**Figure S52.**  $^{13}\text{C}$  NMR (101 MHz,  $\text{CDCl}_3$ ) of compound **6o**  
**Figure S53.**  $^1\text{H}$  NMR (200 MHz,  $\text{CDCl}_3$ ) of compound **6p**  
**Figure S54.**  $^{13}\text{C}$  NMR (101 MHz,  $\text{CDCl}_3$ ) of compound **6p**  
**Figure S55.**  $^1\text{H}$  NMR (200 MHz,  $\text{CDCl}_3$ ) of compound **6q**  
**Figure S56.**  $^{13}\text{C}$  NMR (101 MHz,  $\text{CDCl}_3$ ) of compound **6q**  
**Figure S57.**  $^1\text{H}$  NMR (200 MHz,  $\text{CDCl}_3$ ) of compound **6r**  
**Figure S58.**  $^{13}\text{C}$  NMR (101 MHz,  $\text{CDCl}_3$ ) of compound **6r**  
**Figure S59.**  $^1\text{H}$  NMR (200 MHz,  $\text{CDCl}_3$ ) of compound **6s**  
**Figure S60.**  $^{13}\text{C}$  NMR (50 MHz,  $\text{CDCl}_3$ ) of compound **6s**  
**Figure S61.**  $^1\text{H}$  NMR (200 MHz,  $\text{CDCl}_3$ ) of compound **6t**  
**Figure S62.**  $^{13}\text{C}$  NMR (50 MHz,  $\text{CDCl}_3$ ) of compound **6t**  
**Table S1.** ADME prediction for compounds **5**.  
**Table S2.** ADME prediction for compounds **6**.  
**Table S3.** Variables used for PCA analysis.

Pulse Sequence: s2pul  
Solvent: CDCl3  
Ambient temperature  
GEMINI-200 "gem2000"



Pulse 30.0 degrees  
Acq. time 2.000 sec  
Width 4000.0 Hz  
112 repetitions  
OBSERVE H1, 199.9417676 MHz  
DATA PROCESSING  
F1 size 65536  
Total time 4 min, 29 sec

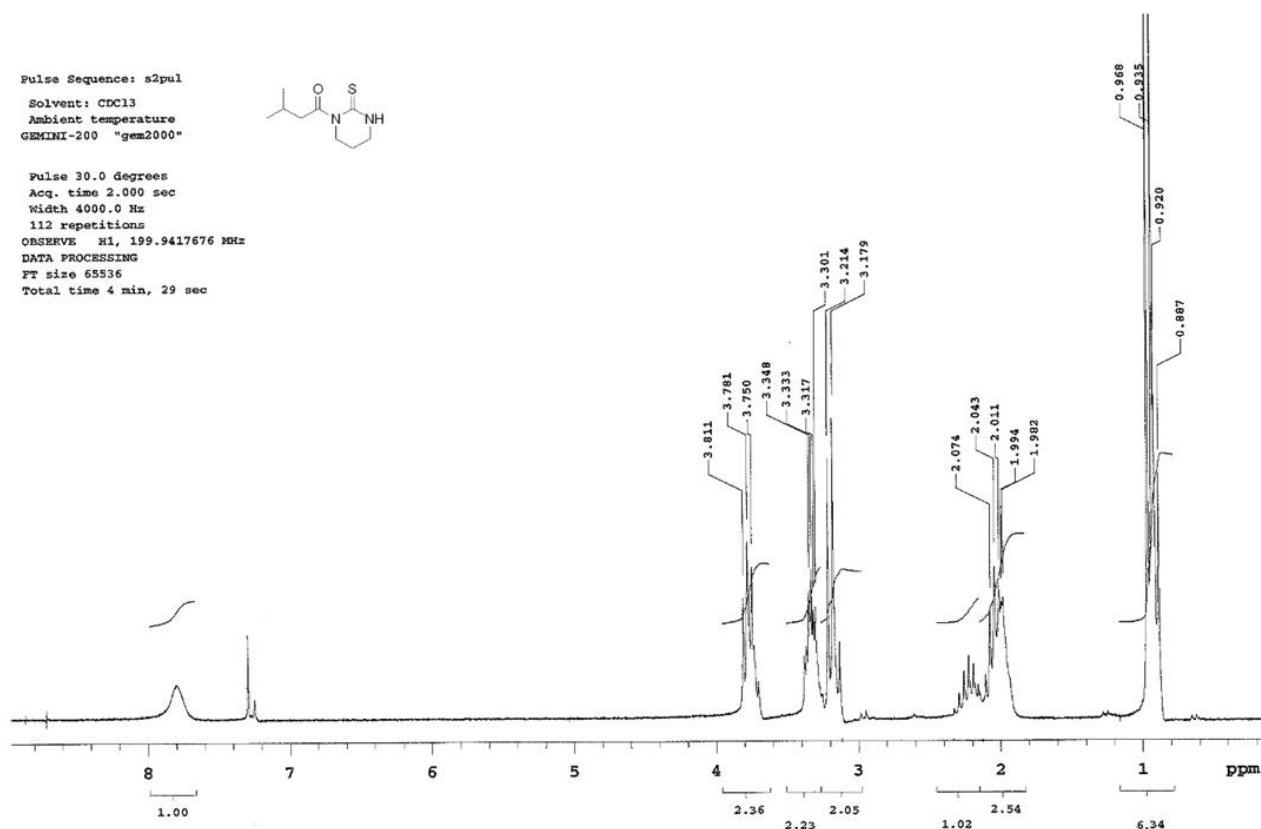


Figure S1. <sup>1</sup>H NMR (200 MHz, CDCl<sub>3</sub>) of compound 5a

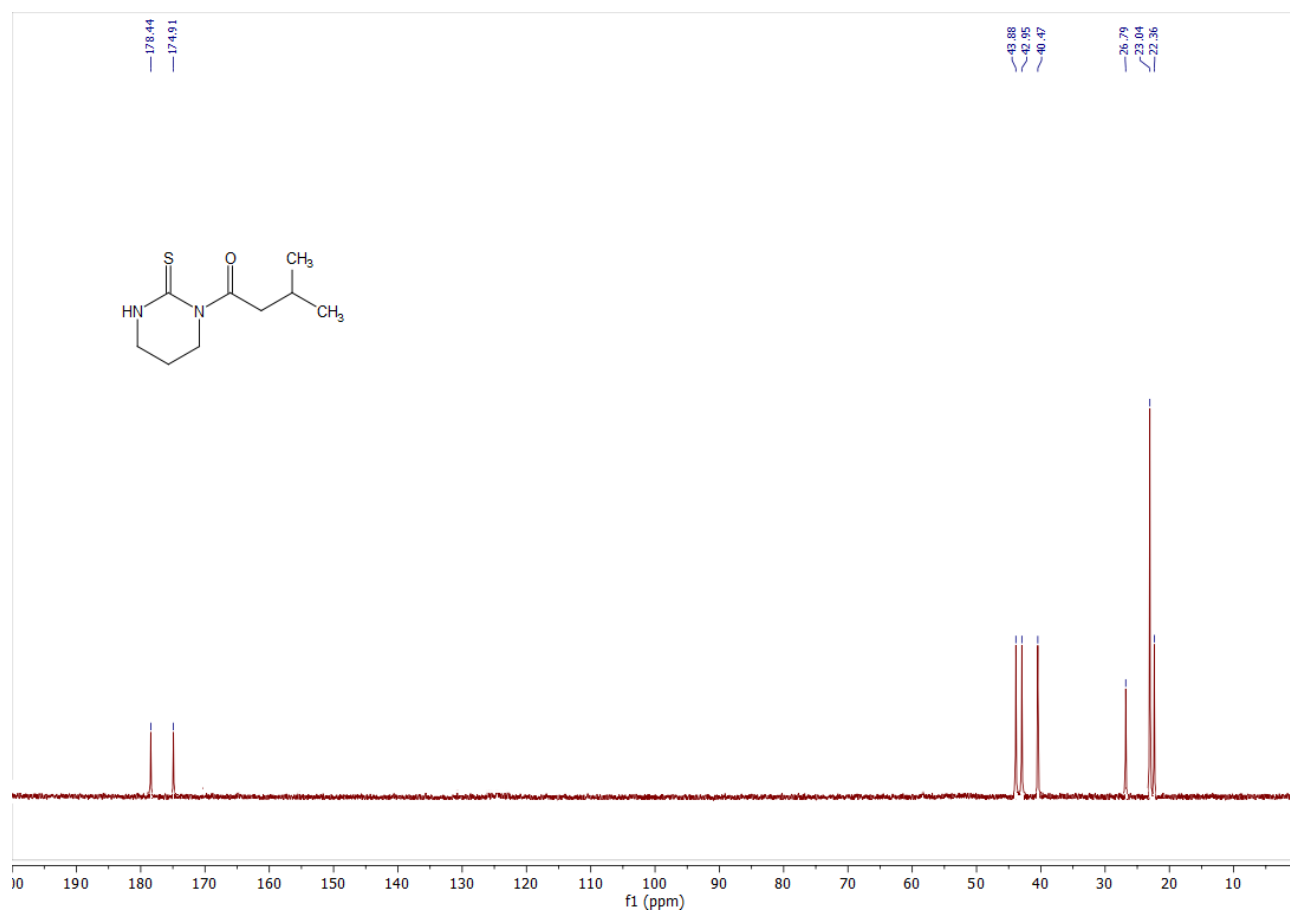
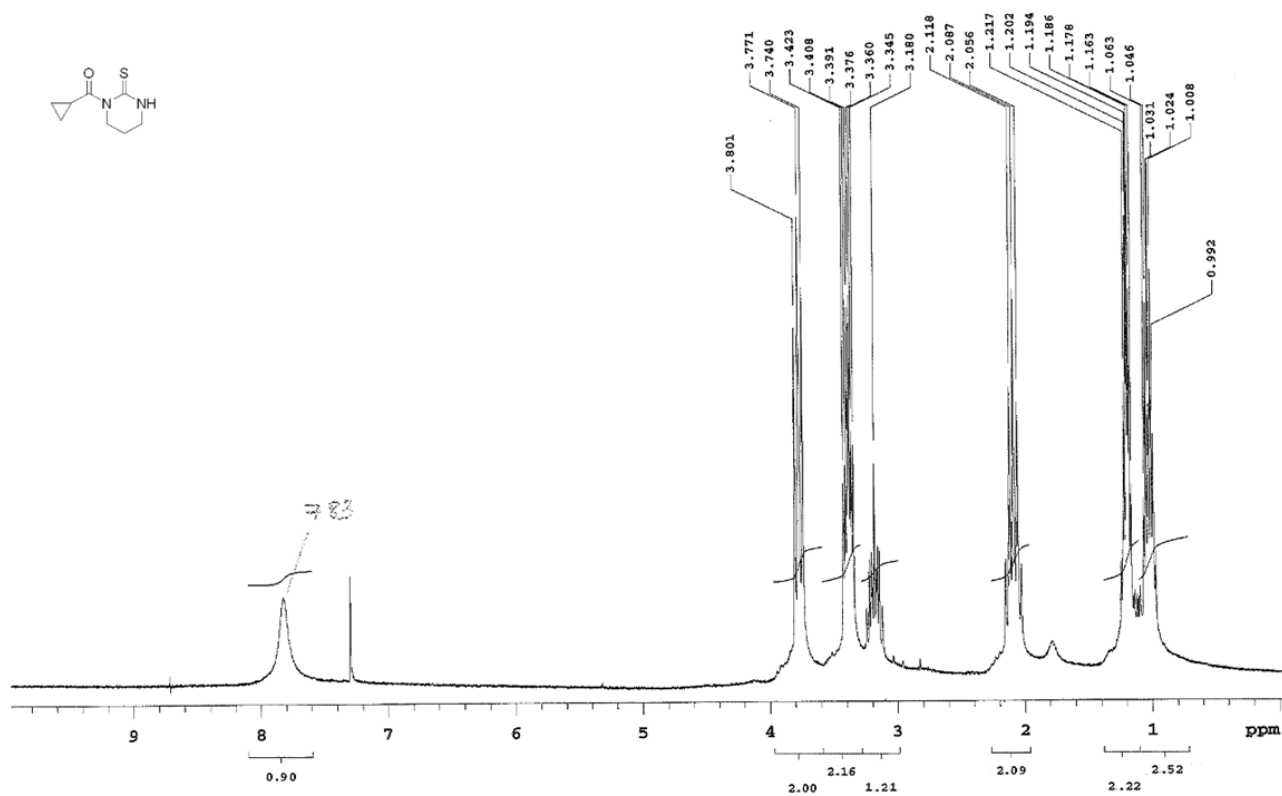
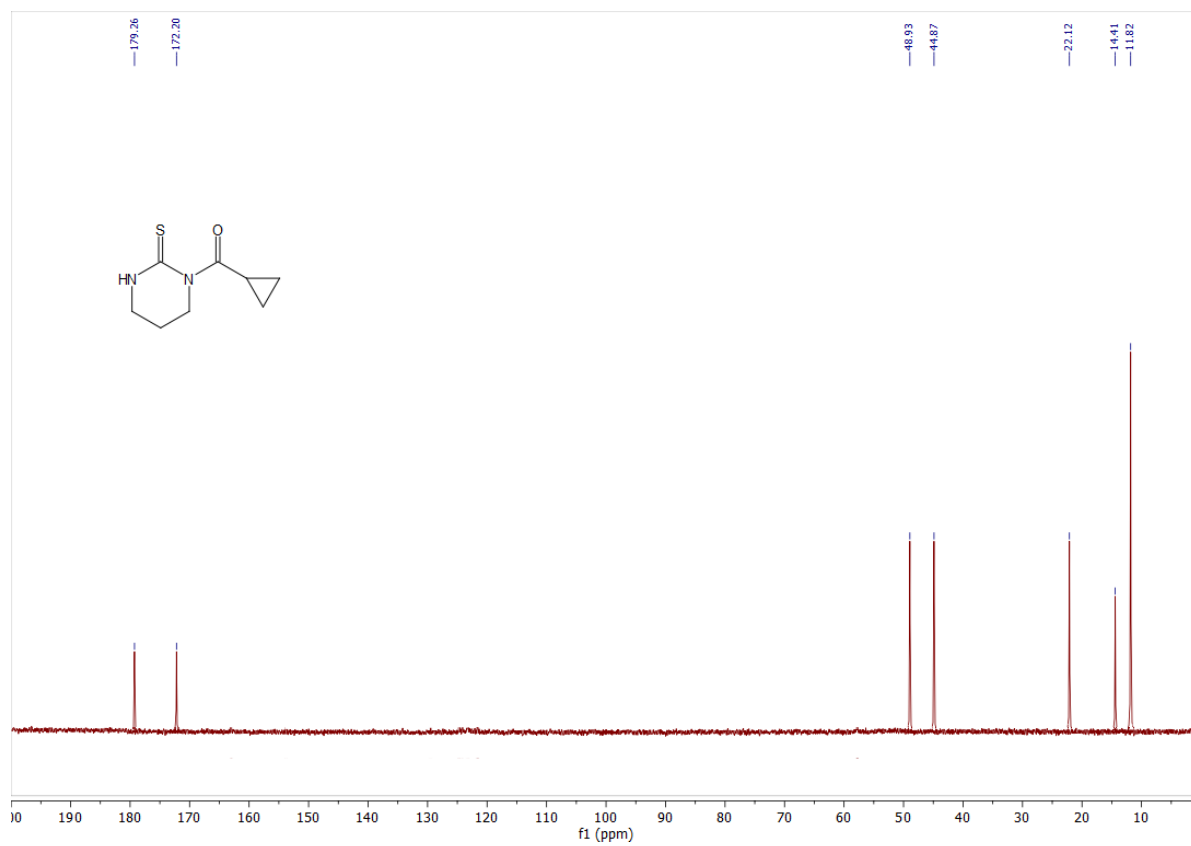


Figure S2. <sup>13</sup>C NMR (50 MHz, CDCl<sub>3</sub>) of compound 5a





**Figure S3.** <sup>1</sup>H NMR (200 MHz, CDCl<sub>3</sub>) of compound **5b**



**Figure S4.** <sup>13</sup>C NMR (50 MHz, CDCl<sub>3</sub>) of compound **5b**

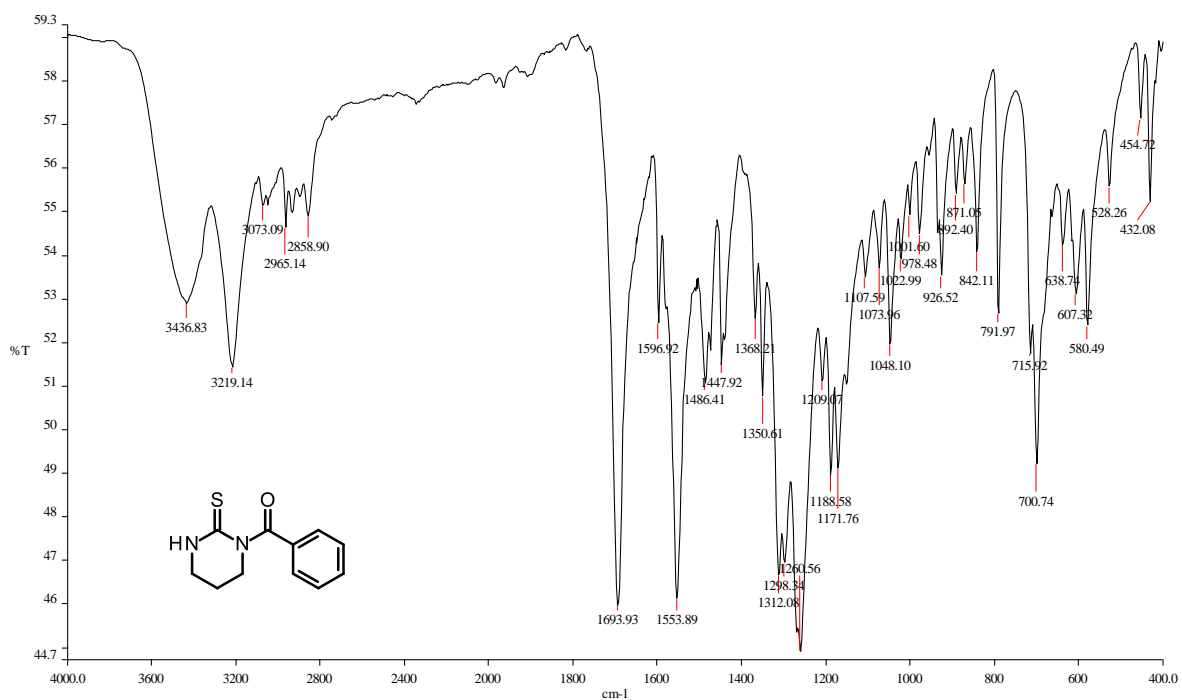


Figure S5. IR (KBr) of compound 5c

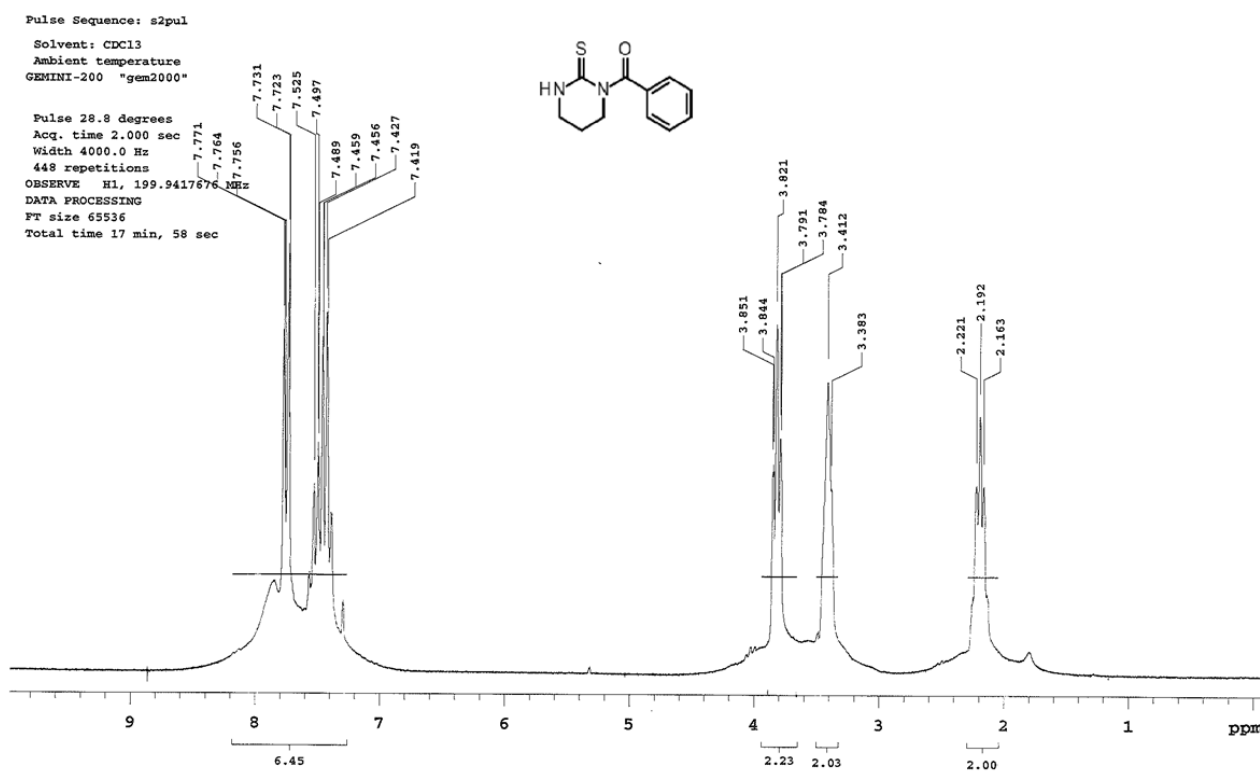
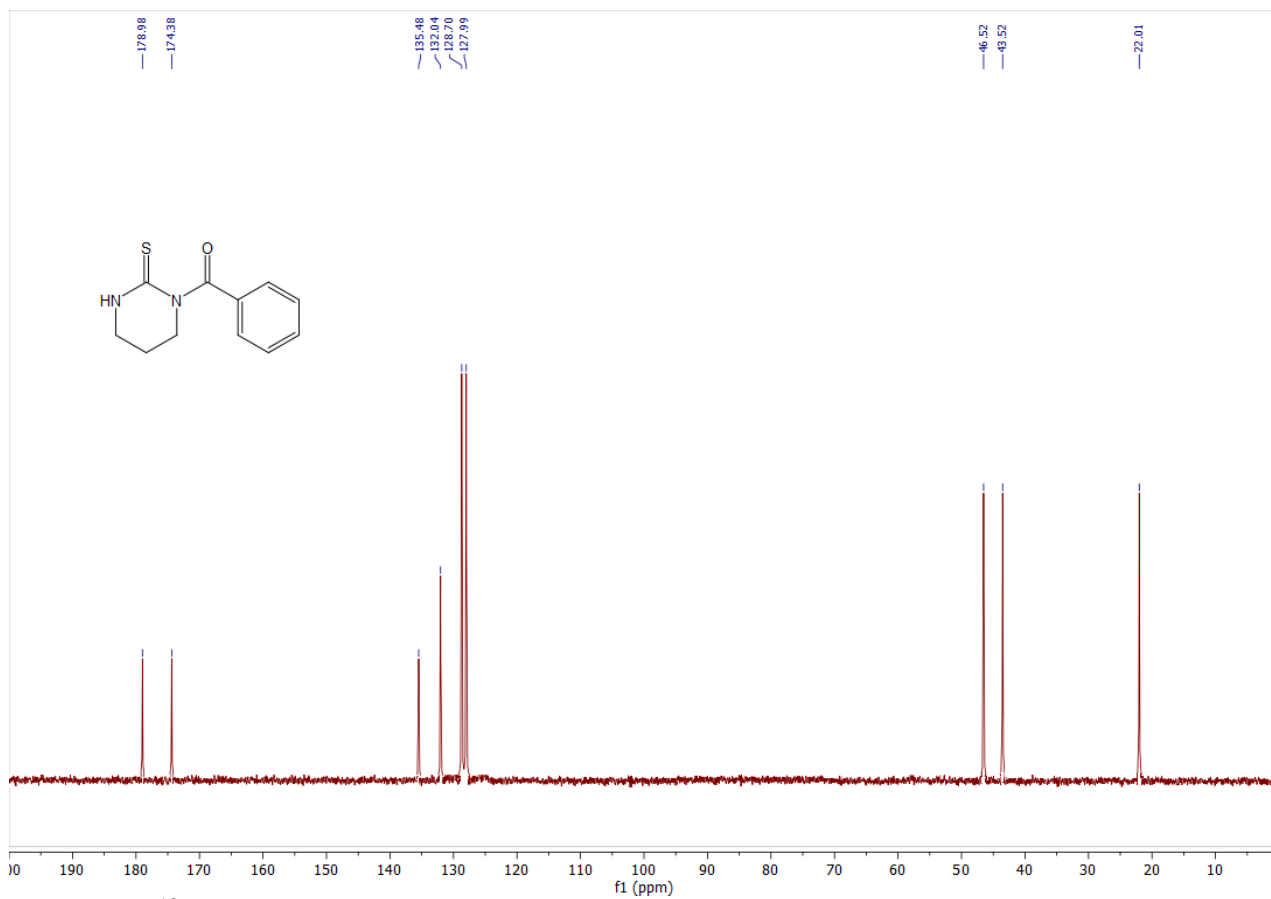
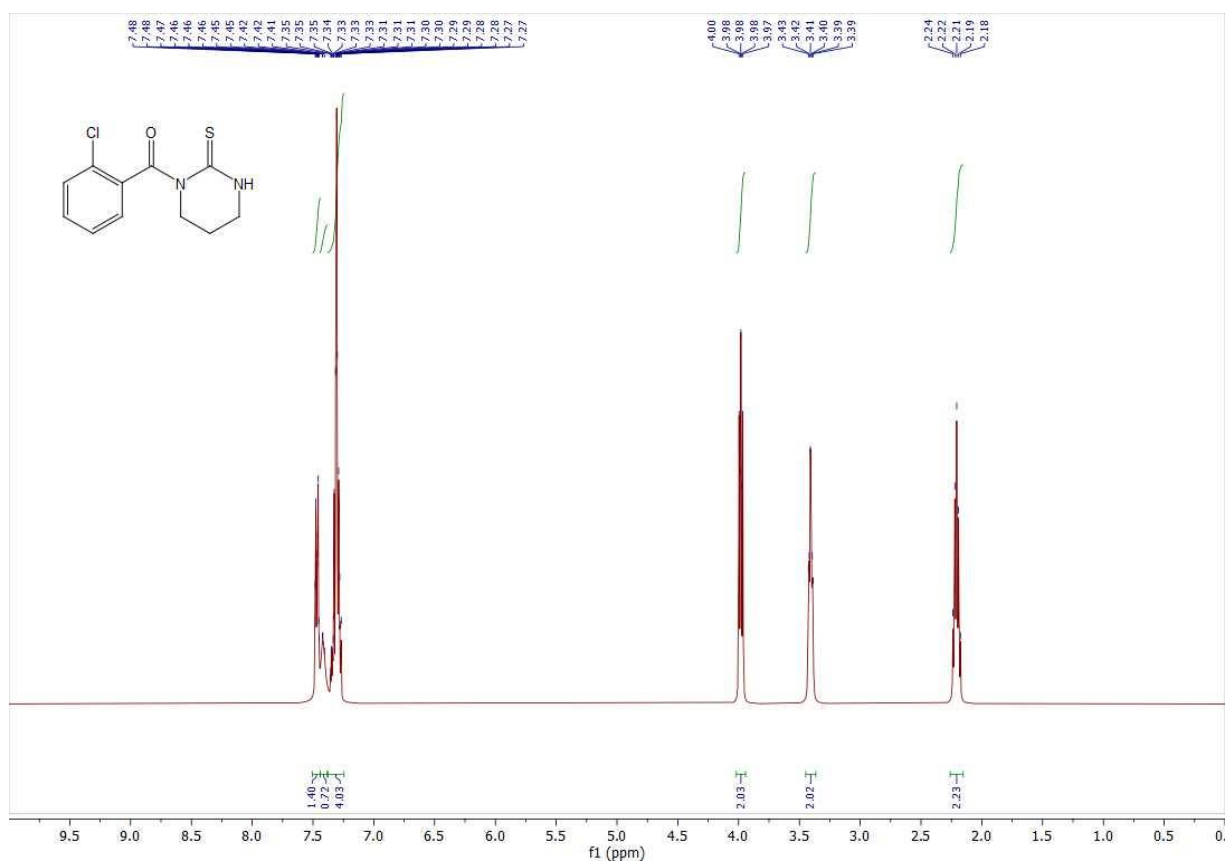


Figure S6. <sup>1</sup>H NMR (200 MHz, CDCl<sub>3</sub>) of compound 5c



**Figure S7.**  $^{13}\text{C}$  NMR (50 MHz,  $\text{CDCl}_3$ ) of compound **5c**



**Figure S8.**  $^1\text{H}$  NMR (400 MHz,  $\text{CDCl}_3$ ) of compound **5d**

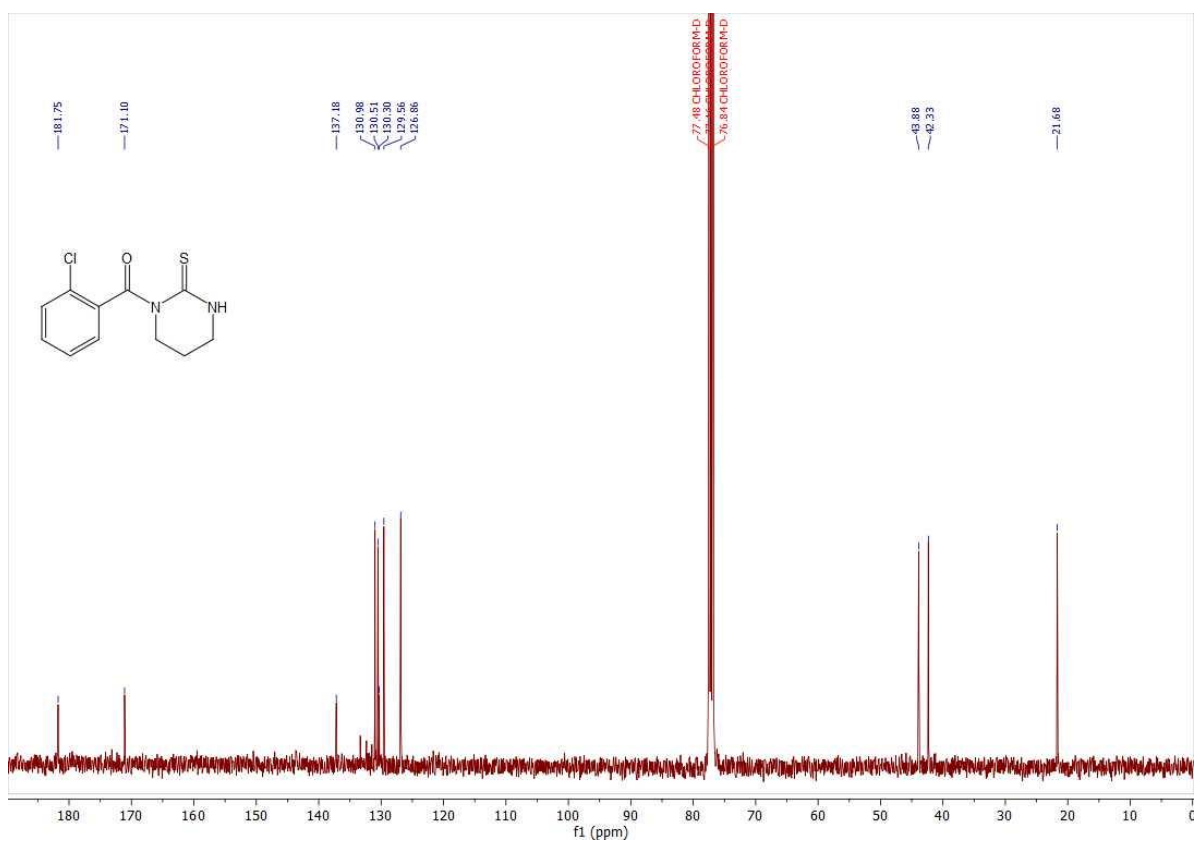


Figure S9.  $^{13}\text{C}$  NMR (101 MHz,  $\text{CDCl}_3$ ) of compound 5d

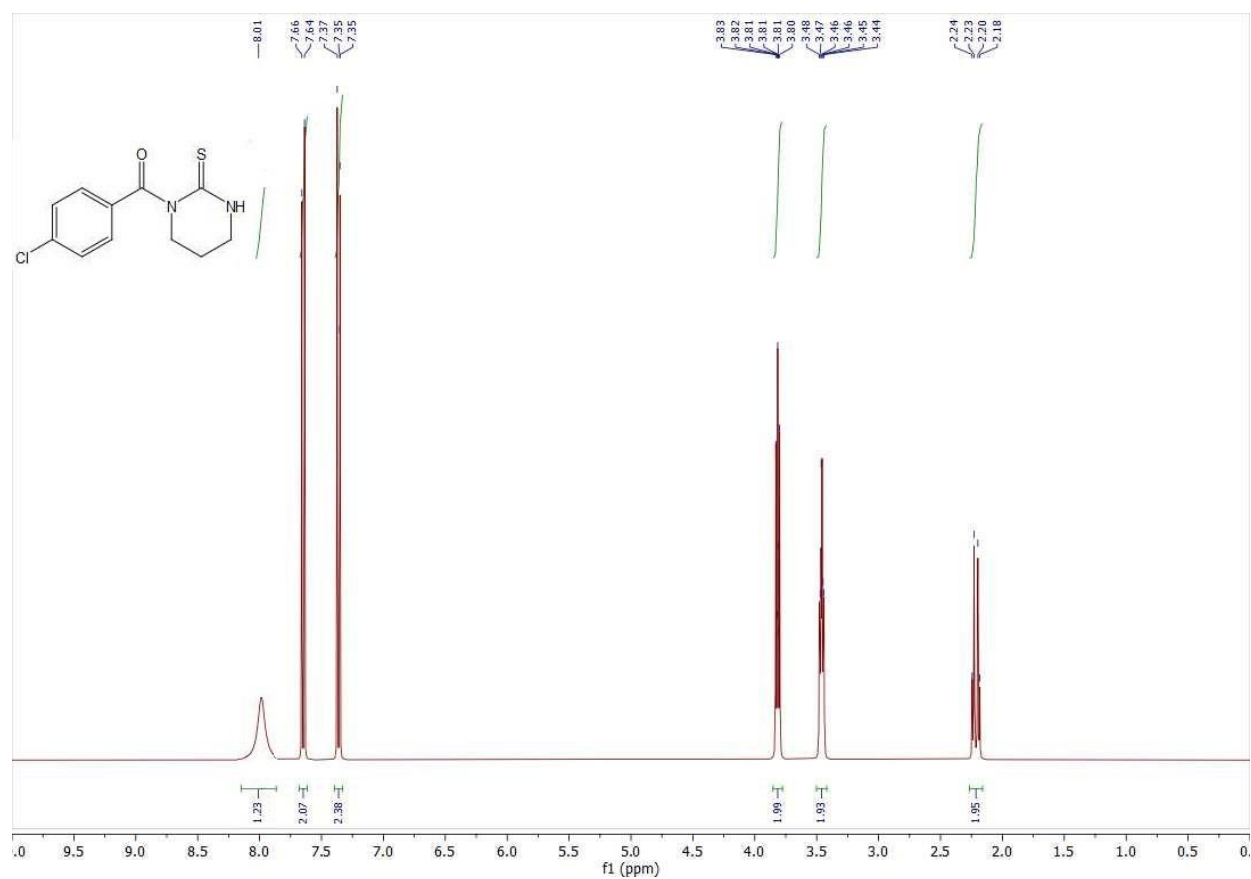


Figure S10.  $^1\text{H}$  NMR (400 MHz,  $\text{CDCl}_3$ ) of compound 5e

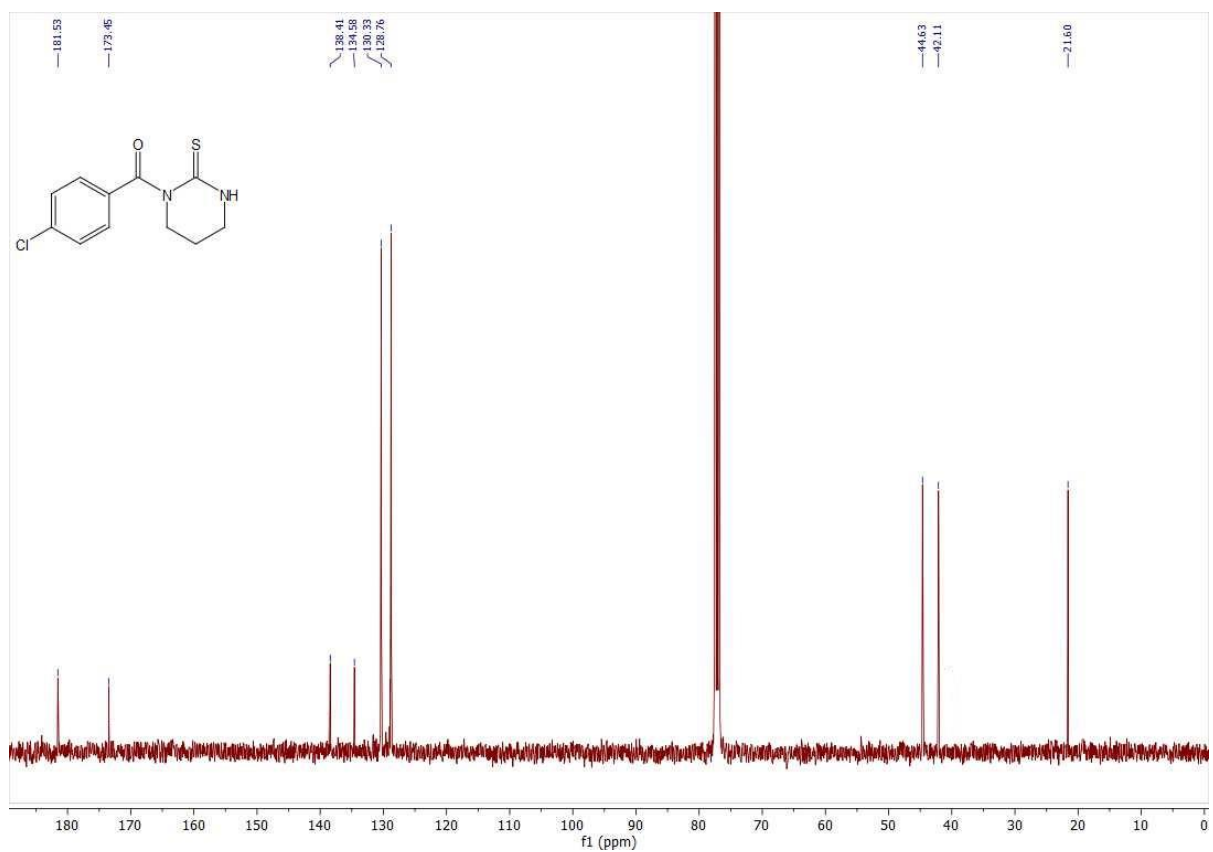


Figure S11. <sup>13</sup>C NMR (101 MHz, CDCl<sub>3</sub>) of compound 5e

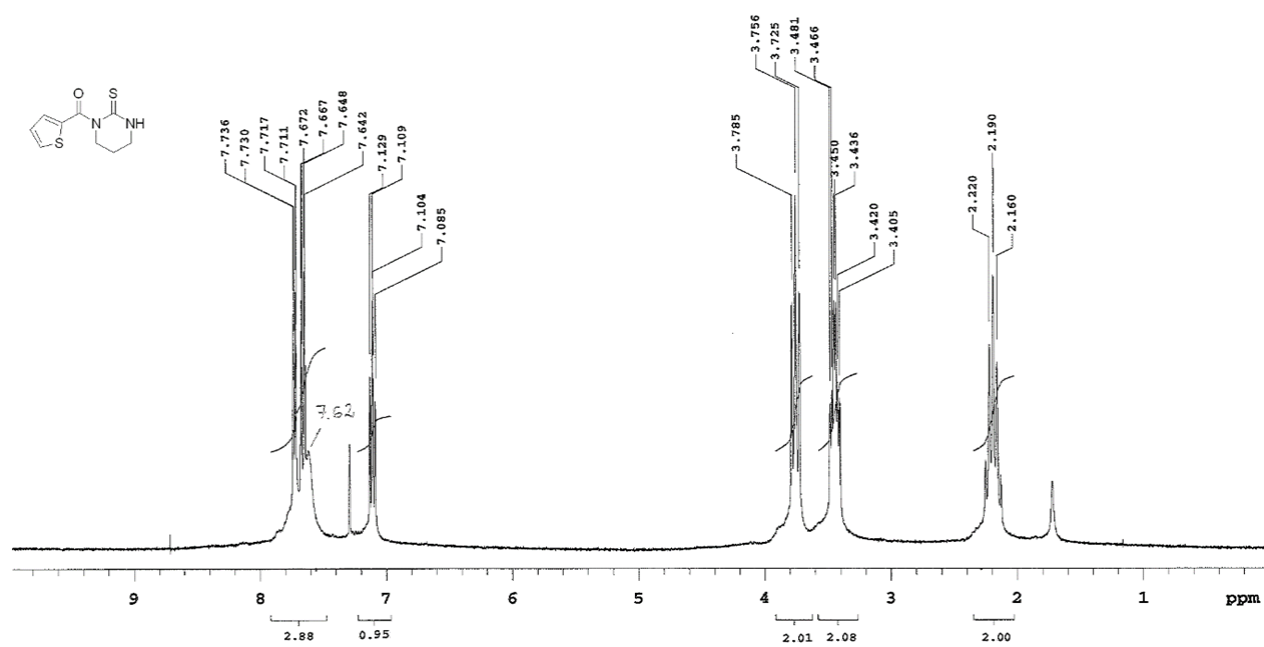
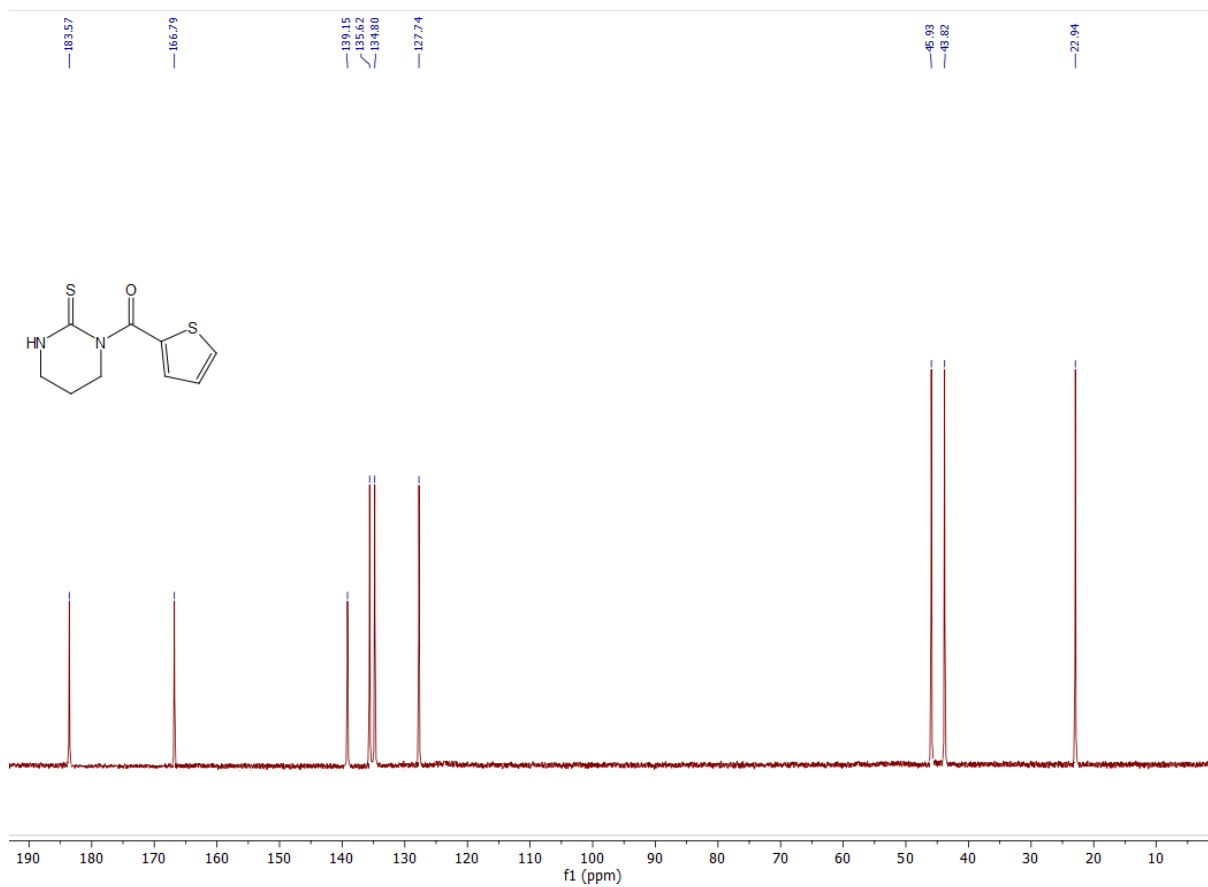
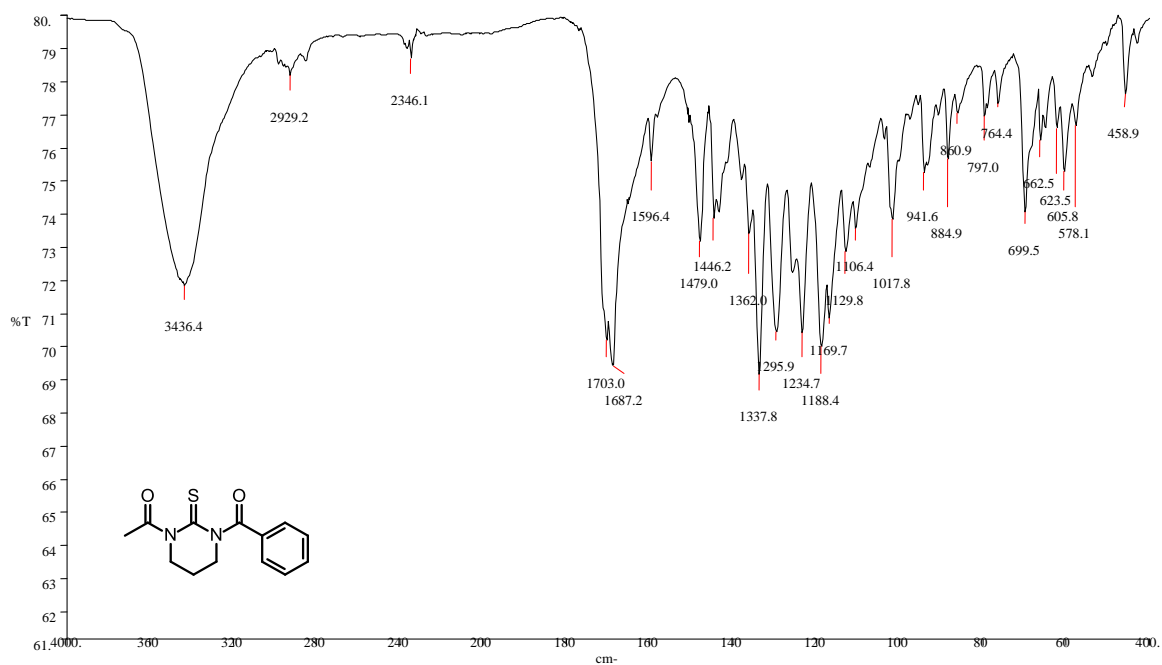


Figure S12. <sup>1</sup>H NMR (200 MHz, CDCl<sub>3</sub>) of compound 5f



**Figure S13.**  $^{13}\text{C}$  NMR (50 MHz,  $\text{CDCl}_3$ ) of compound **5f**



**Figure S14.** IR (KBr) of compound **6a**

Pulse Sequence: s2pul  
Solvent: CDCl3  
Ambient temperature  
GEMINI-200 "gem2000"

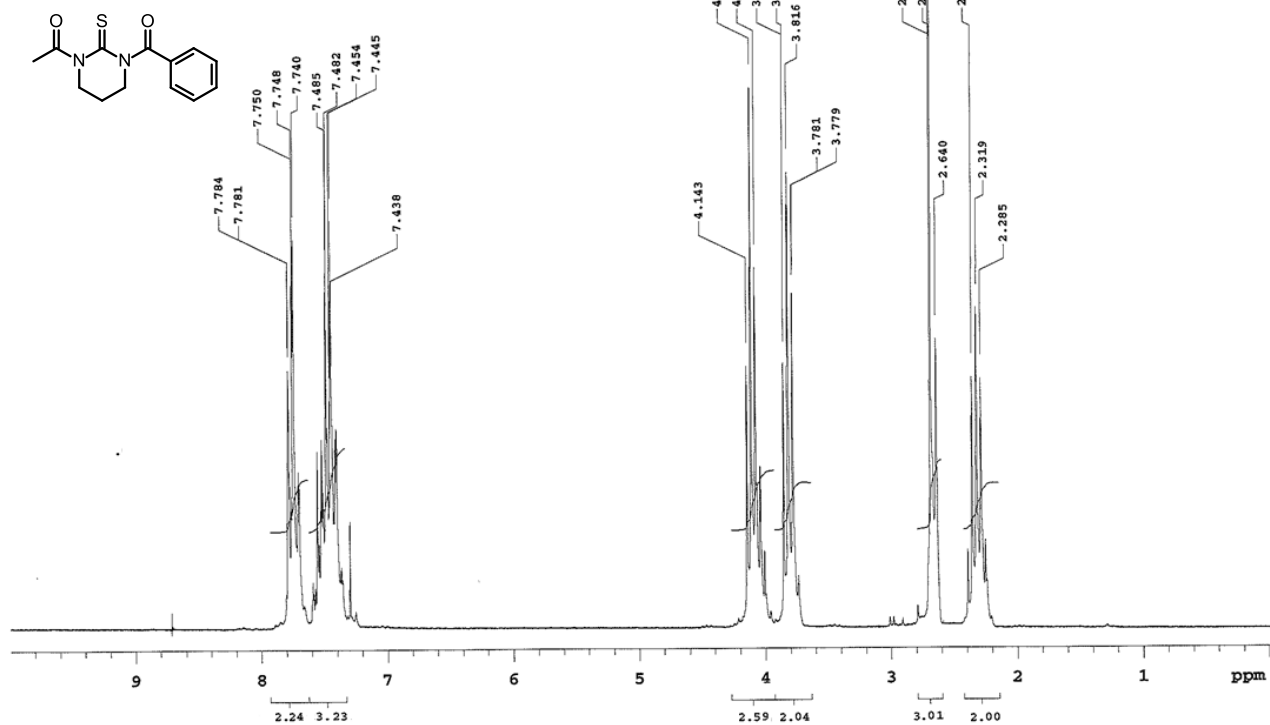


Figure S15. <sup>1</sup>H NMR (200 MHz, CDCl<sub>3</sub>) of compound 6a

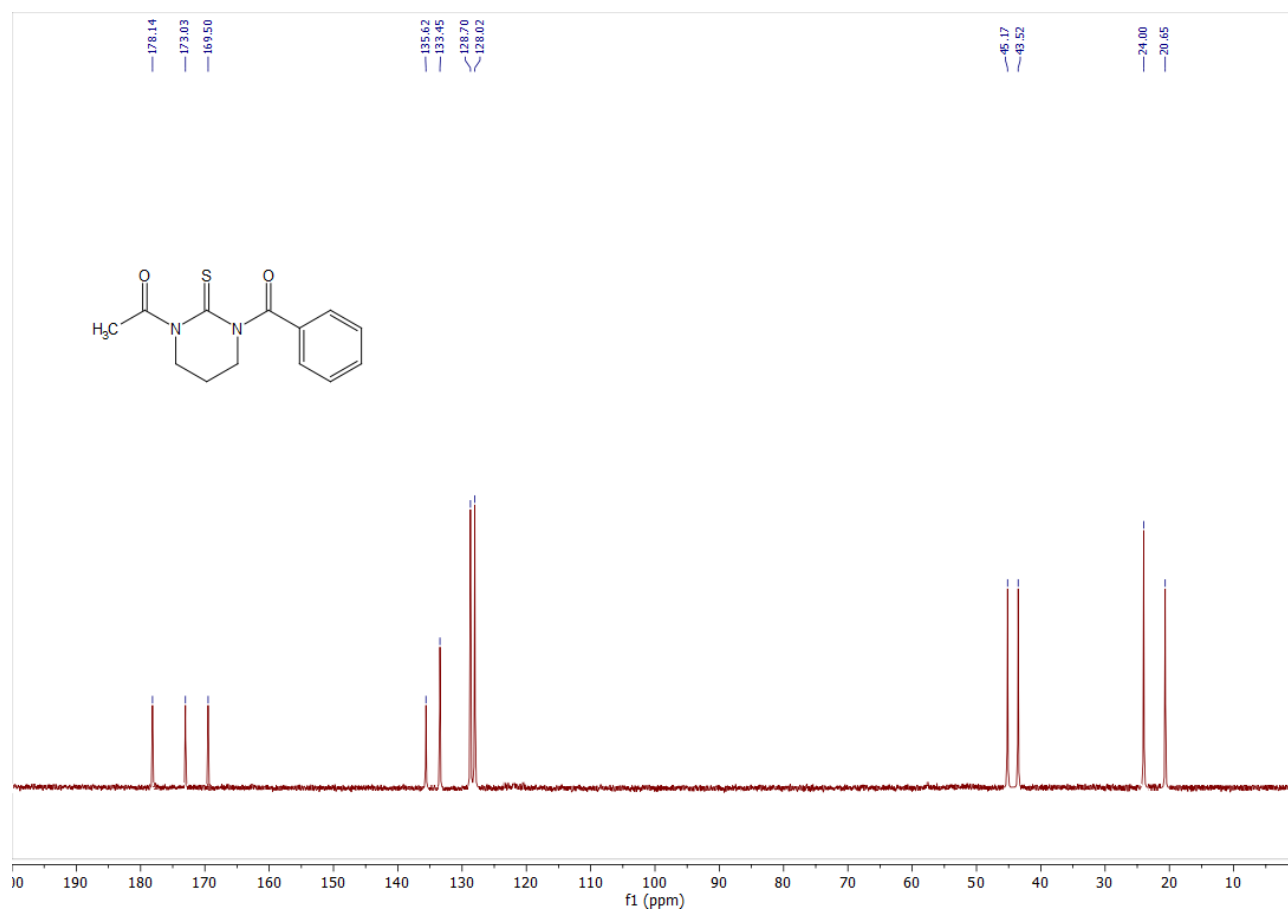


Figure S16. <sup>13</sup>C NMR (50 MHz, CDCl<sub>3</sub>) of compound 6a

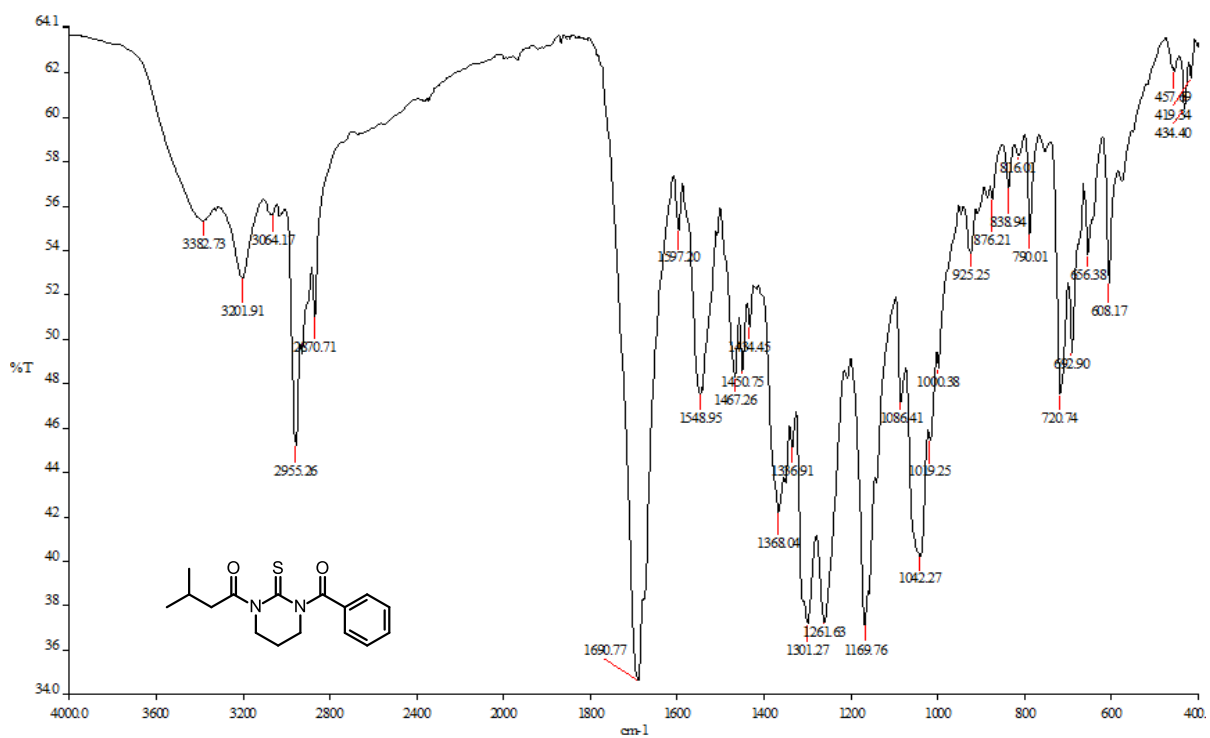


Figure S17. IR (KBr) of compound **6b**

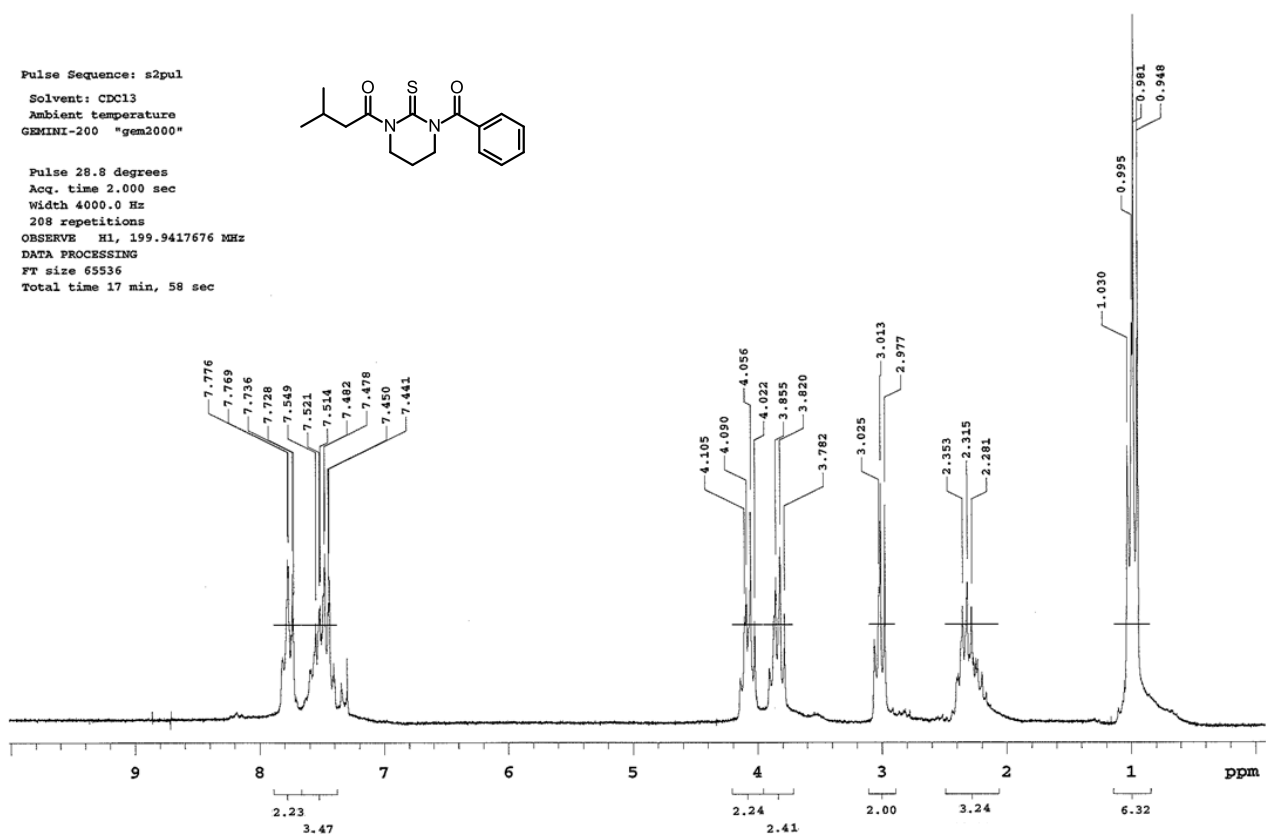
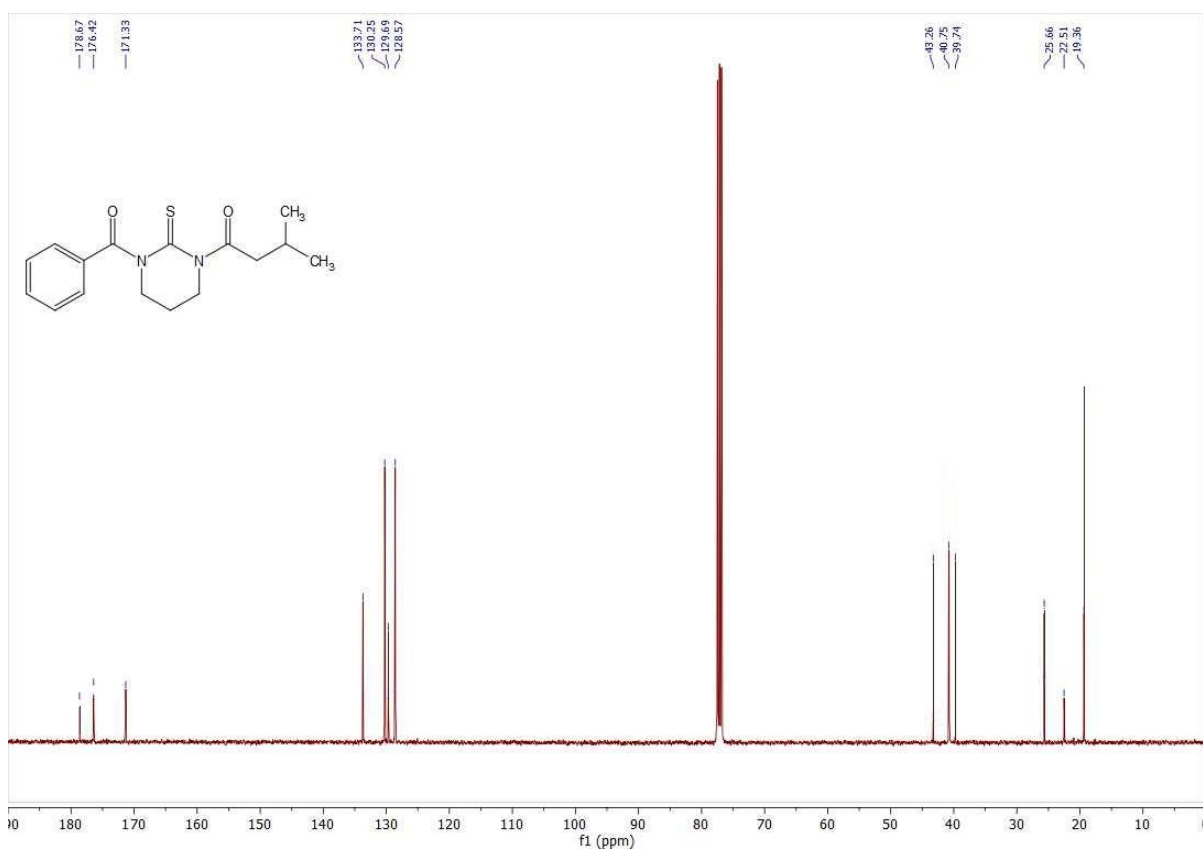
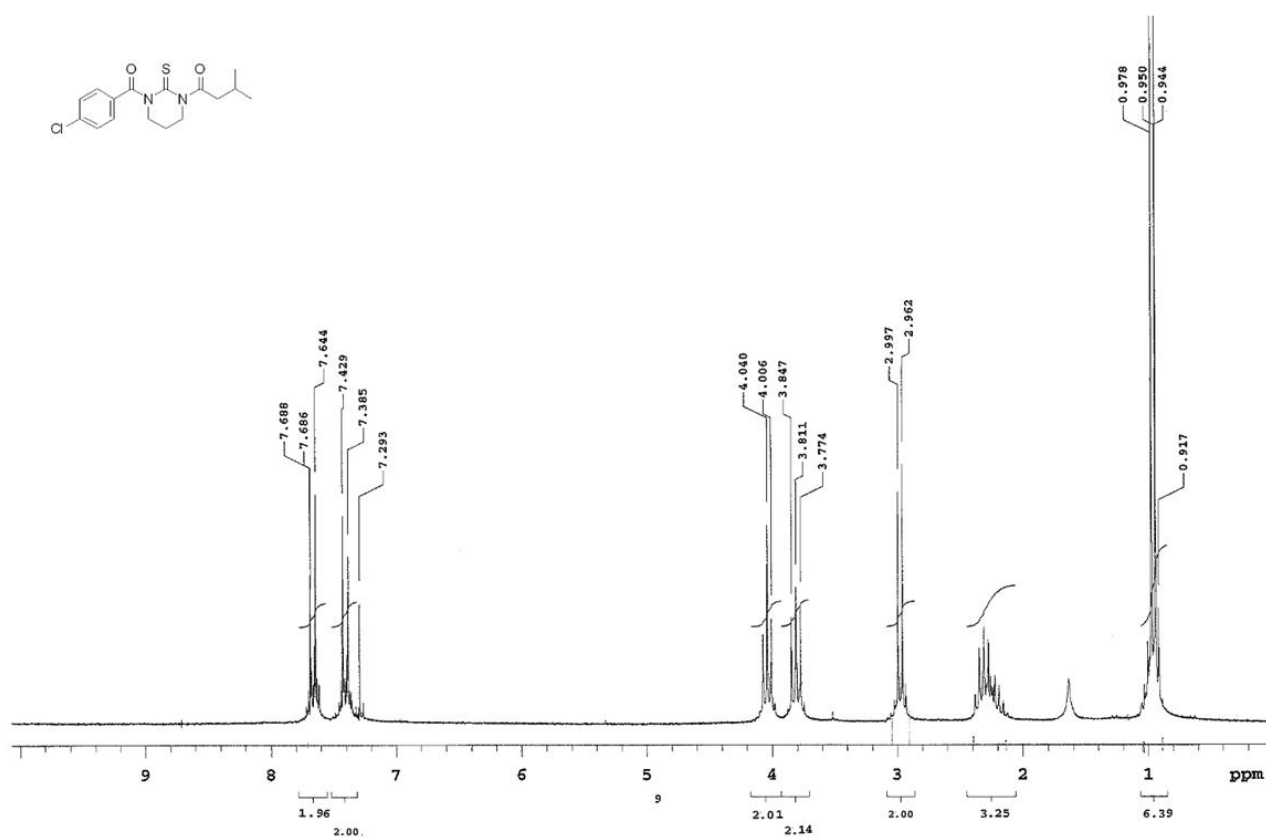


Figure S18.  $^1\text{H}$  NMR (200 MHz,  $\text{CDCl}_3$ ) of compound **6b**





**Figure S19.**  $^{13}\text{C}$  NMR (400 MHz,  $\text{CDCl}_3$ ) of compound **6b**



**Figure S20.**  $^1\text{H}$  NMR (200 MHz,  $\text{CDCl}_3$ ) of compound **6c**

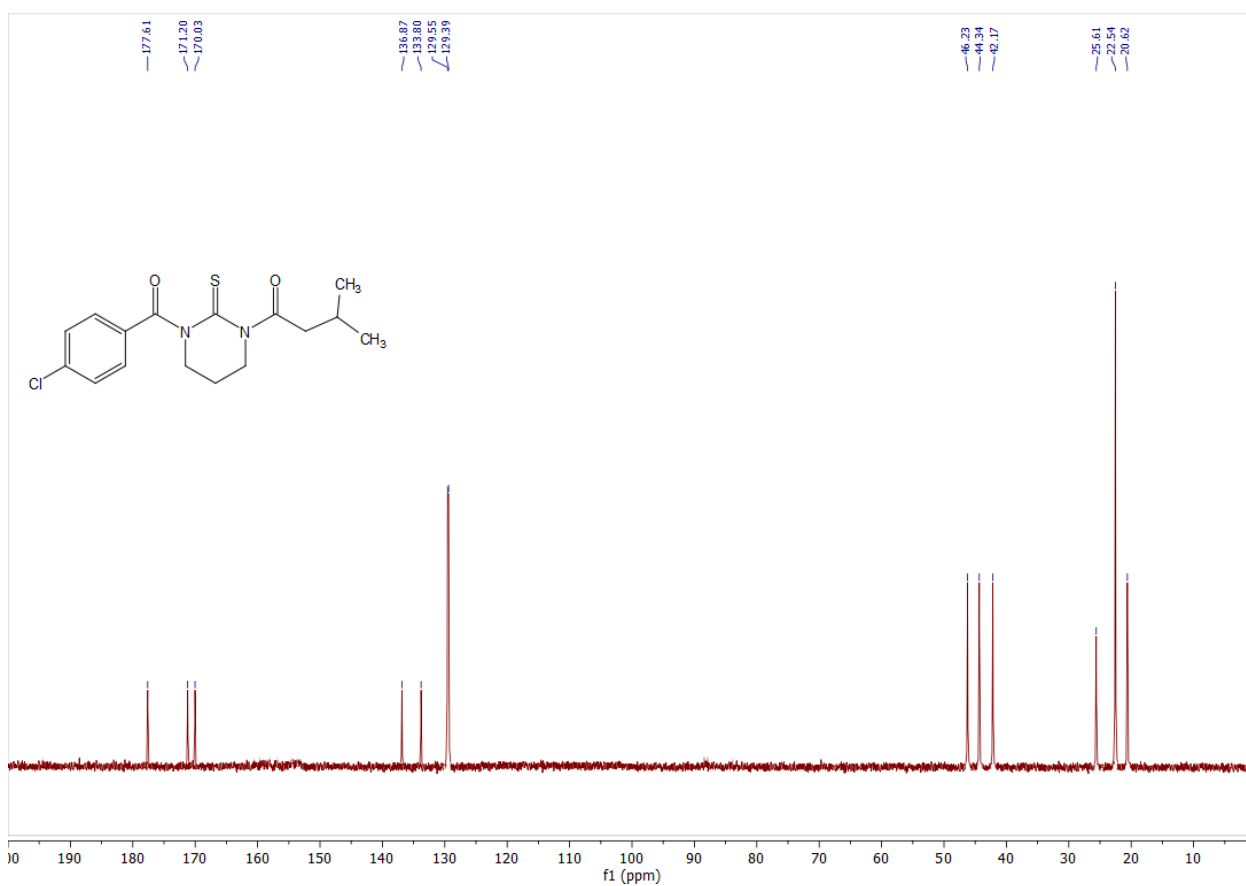


Figure S21.  $^{13}\text{C}$  NMR (50 MHz,  $\text{CDCl}_3$ ) of compound **6c**

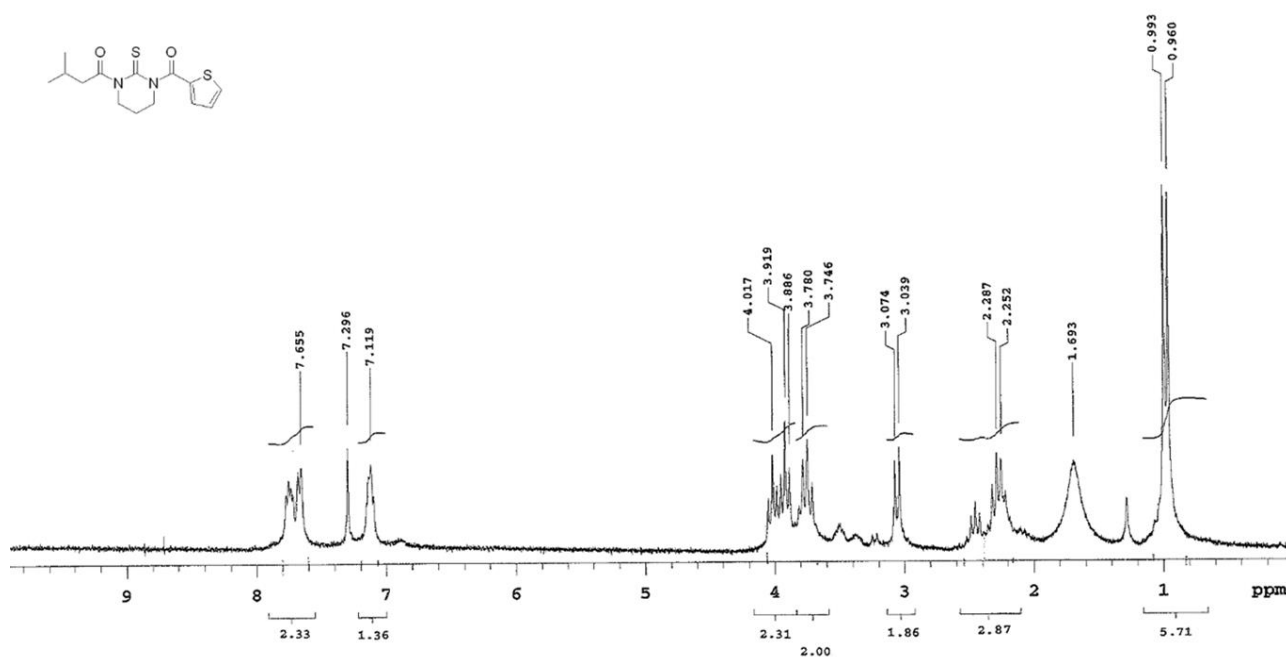


Figure S22.  $^1\text{H}$  NMR (200 MHz,  $\text{CDCl}_3$ ) of compound **6d**

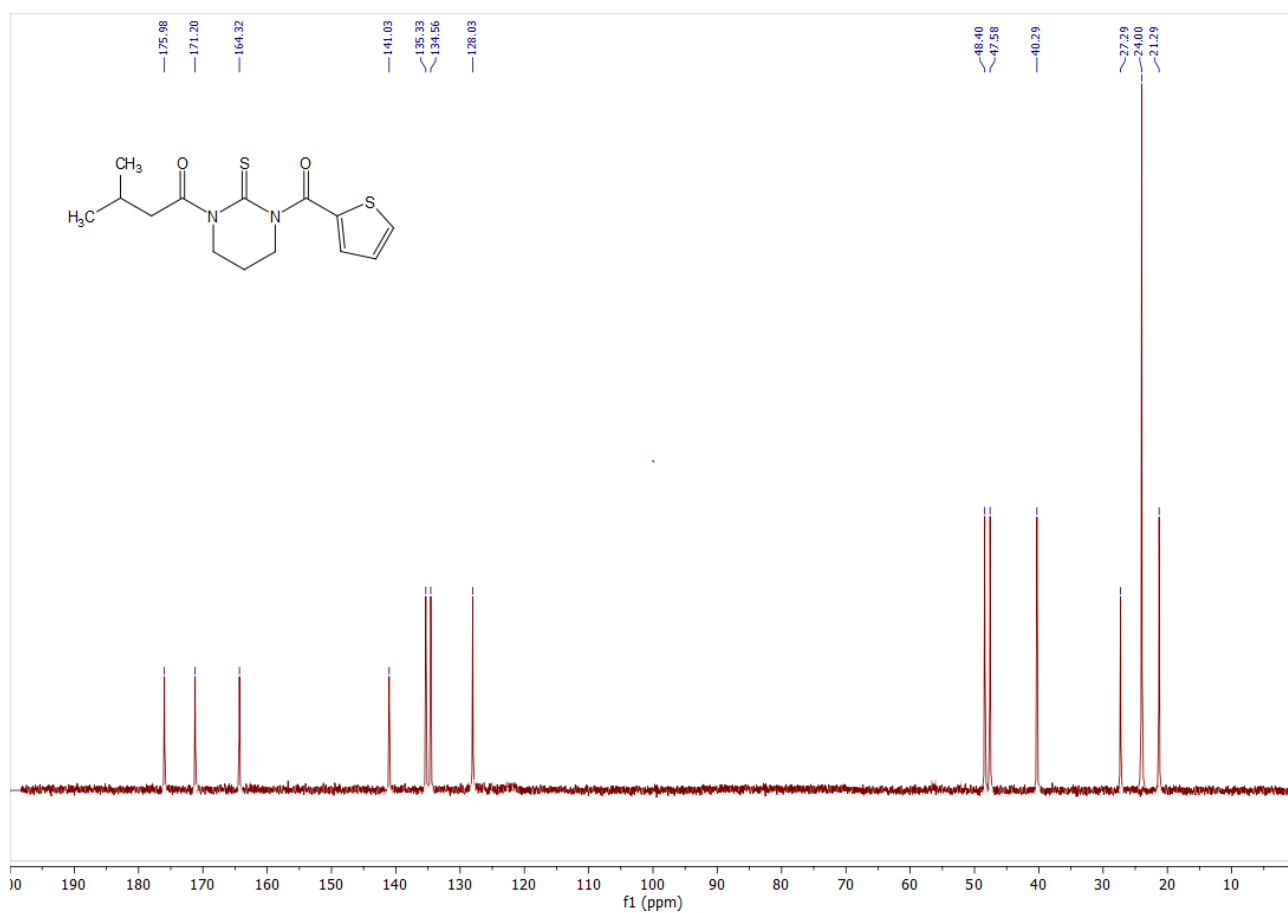


Figure S23.  $^{13}\text{C}$  NMR (50 MHz,  $\text{CDCl}_3$ ) of compound 6d

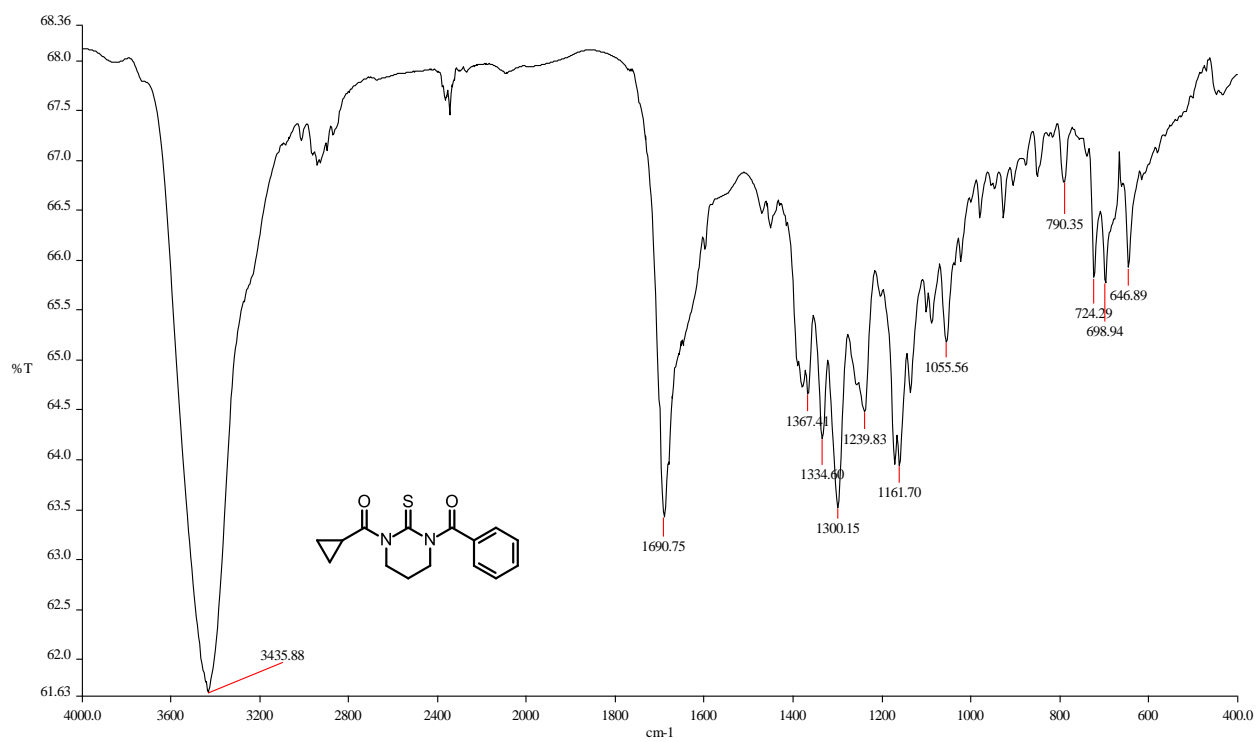


Figure S24. IR (KBr) of compound 6e

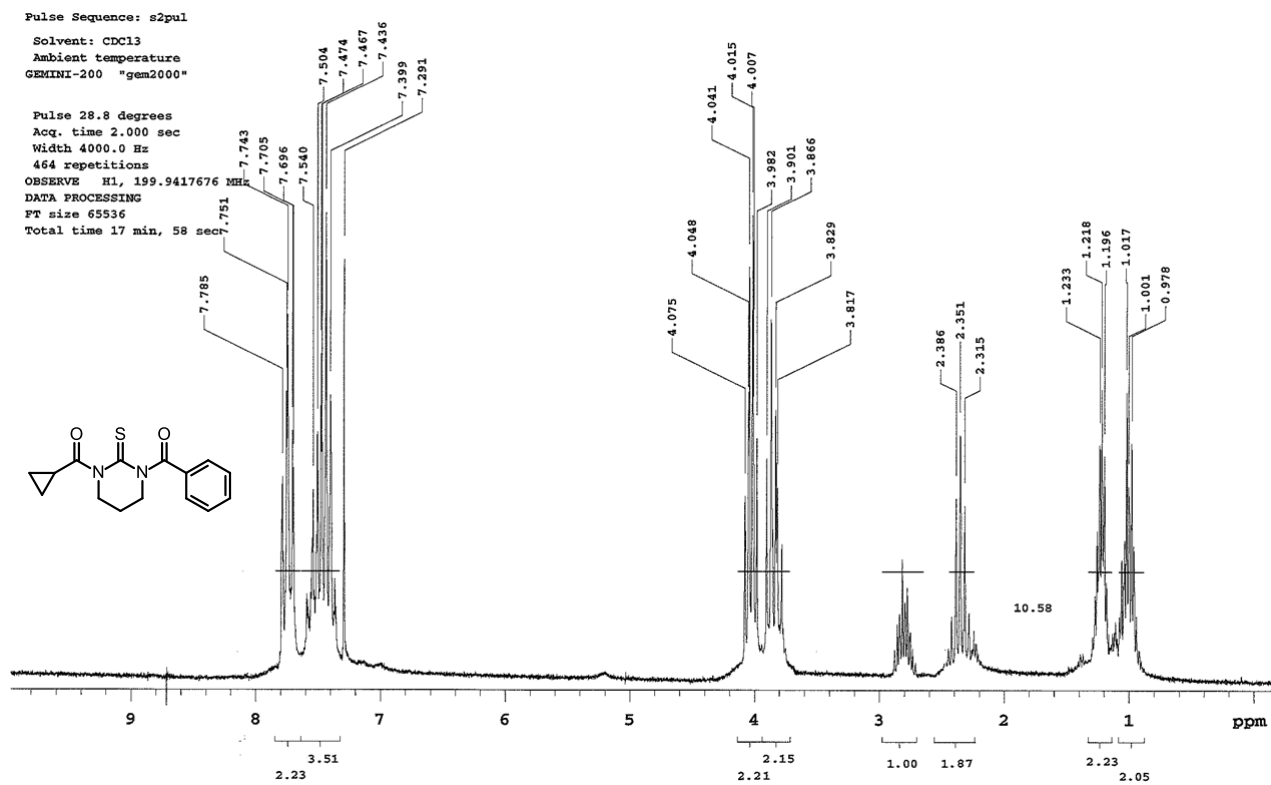


Figure S25. <sup>1</sup>H NMR (200 MHz, CDCl<sub>3</sub>) of compound **6e**

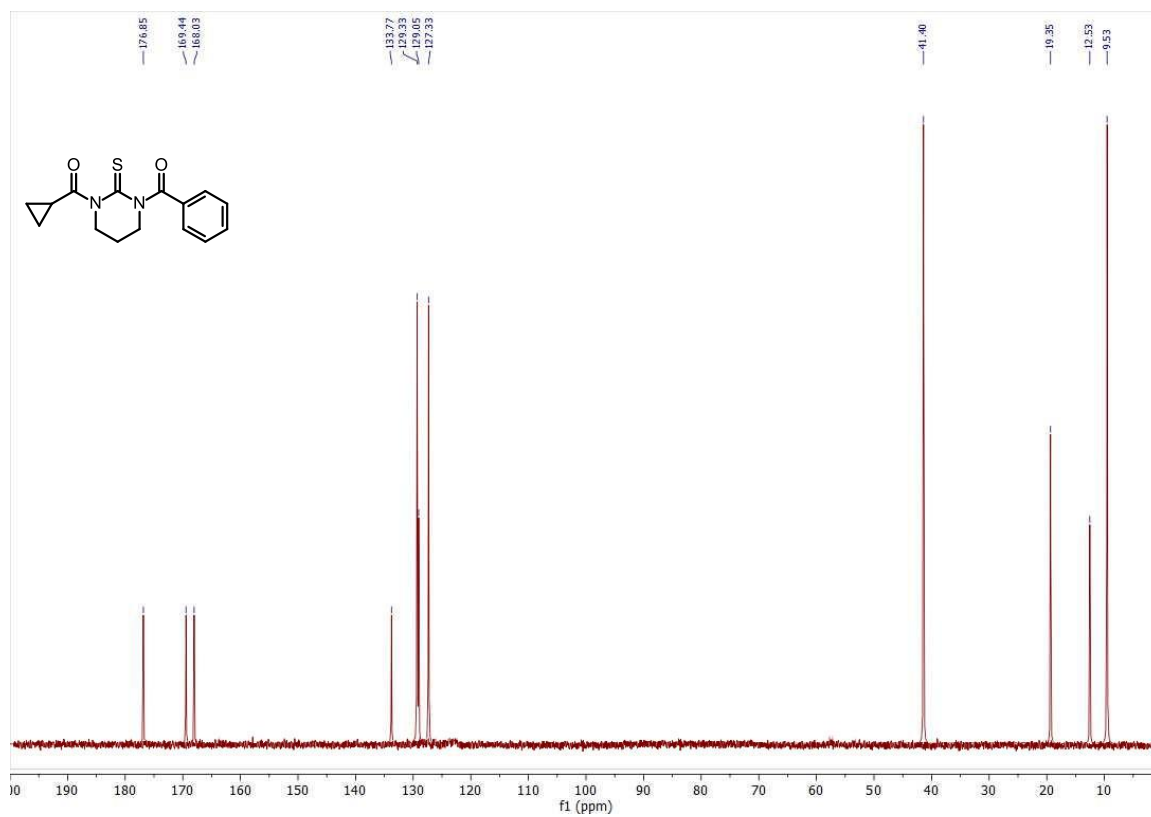


Figure S26. <sup>13</sup>C NMR (101 MHz, CDCl<sub>3</sub>) of compound **6e**

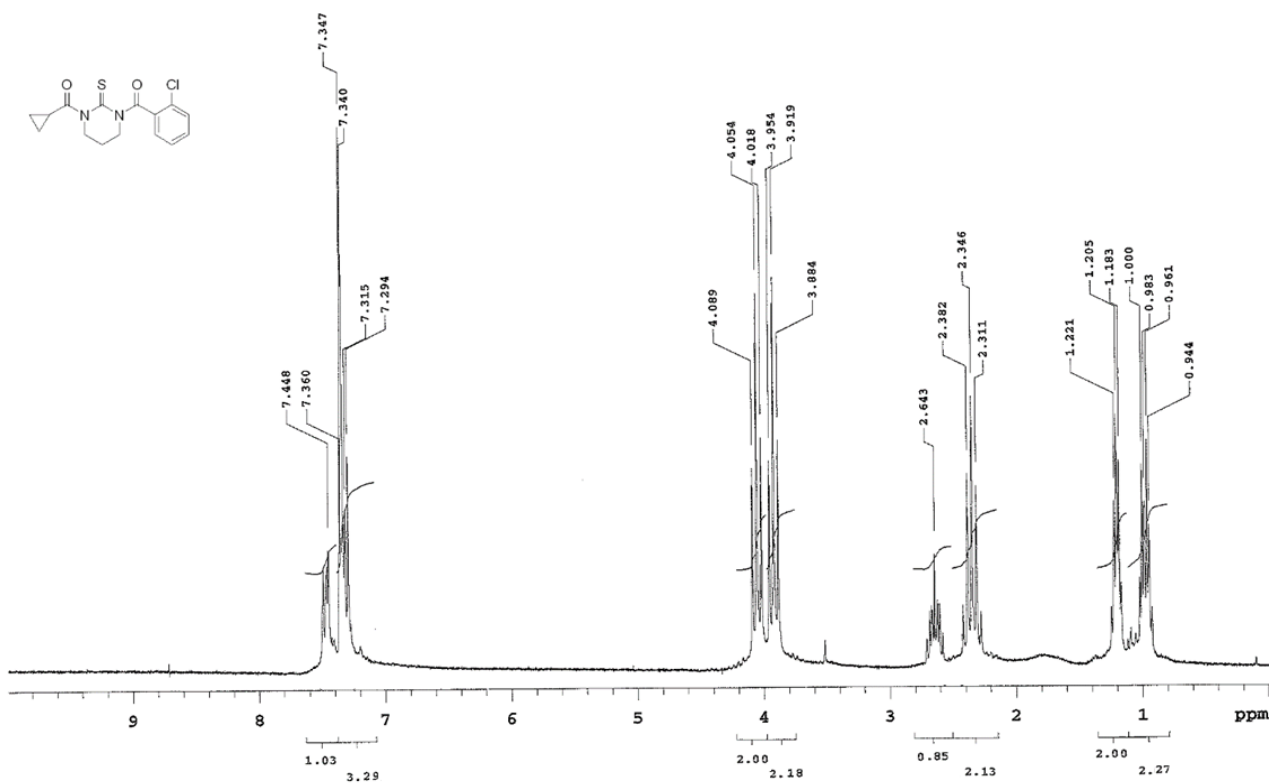


Figure S27. <sup>1</sup>H NMR (200 MHz, CDCl<sub>3</sub>) of compound **6f**

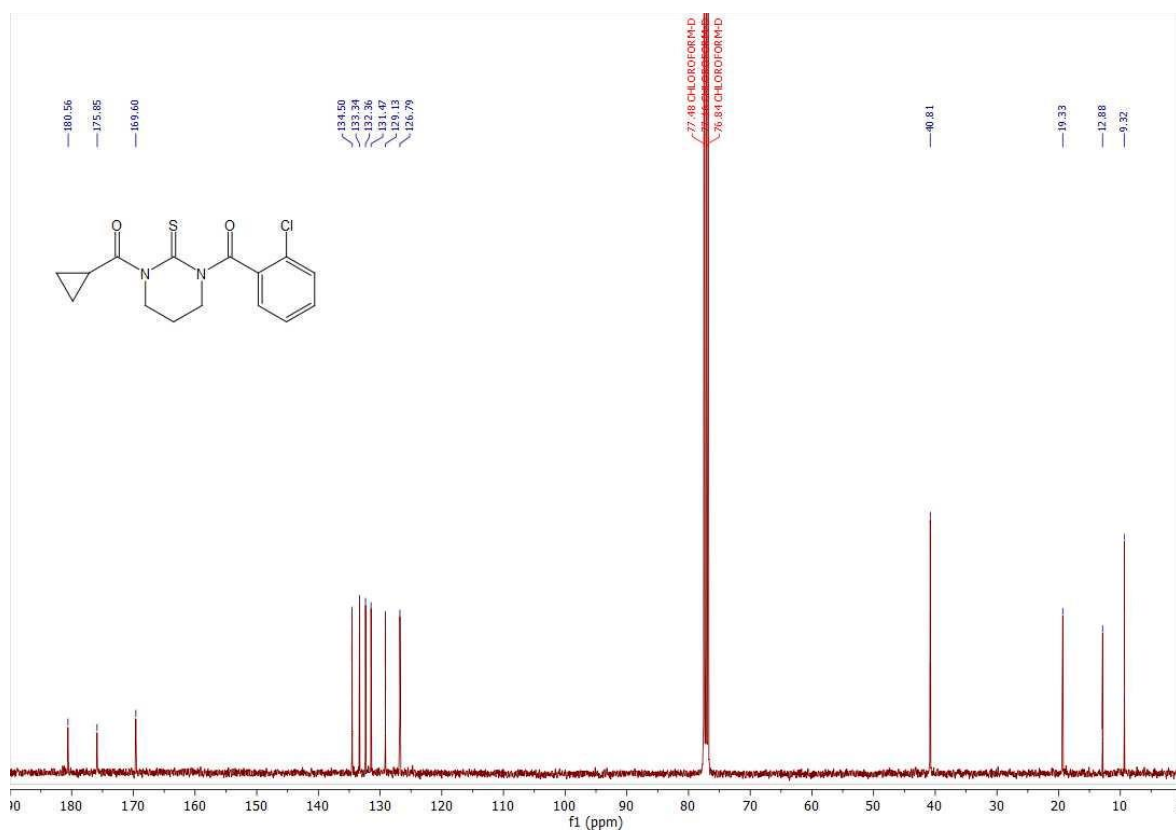


Figure S28. <sup>13</sup>C NMR (101 MHz, CDCl<sub>3</sub>) of compound **6f**

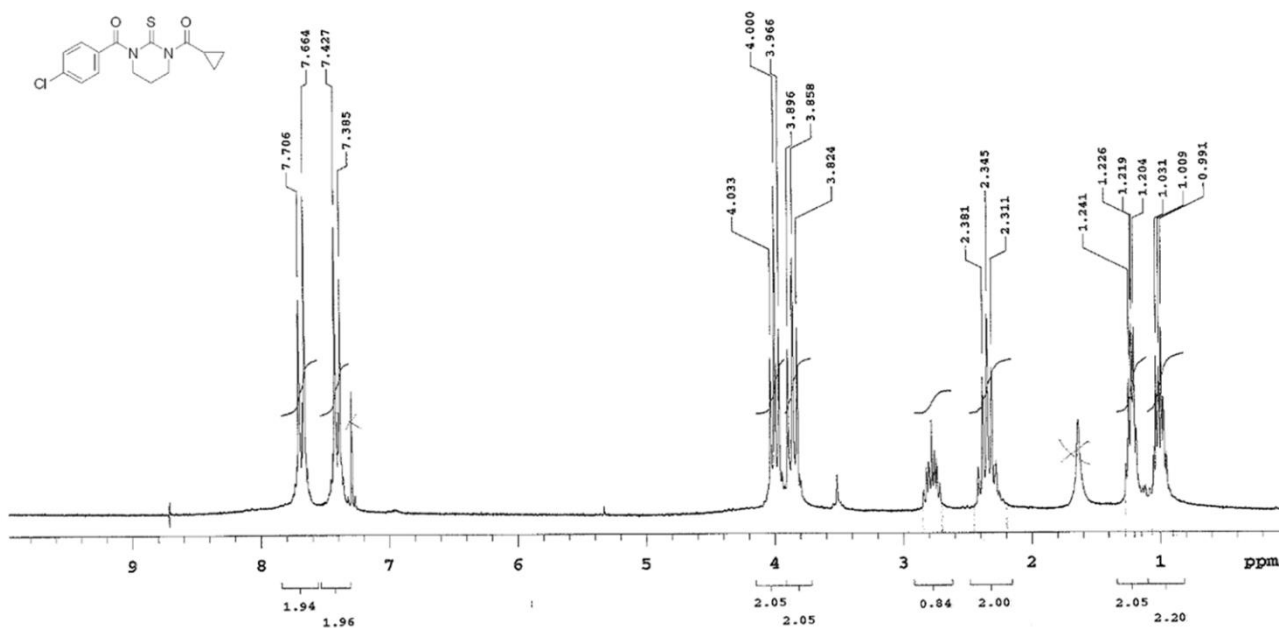


Figure S29. <sup>1</sup>H NMR (200 MHz, CDCl<sub>3</sub>) of compound 6g

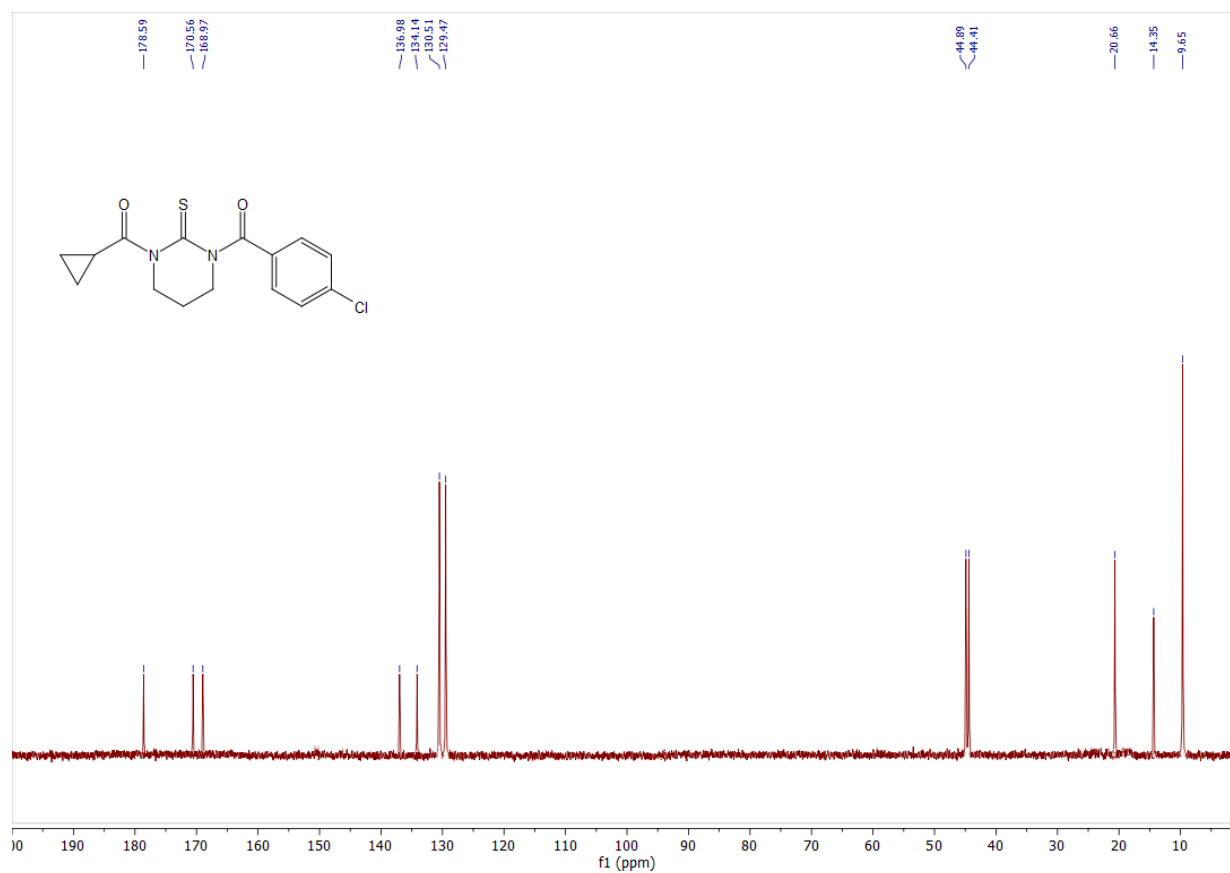
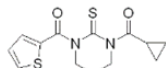


Figure S30. <sup>13</sup>C NMR (50 MHz, CDCl<sub>3</sub>) of compound 6g

Pulse Sequence: s2pul

Solvent: CDCl<sub>3</sub>  
Ambient temperature  
GEMINI-200 "gem2000"



Pulse 30.0 degrees  
Acq. time 2.000 sec  
Width 4000.0 Hz  
128 repetitions  
OBSERVE H1, 199.9417676 MHz  
DATA PROCESSING  
FT size 65536  
Total time 17 min, 58 sec

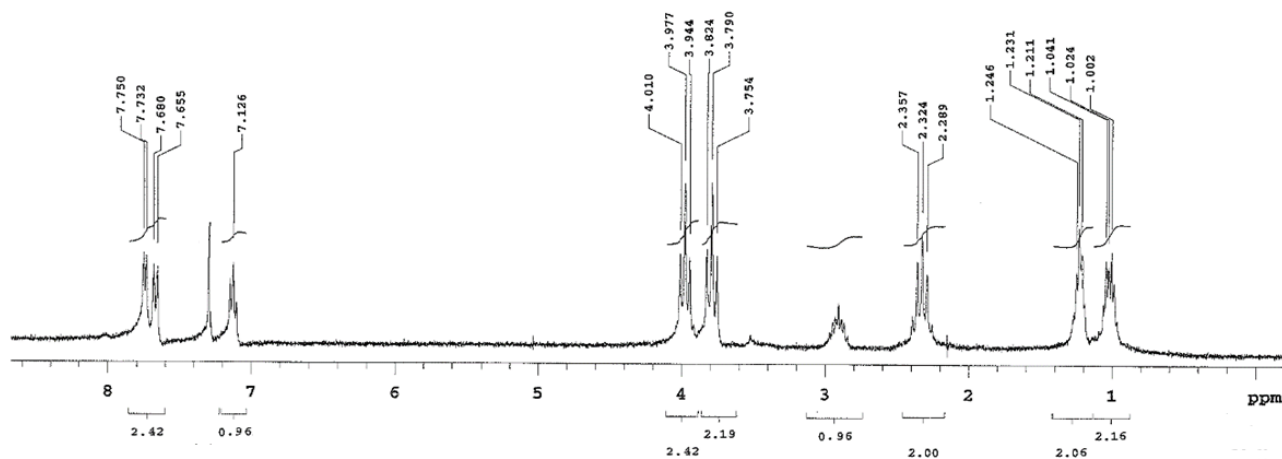


Figure S31. <sup>1</sup>H NMR (200 MHz, CDCl<sub>3</sub>) of compound **6h**

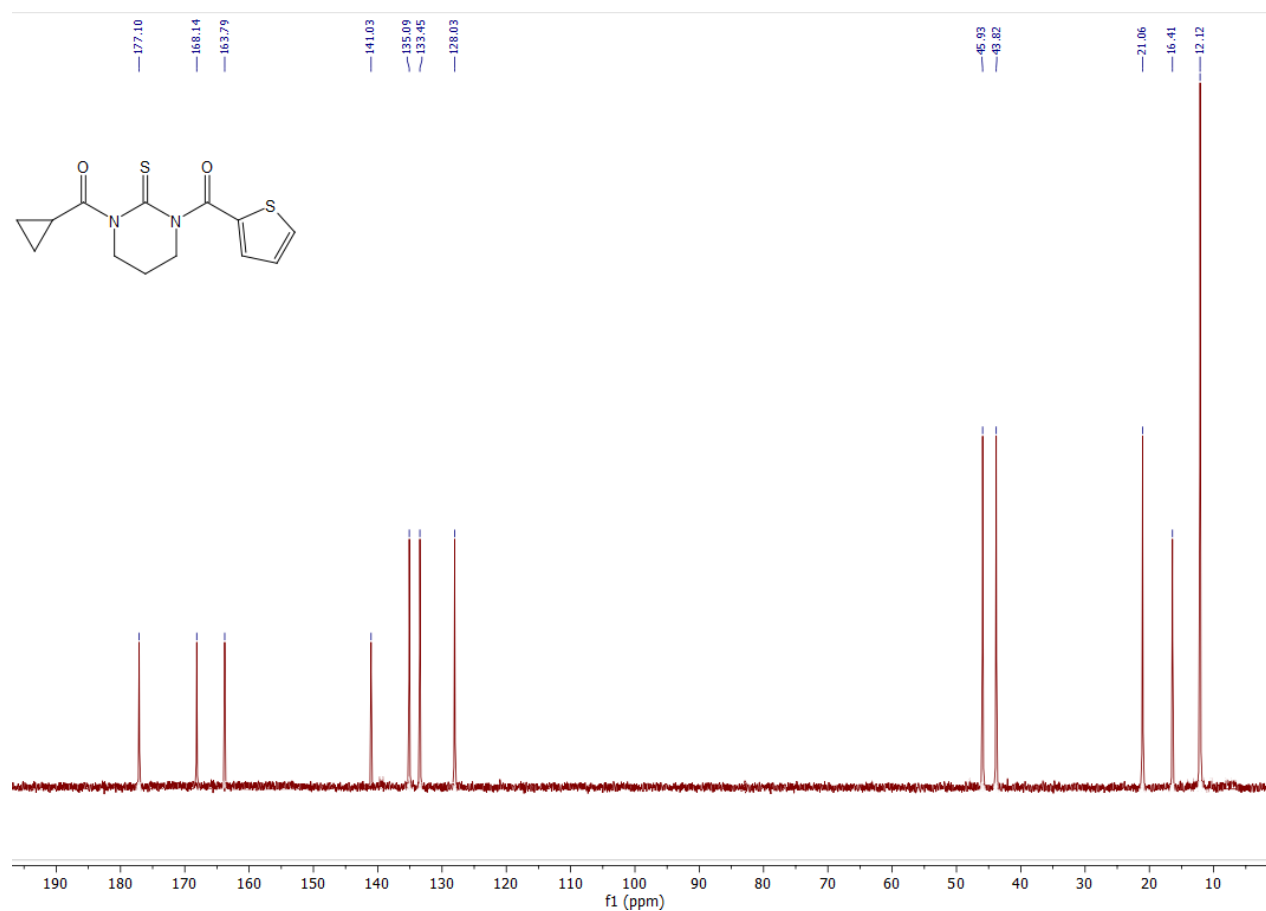


Figure S32. <sup>13</sup>C NMR (50 MHz, CDCl<sub>3</sub>) of compound **6h**

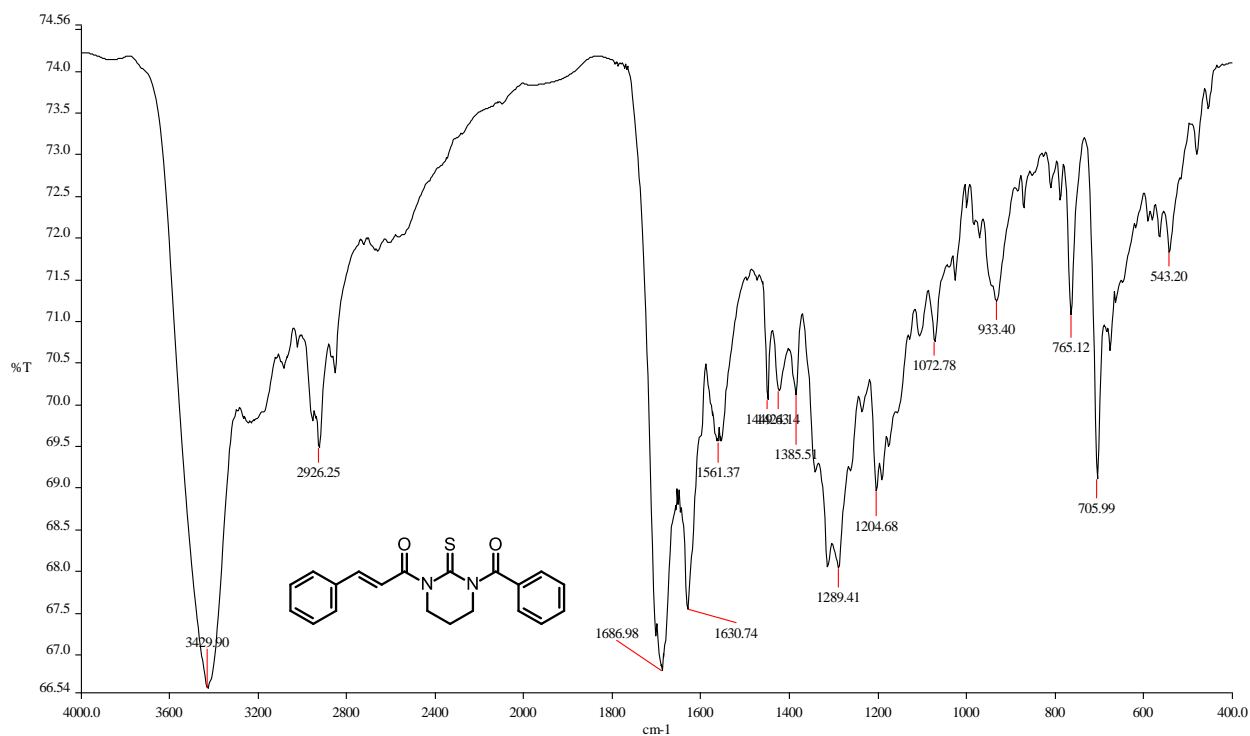


Figure S33. IR (KBr) of compound 6i

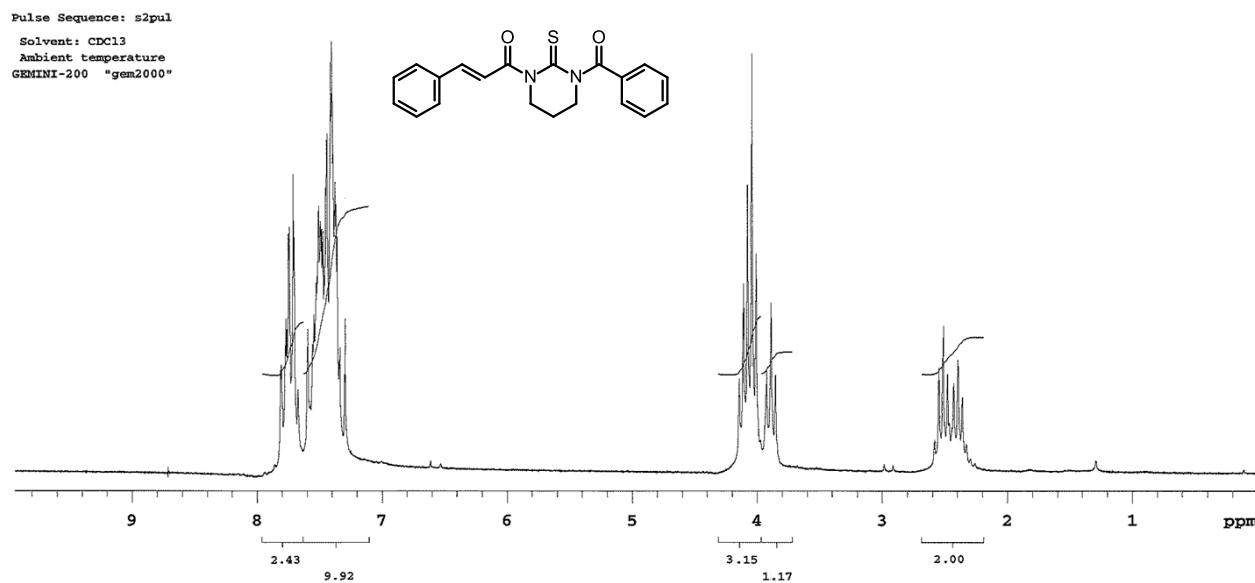


Figure S34. <sup>1</sup>H NMR (200 MHz, CDCl<sub>3</sub>) of compound 6i



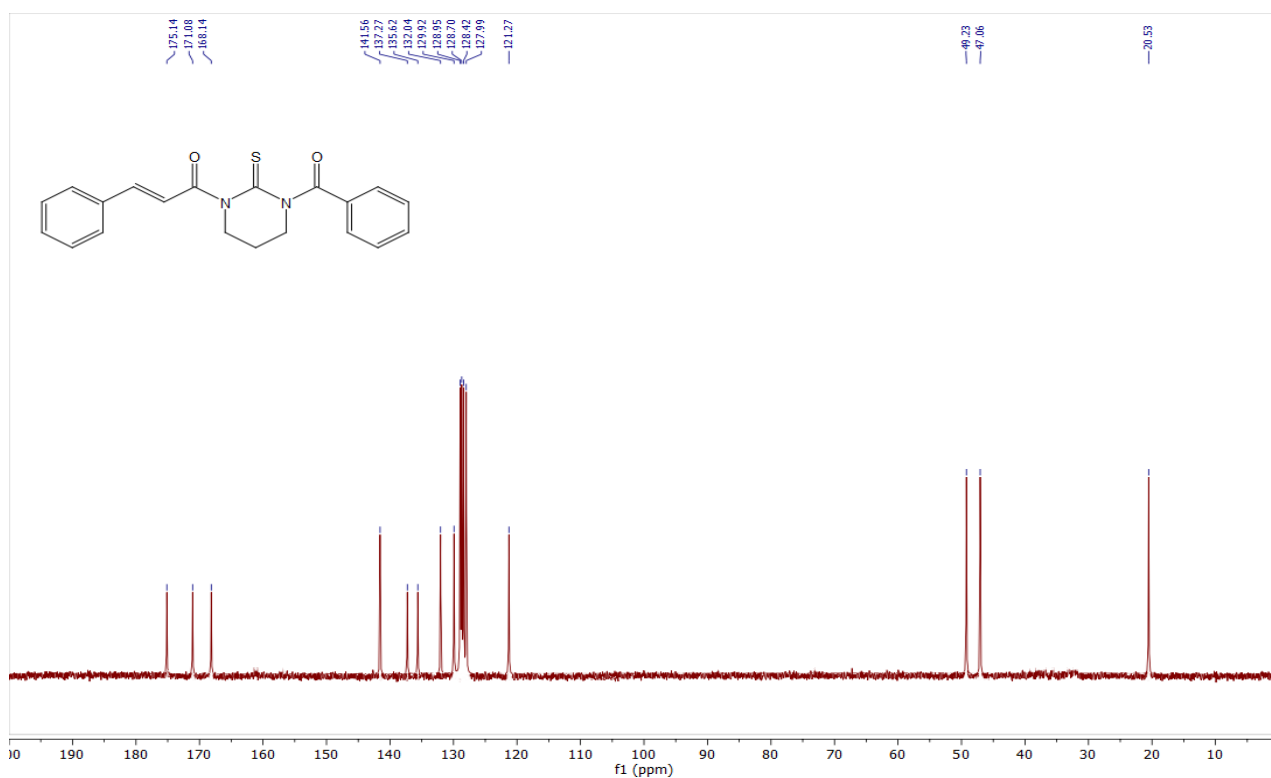


Figure S35.  $^{13}\text{C}$  NMR (50 MHz,  $\text{CDCl}_3$ ) of compound **6i**

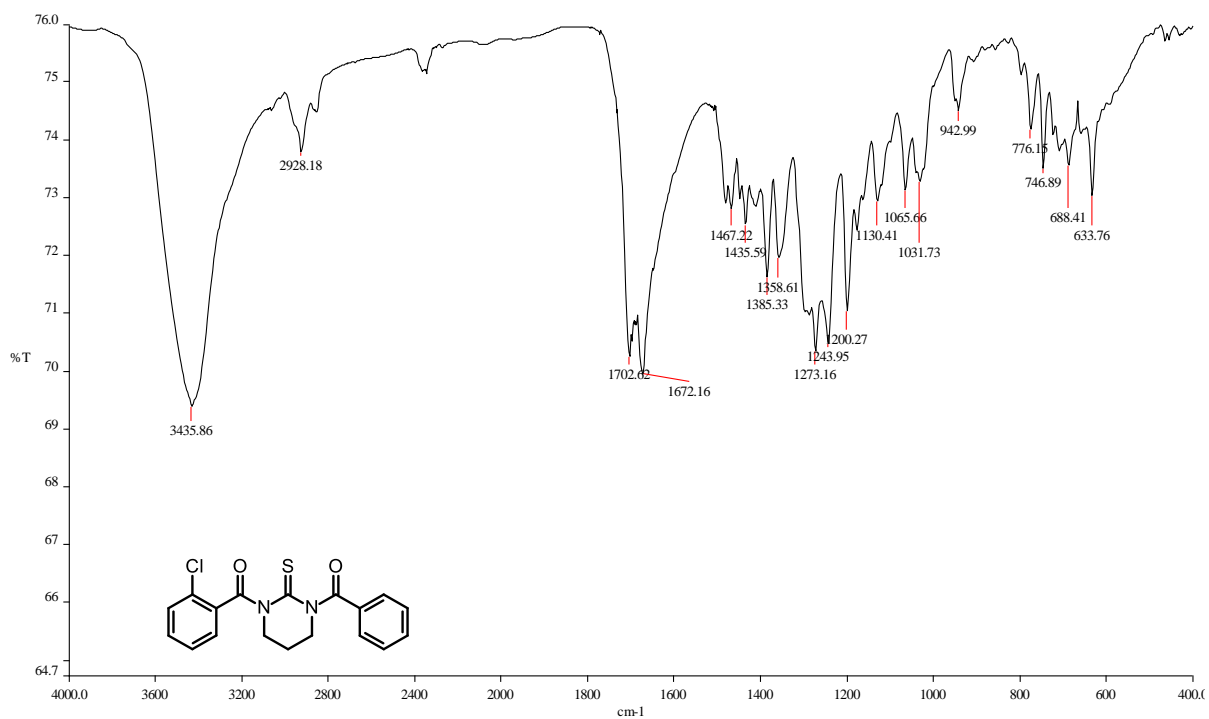


Figure S36. IR (KBr) of compound **6j**

Pulse Sequence: s2pul  
Solvent: CDCl3  
Ambient temperature  
GEMINI-200 "gem2000"

Pulse 28.8 degrees  
Acq. time 2.000 sec  
Width 4000.0 Hz  
512 repetitions  
OBSERVE H1, 199.9417676 MHz  
DATA PROCESSING  
FT size 65536  
Total time 17 min, 58 sec

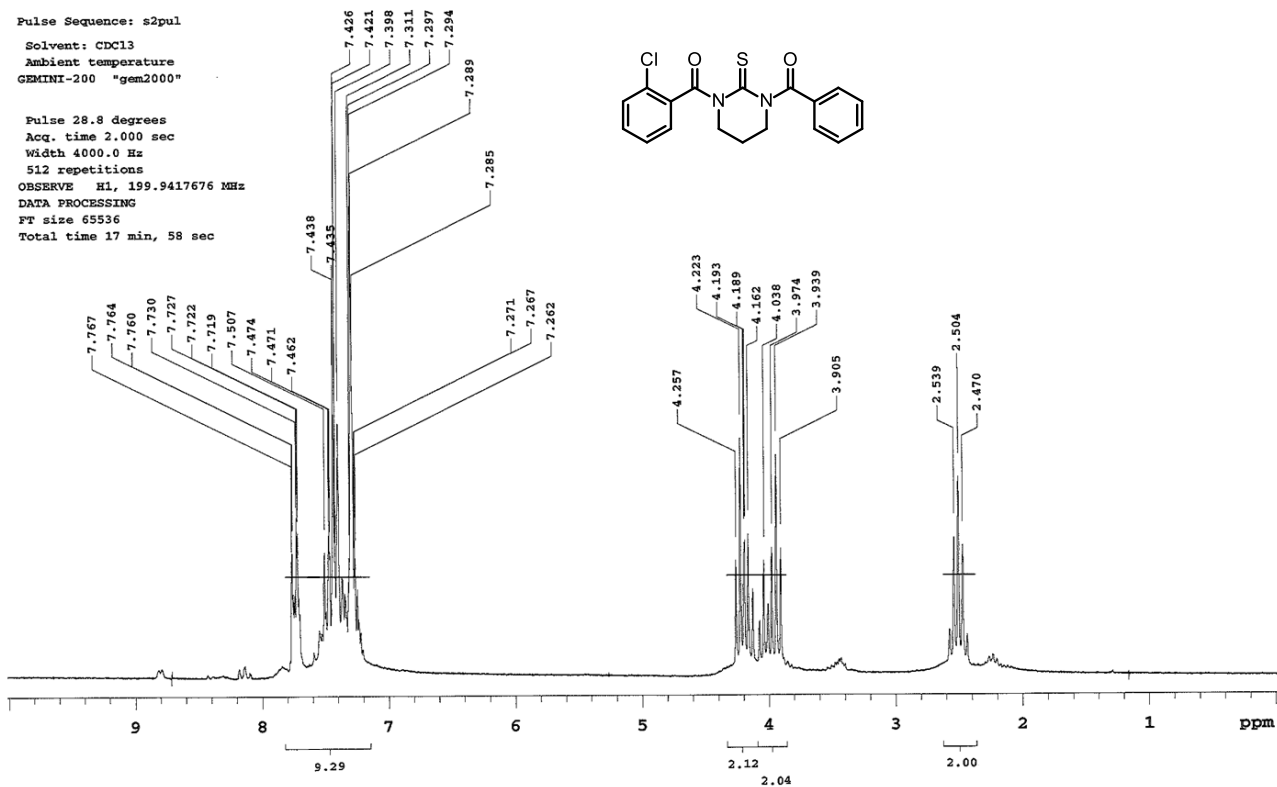
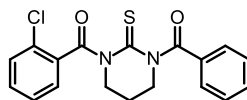


Figure S37.  $^1\text{H}$  NMR (200 MHz,  $\text{CDCl}_3$ ) of compound **6j**

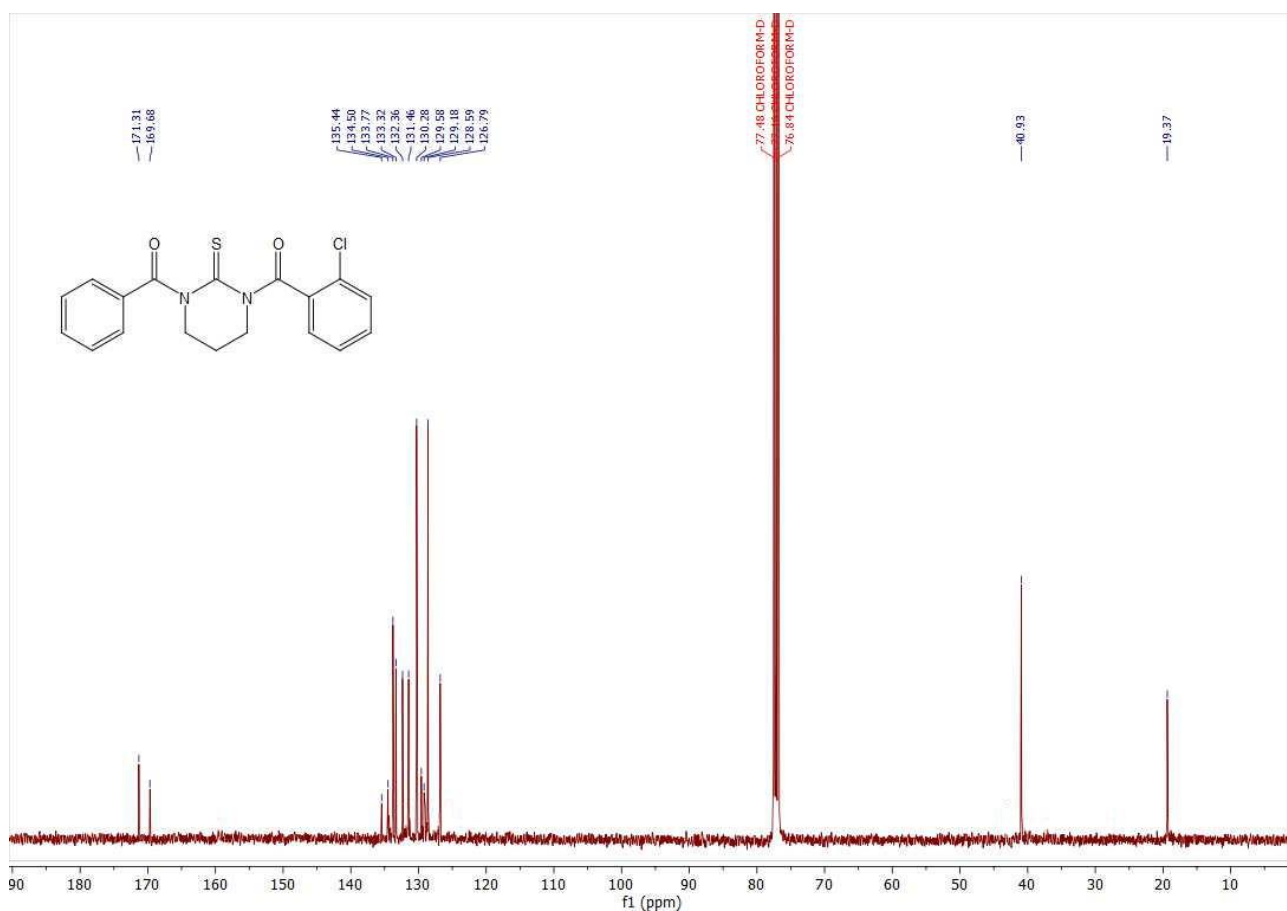


Figure S38.  $^{13}\text{C}$  NMR (101 MHz,  $\text{CDCl}_3$ ) of compound **6j**

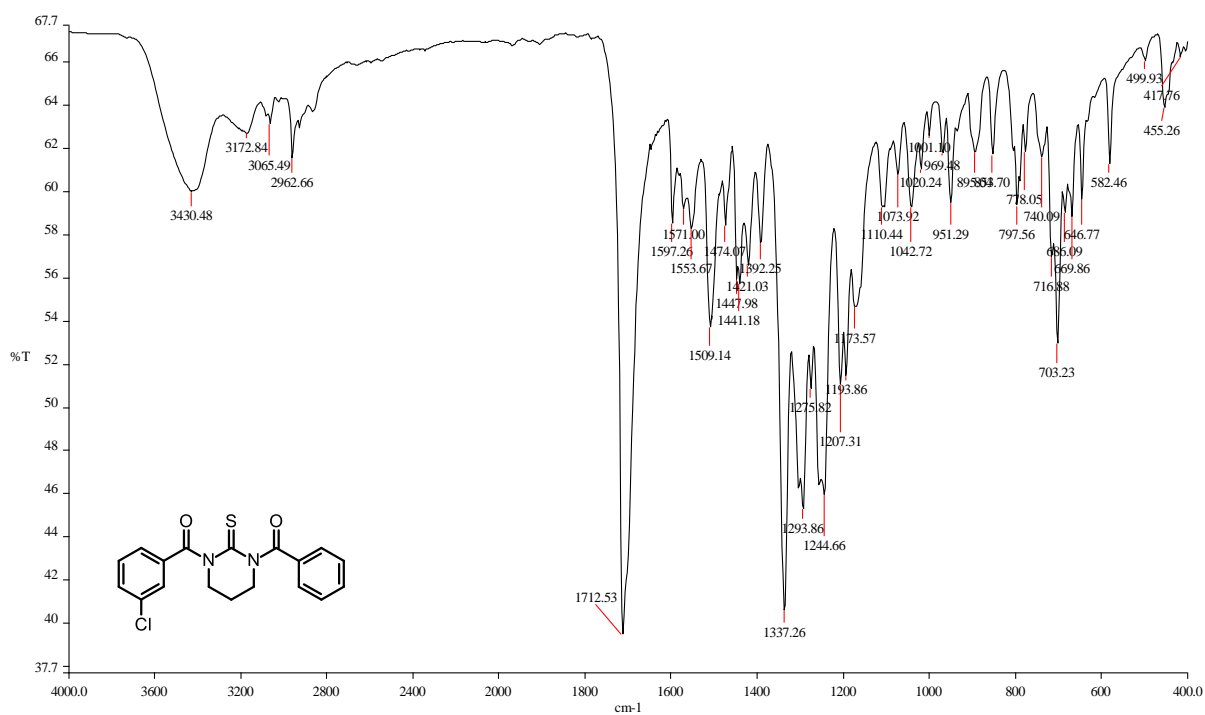


Figure S39. IR (KBr) of compound **6k**

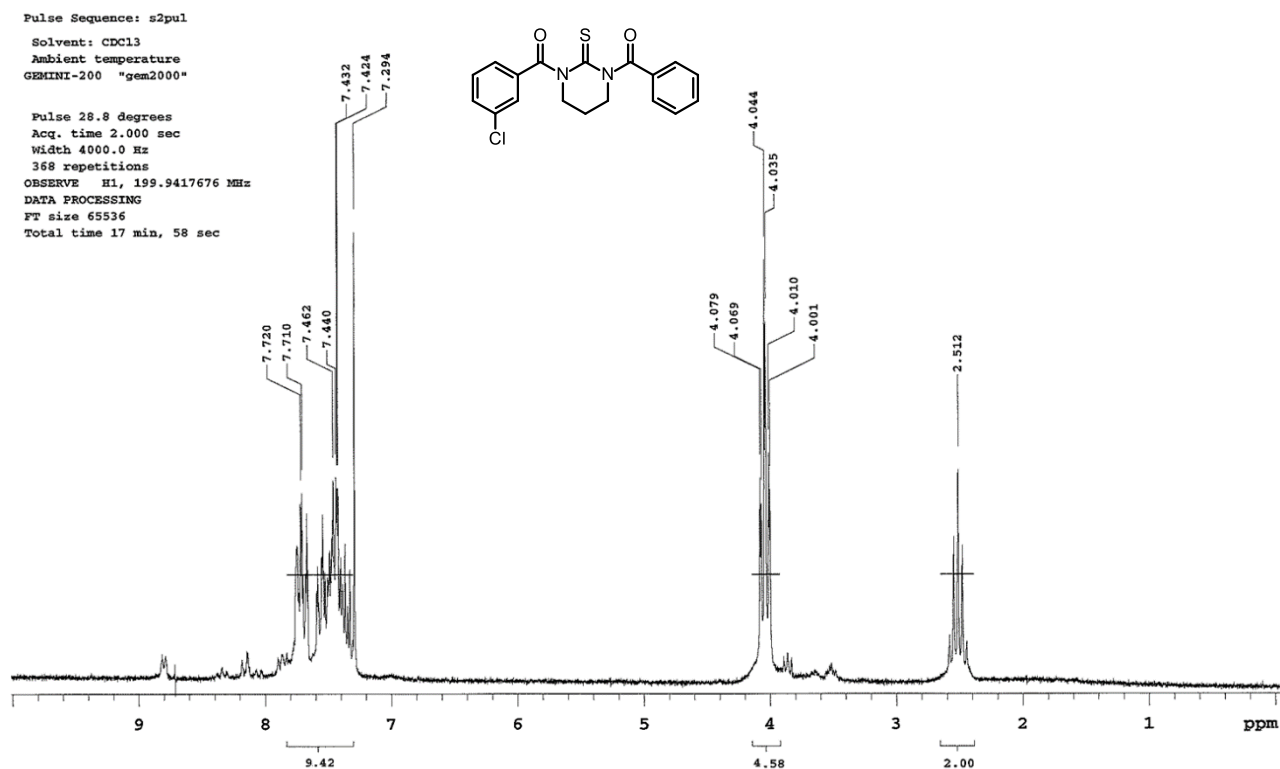


Figure S40.  $^1\text{H}$  NMR (200 MHz,  $\text{CDCl}_3$ ) of compound **6k**

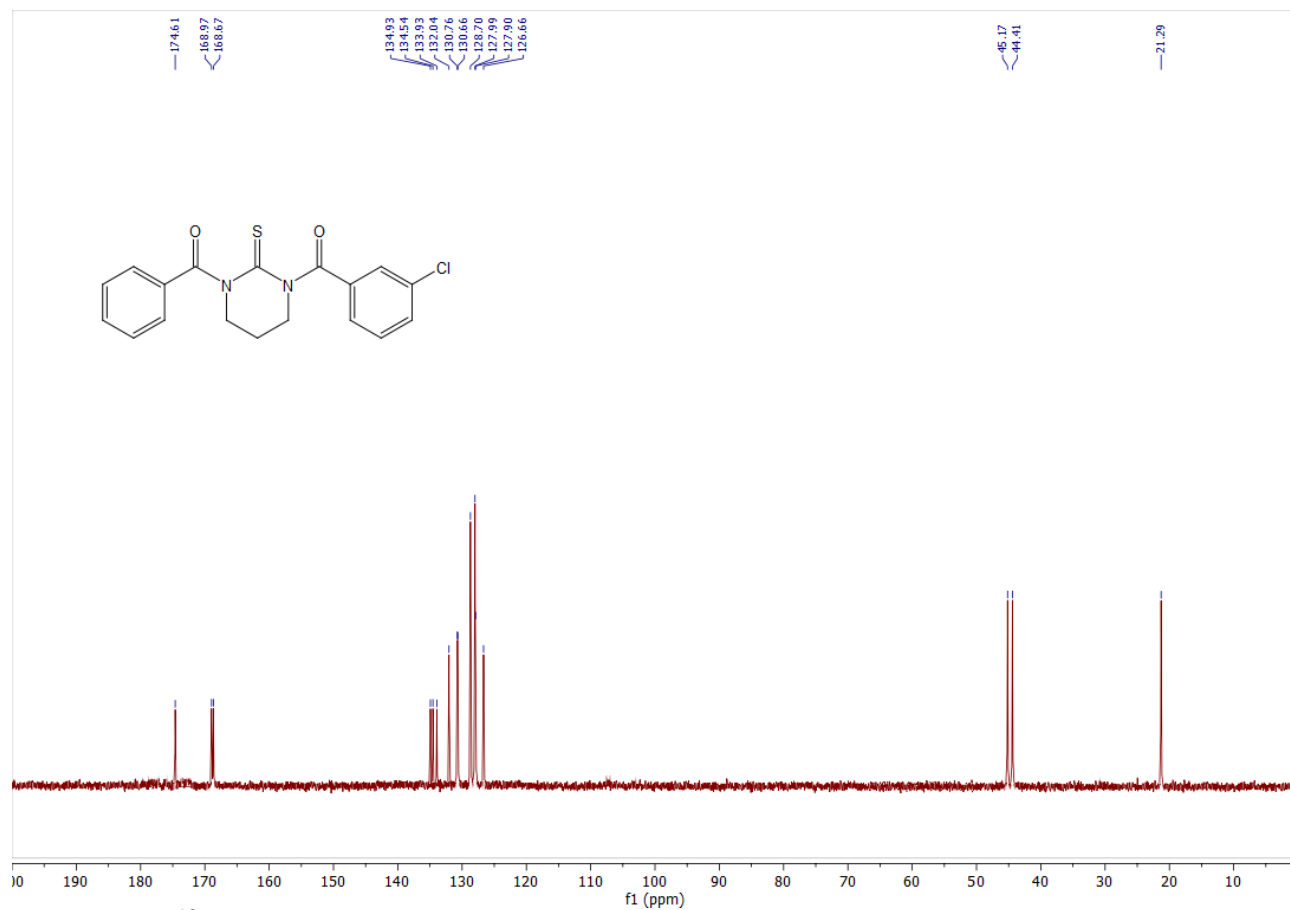


Figure S41. <sup>13</sup>C NMR (50 MHz, CDCl<sub>3</sub>) of compound 6k

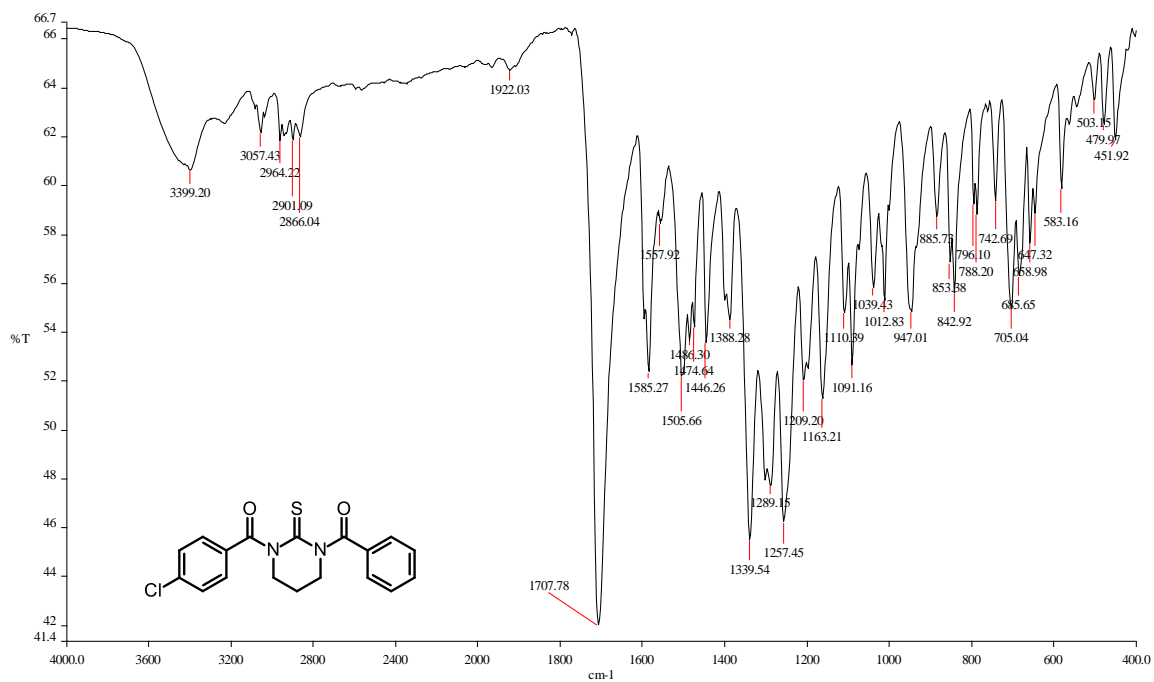
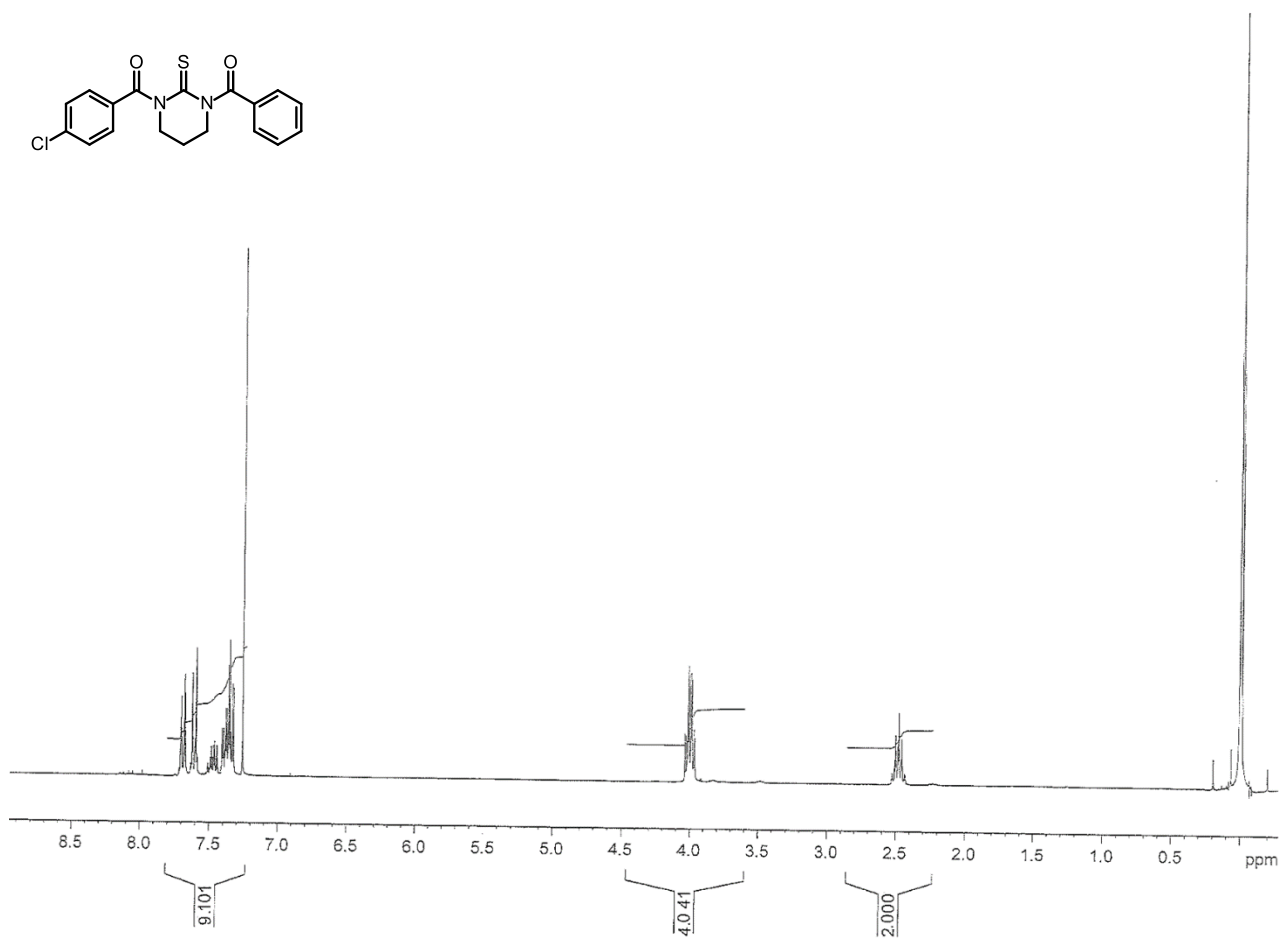
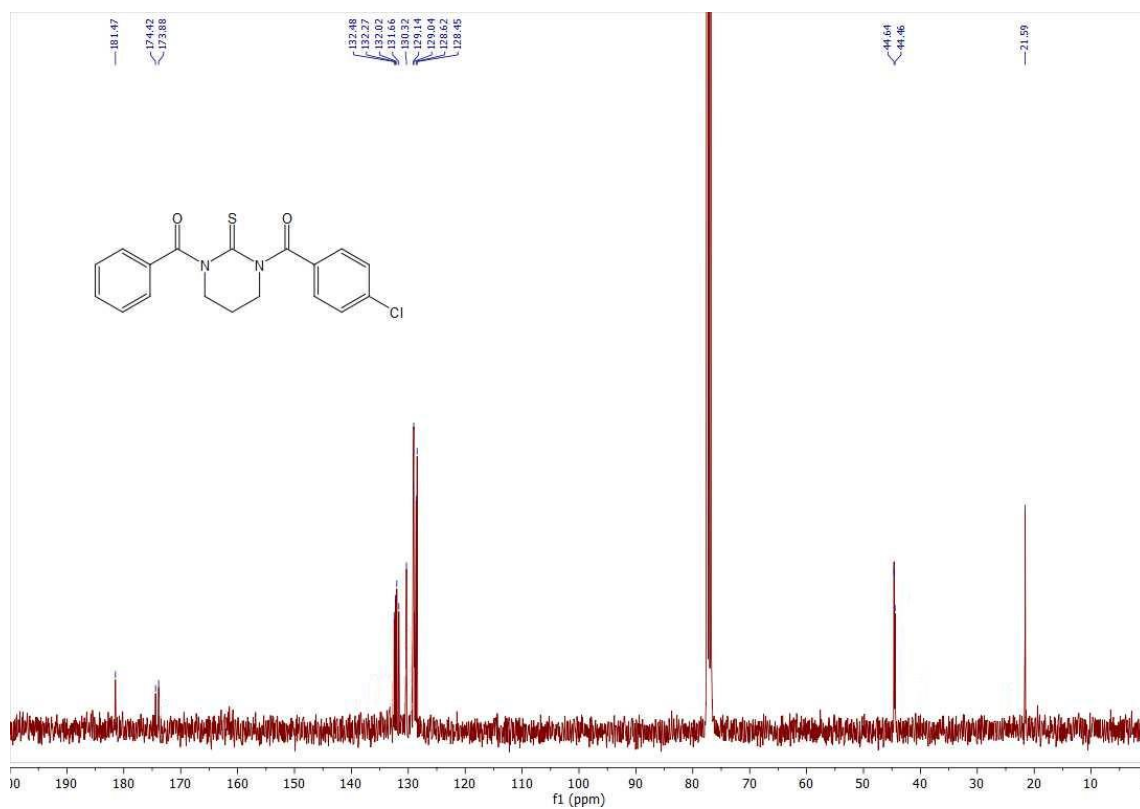


Figure S42. IR (KBr) of compound 6l



**Figure S43.** <sup>1</sup>H NMR (300 MHz, CDCl<sub>3</sub>) of compound **6l**



**Figure S44.** <sup>13</sup>C NMR (101 MHz, CDCl<sub>3</sub>) of compound **6l**

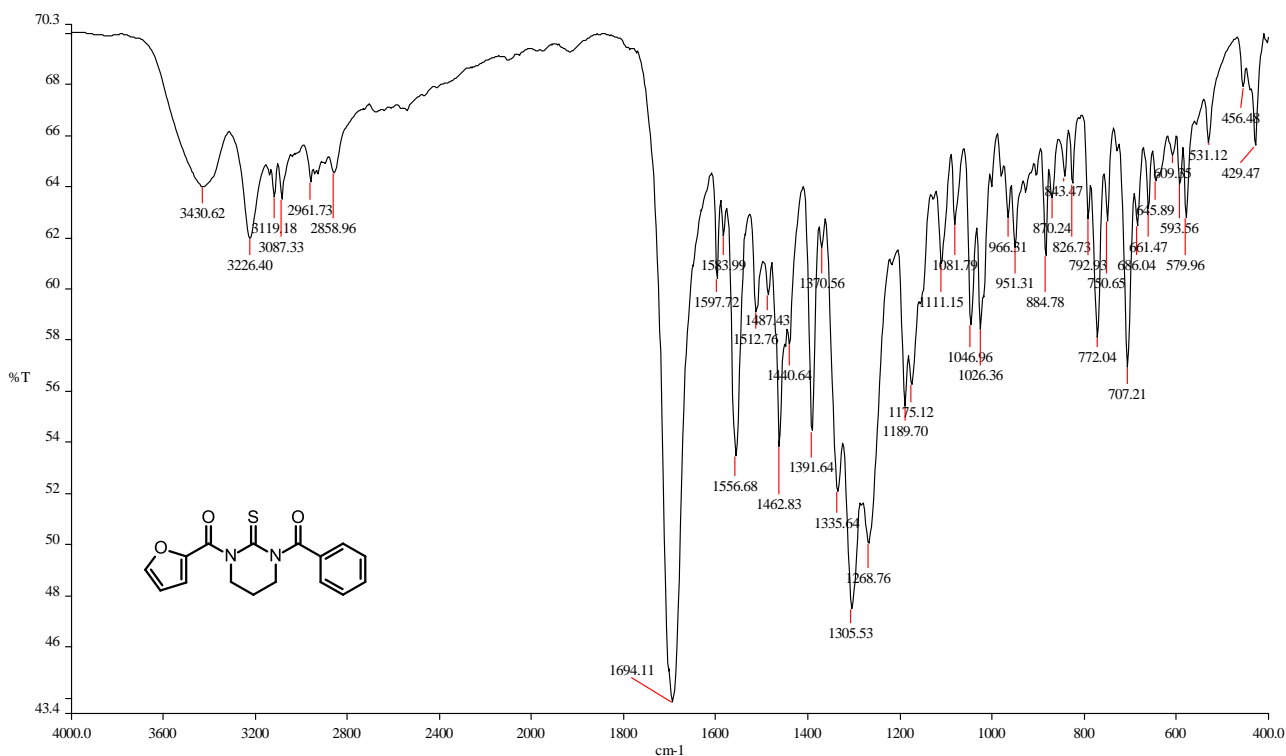


Figure S45. IR (KBr) of compound **6m**

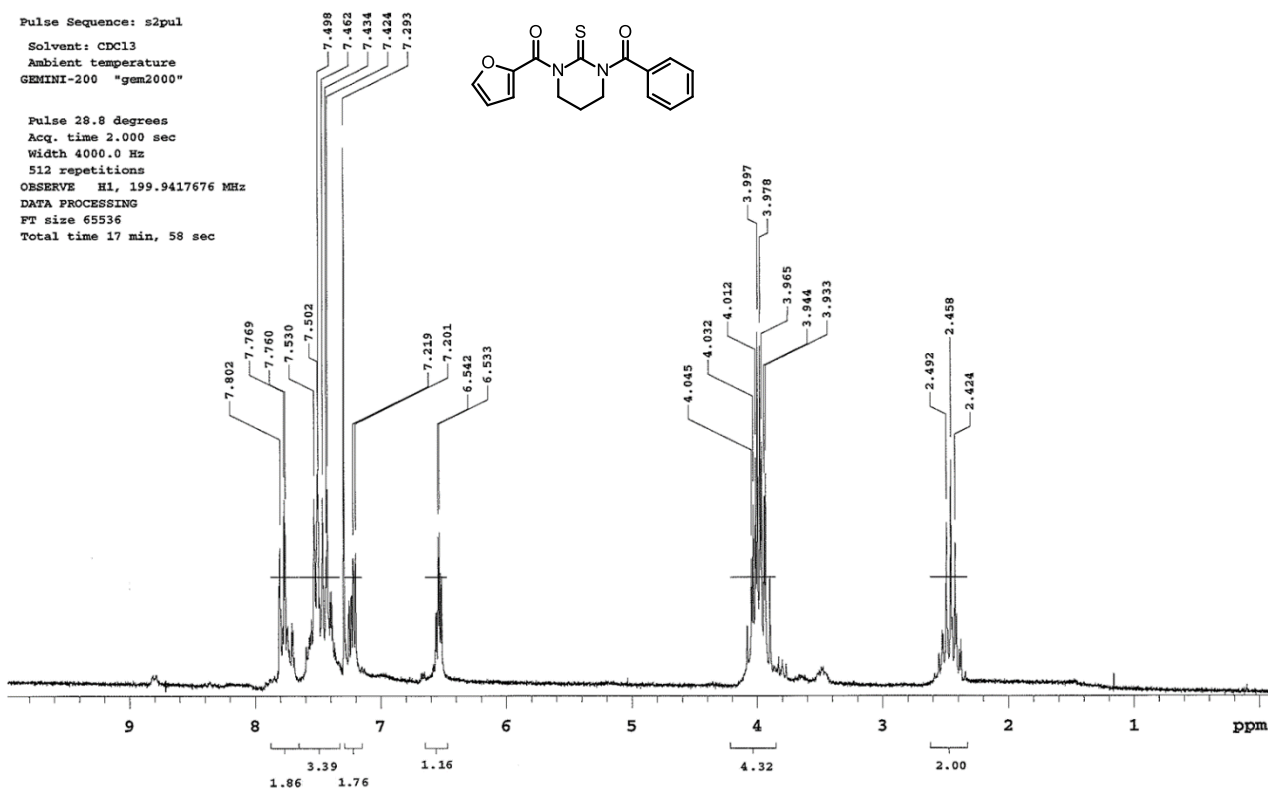
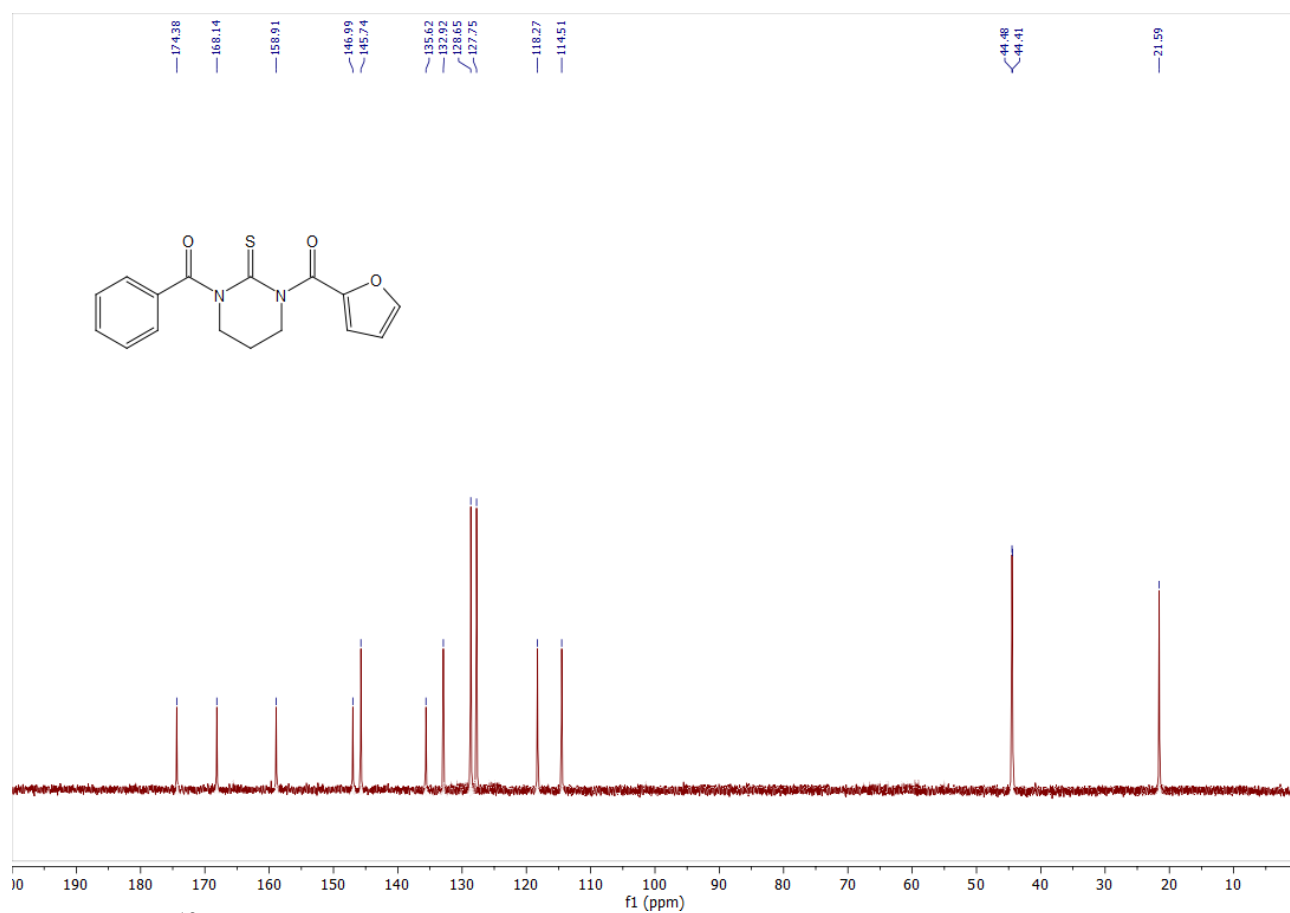
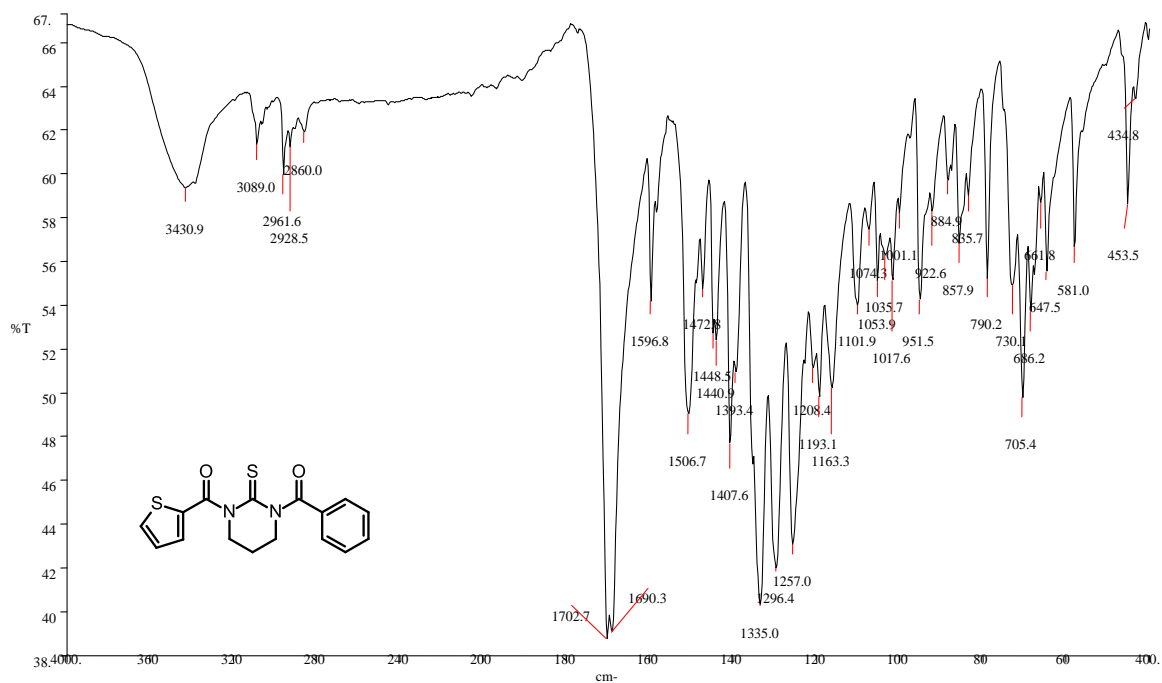


Figure S46.  $^1\text{H}$  NMR (200 MHz,  $\text{CDCl}_3$ ) of compound **6m**



**Figure S47.** <sup>13</sup>C NMR (50 MHz, CDCl<sub>3</sub>) of compound **6m**



**Figure S48.** IR (KBr) of compound **6n**

Pulse Sequence: s2pul  
Solvent: CDCl3  
Ambient temperature  
GEMINI-200 "gem2000"

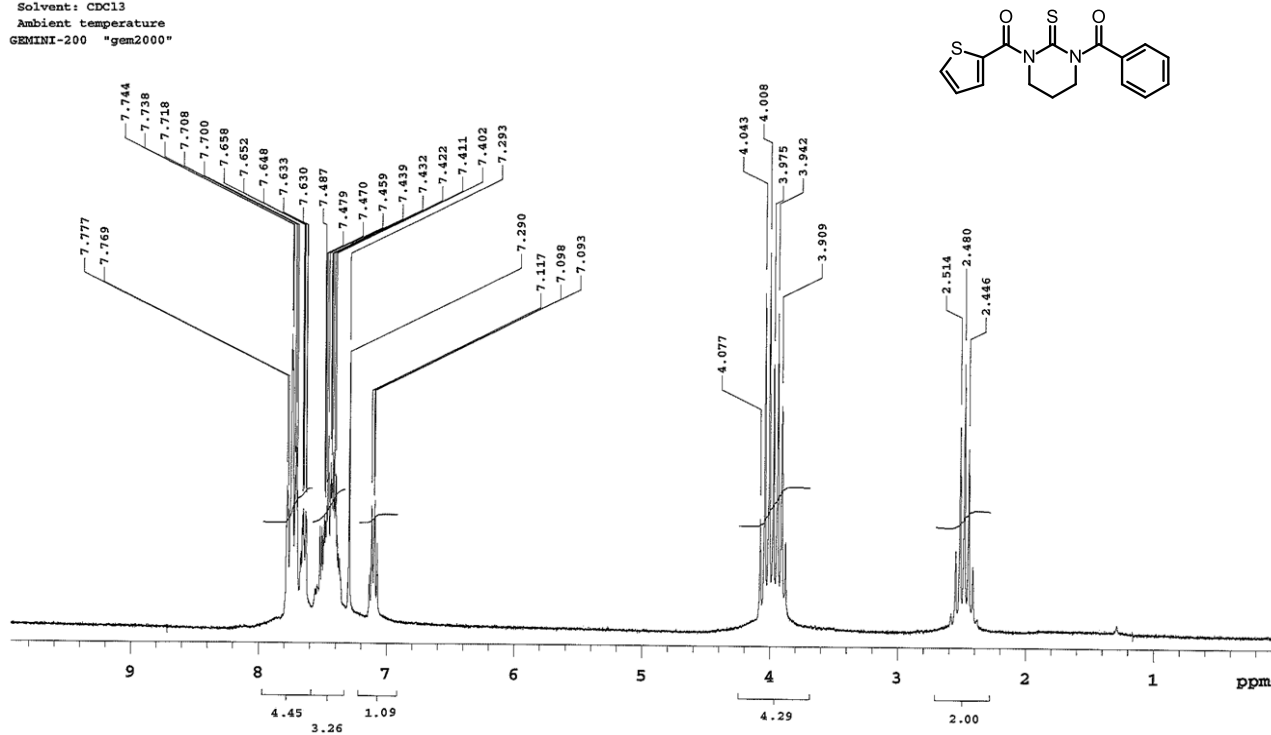


Figure S49. <sup>1</sup>H NMR (200 MHz, CDCl<sub>3</sub>) of compound **6n**

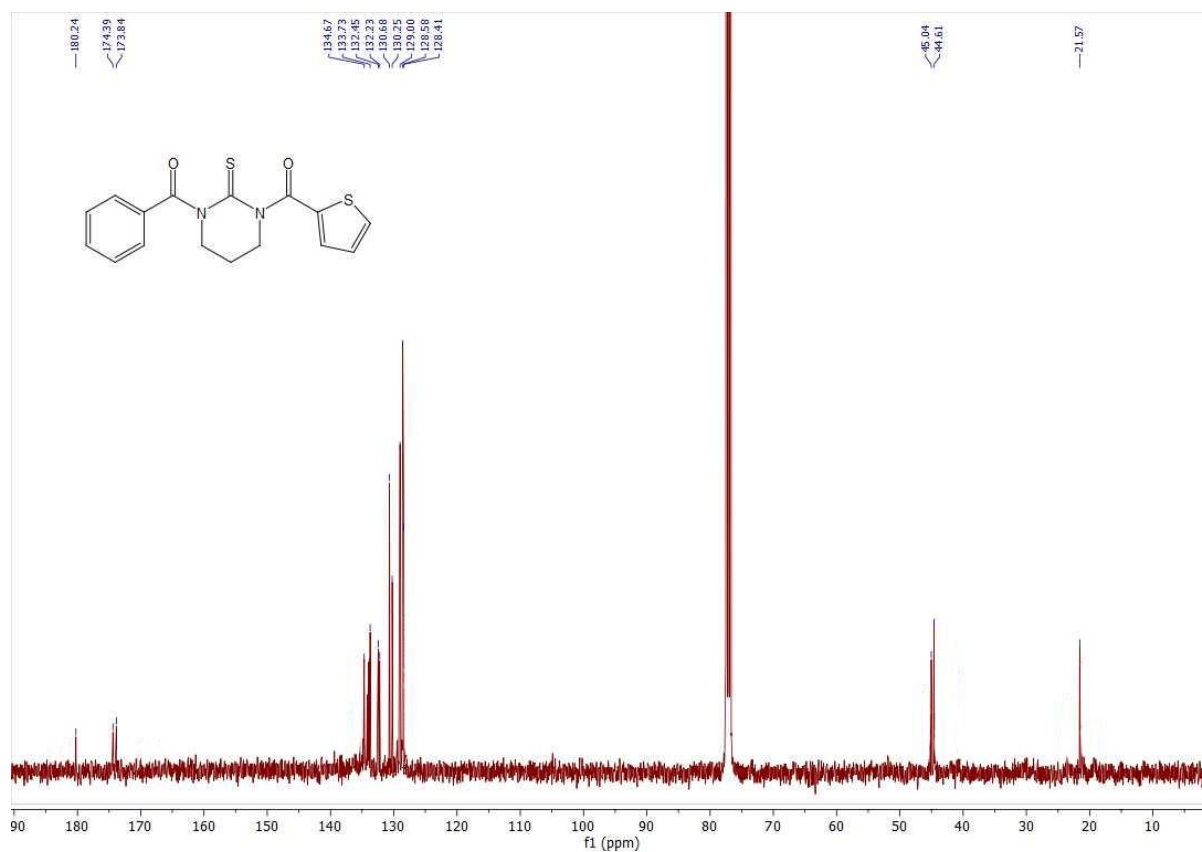


Figure S50. <sup>13</sup>C NMR (101 MHz, CDCl<sub>3</sub>) of compound **6n**



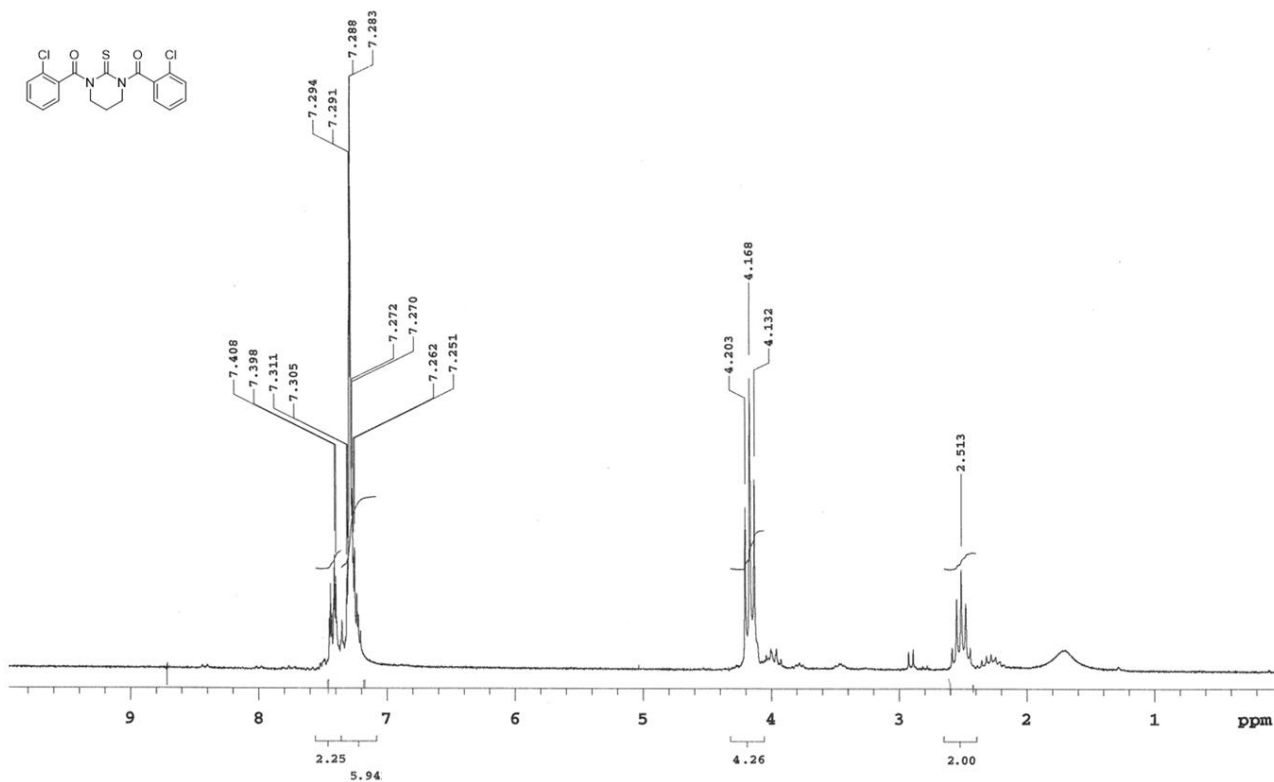


Figure S51. <sup>1</sup>H NMR (200 MHz, CDCl<sub>3</sub>) of compound 60

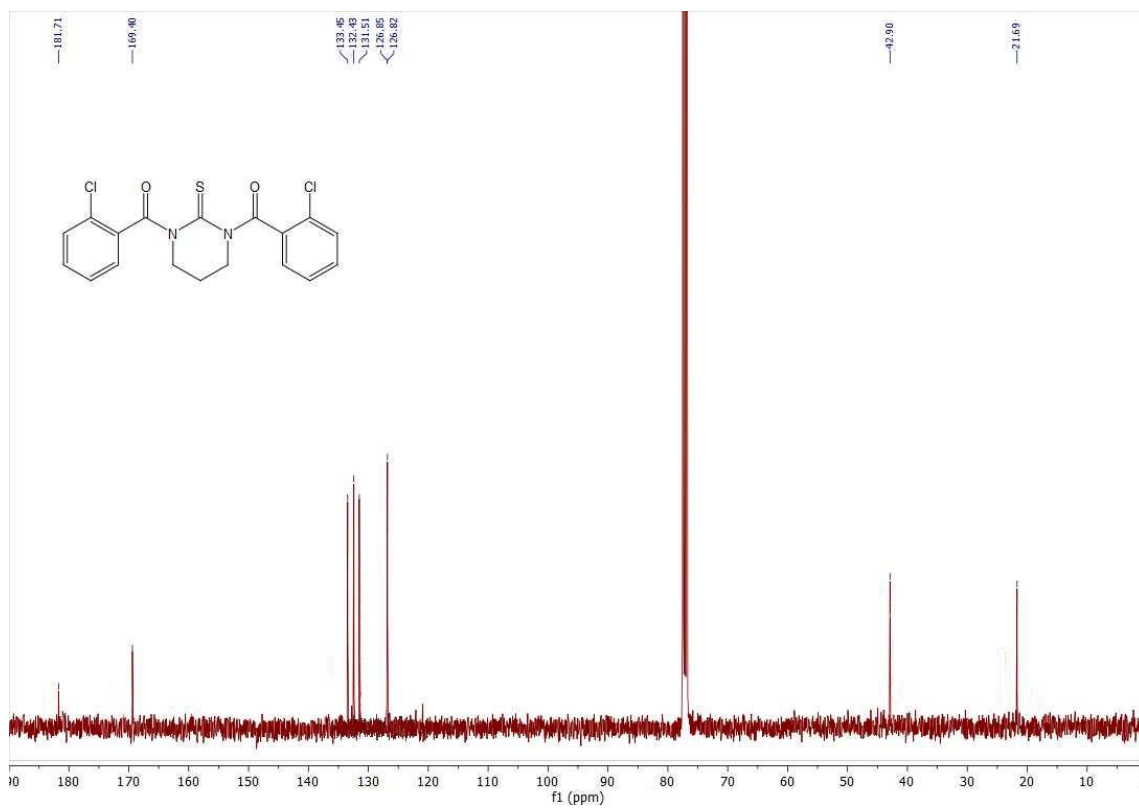


Figure S52. <sup>13</sup>C NMR (101 MHz, CDCl<sub>3</sub>) of compound 60

Pulse Sequence: s2pul  
Solvent: CDCl3  
Ambient temperature  
GEMINI-200 "gem2000"

Pulse 30.0 degrees  
Acq. time 2.000 sec  
Width 4000.0 Hz  
288 repetitions  
OBSERVE H1, 199.9417676 MHz  
DATA PROCESSING  
FT size 65536  
Total time 17 min, 58 sec

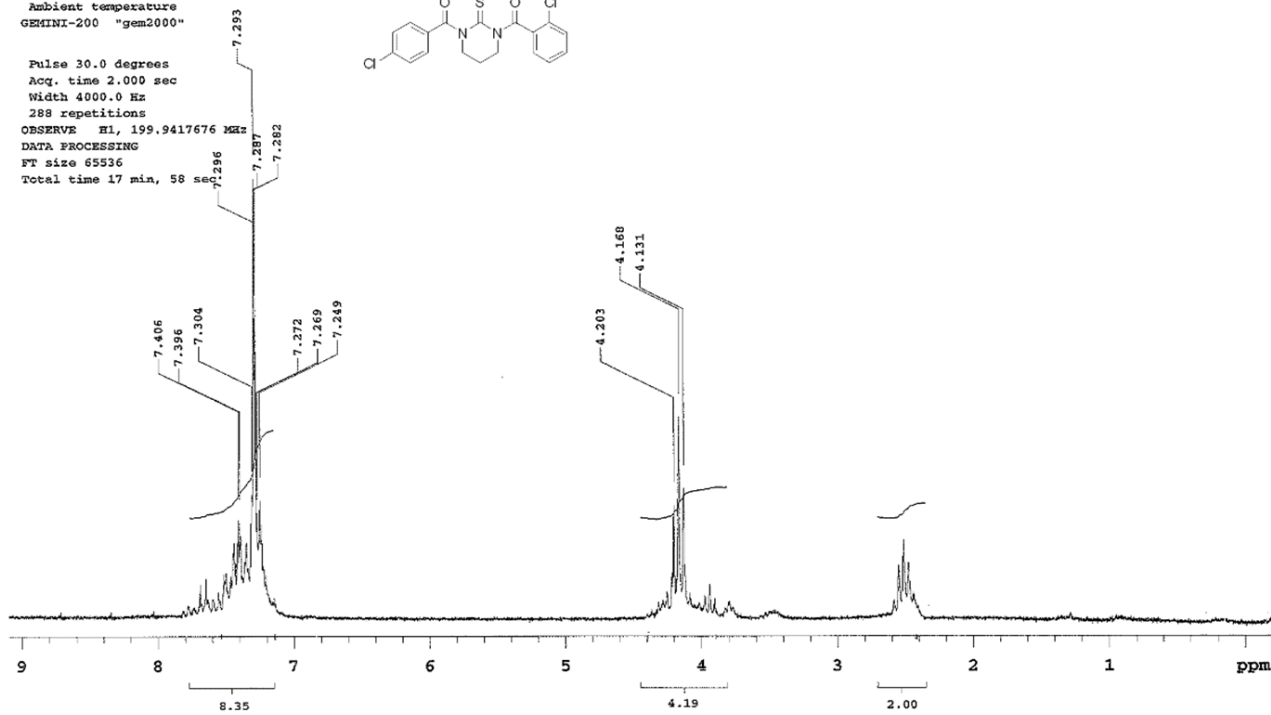
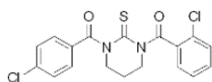


Figure S53.  $^1\text{H}$  NMR (200 MHz,  $\text{CDCl}_3$ ) of compound **6p**

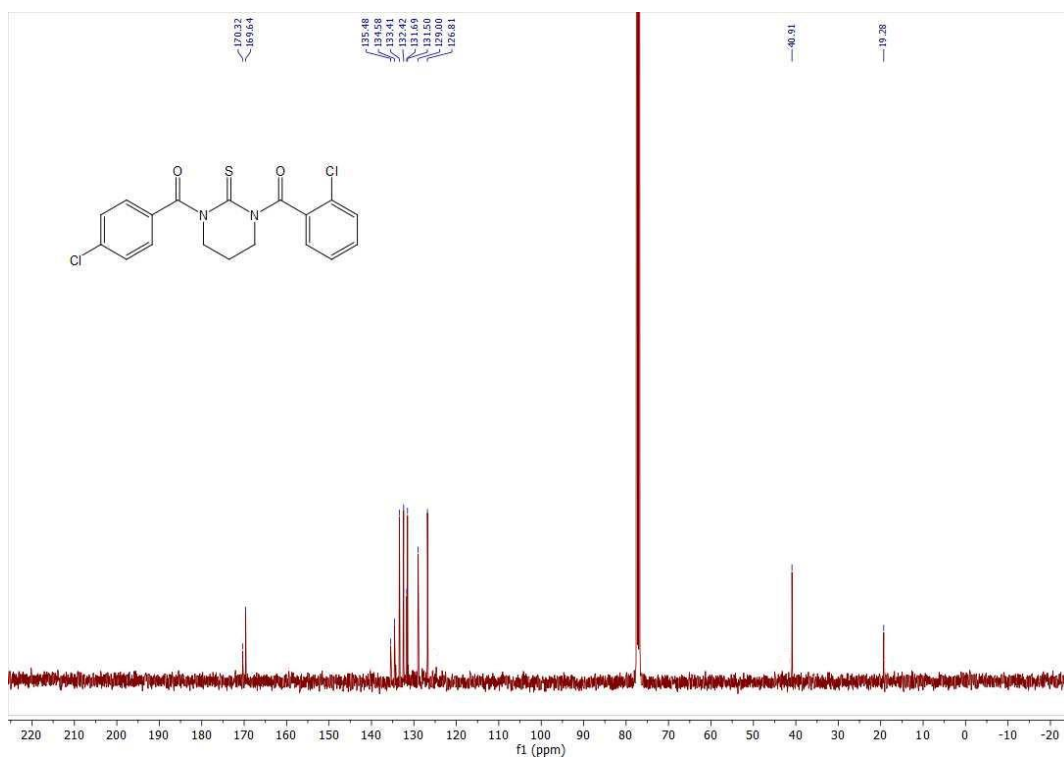


Figure S54.  $^{13}\text{C}$  NMR (101 MHz,  $\text{CDCl}_3$ ) of compound **6p**

Pulse Sequence: s2pul  
Solvent: CDCl3  
Ambient temperature  
GEMINI-200 "gem2000"  
  
Pulse 30.0 degrees  
Acq. time 2.000 sec  
Width 4000.0 Hz  
192 repetitions  
OBSERVE H1, 199.9977676 MHz  
DATA PROCESSING  
FT size 65536  
Total time 17 min, 39 sec

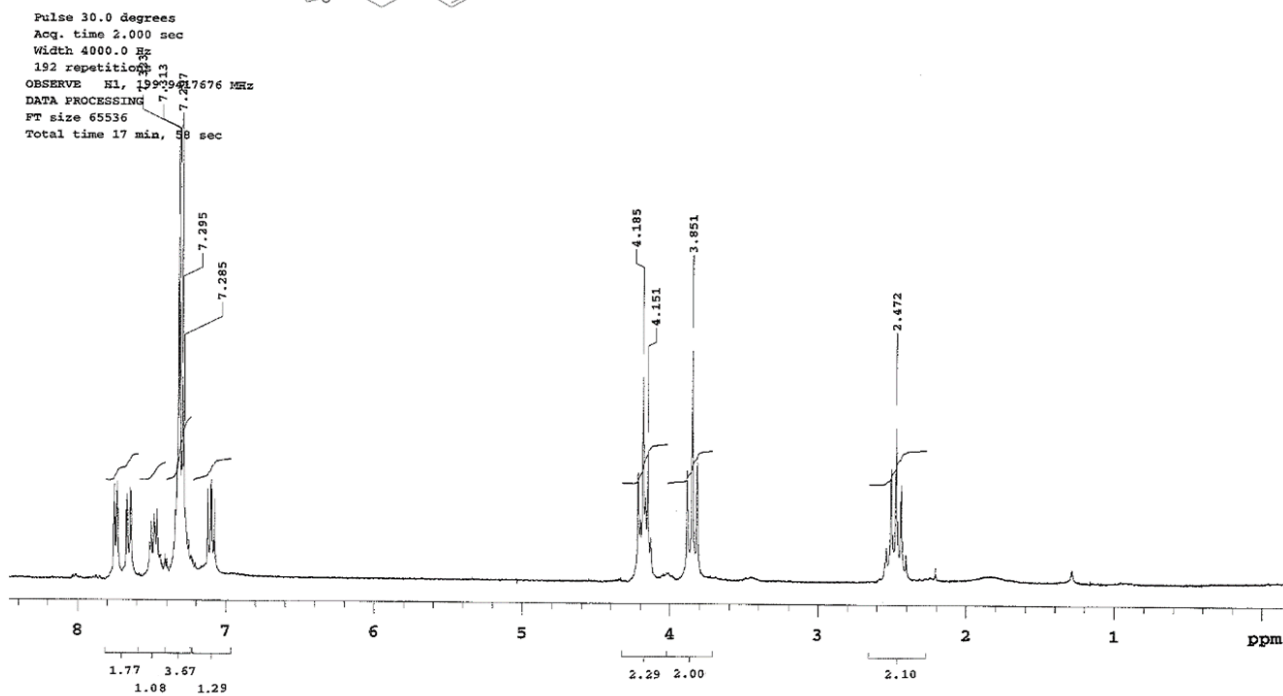
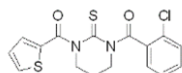


Figure S55.  $^1\text{H}$  NMR (200 MHz,  $\text{CDCl}_3$ ) of compound **6q**

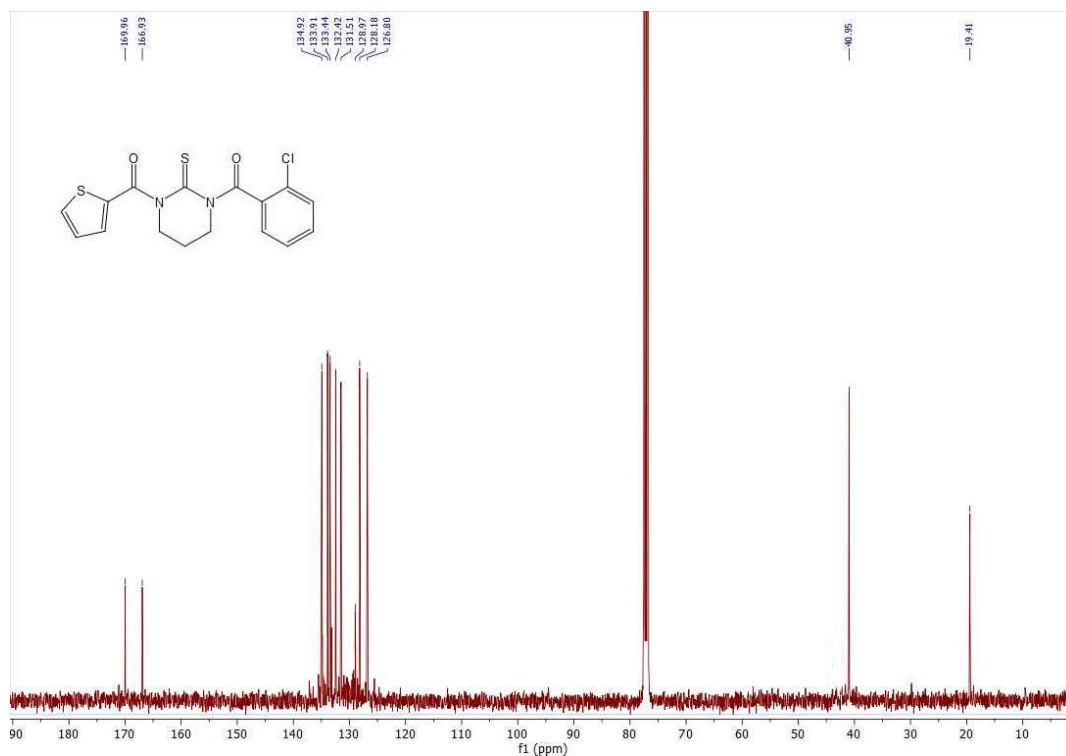


Figure S56.  $^{13}\text{C}$  NMR (101 MHz,  $\text{CDCl}_3$ ) of compound **6q**

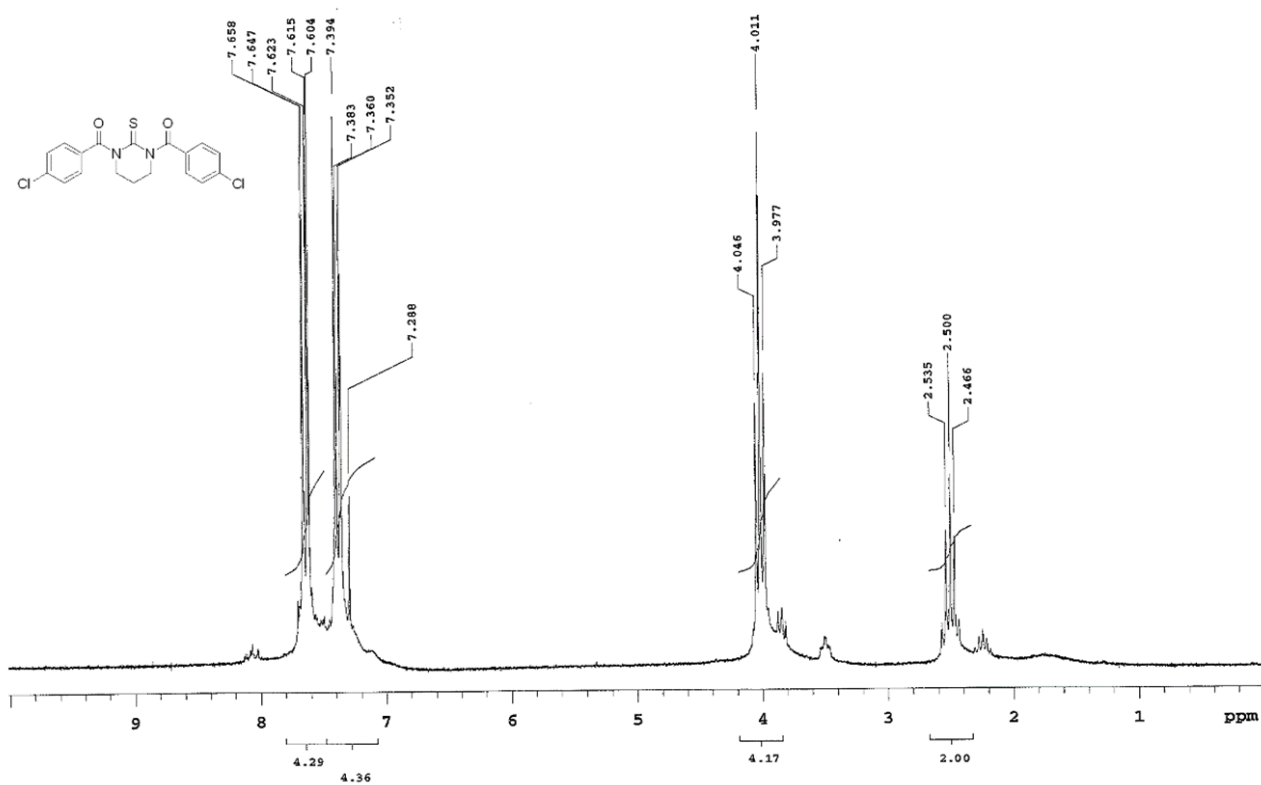


Figure S57. <sup>1</sup>H NMR (200 MHz, CDCl<sub>3</sub>) of compound **6r**

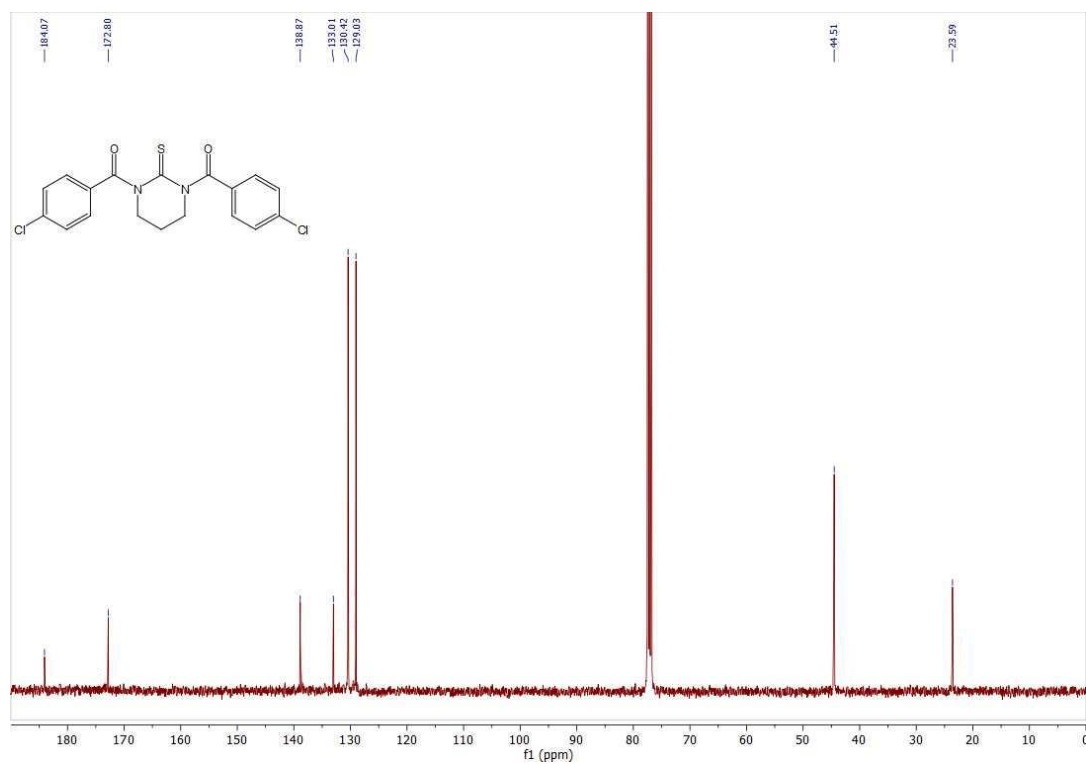
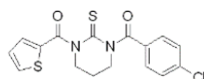


Figure S58. <sup>13</sup>C NMR (101 MHz, CDCl<sub>3</sub>) of compound **6r**

Pulse Sequence: s2pul  
Solvent: CDCl3  
Ambient temperature  
GEMINI-200 "gem2000"



Pulse 30.0 degrees  
Acq. time 2.000 sec  
Width 4000.0 Hz  
128 repetitions  
OBSERVE H1, 199.9417676 MHz  
DATA PROCESSING  
FT size 65536  
Total time 17 min, 56 sec

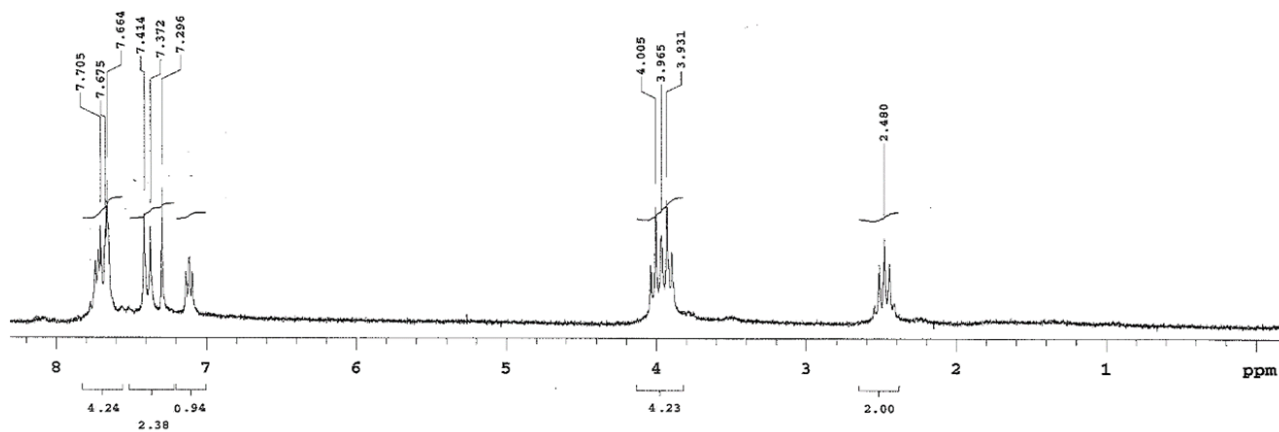


Figure S59. <sup>1</sup>H NMR (200 MHz, CDCl<sub>3</sub>) of compound 6s

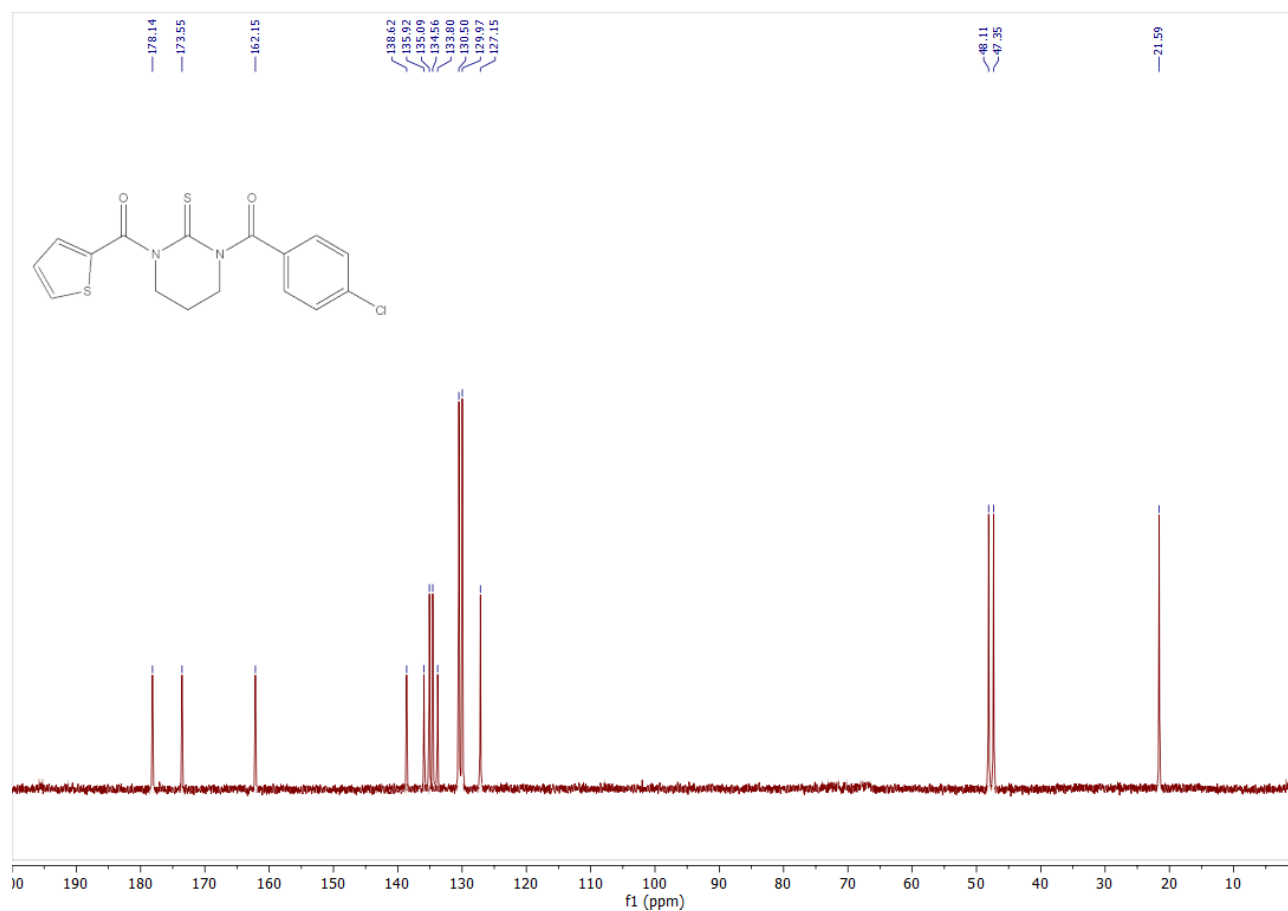
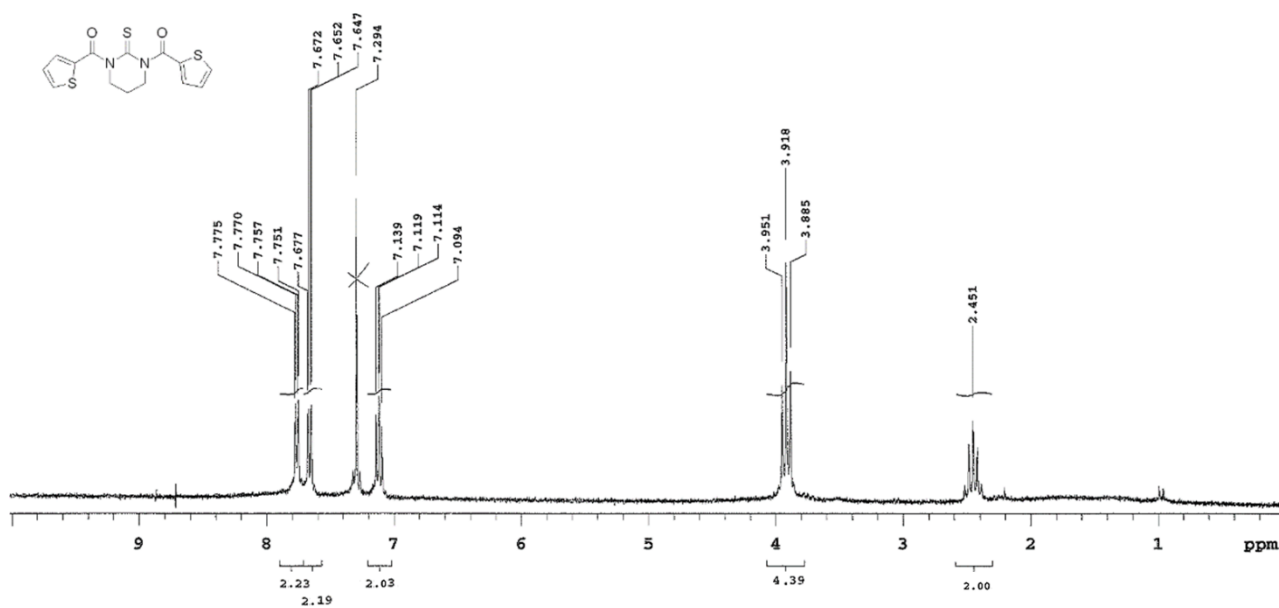
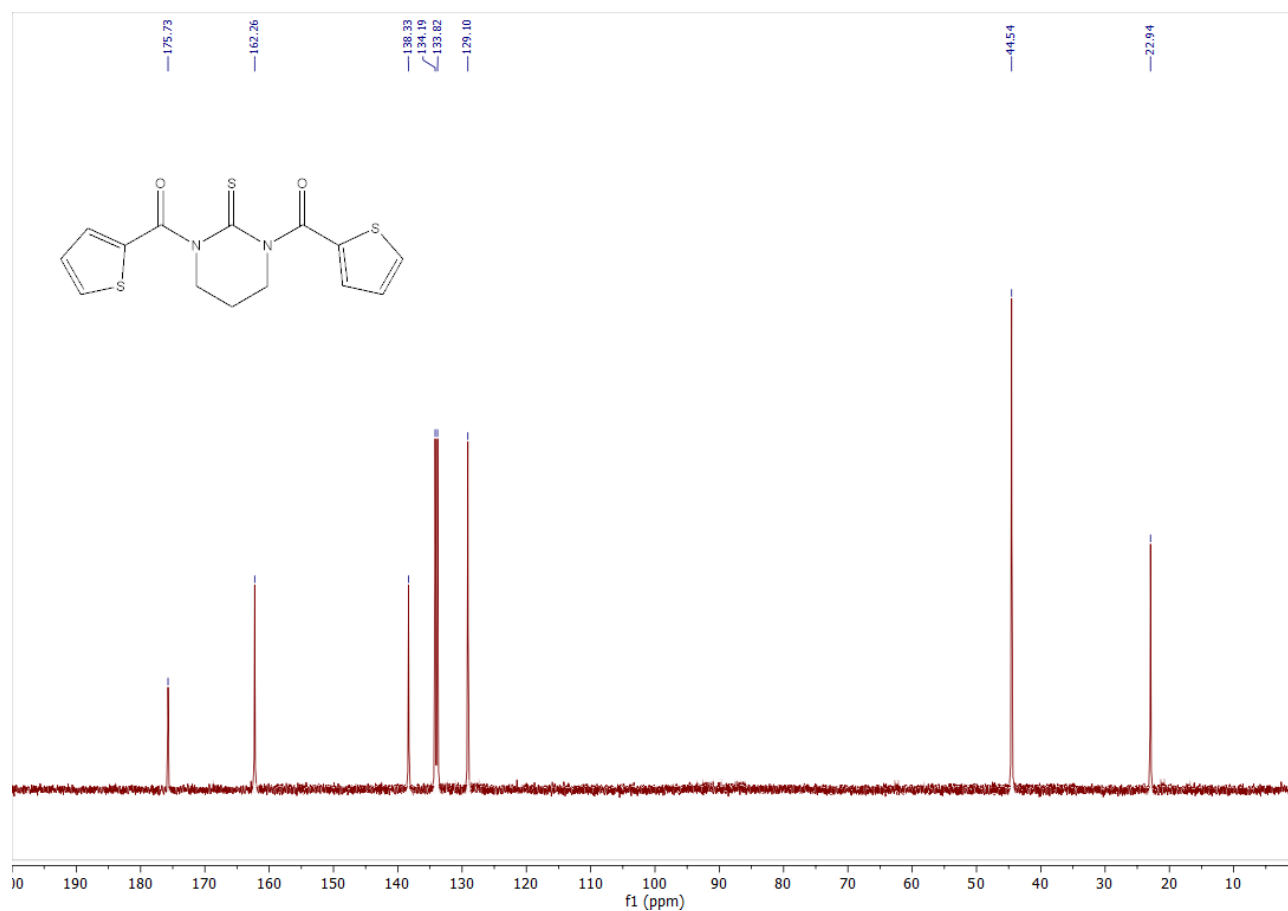


Figure S60. <sup>13</sup>C NMR (50 MHz, CDCl<sub>3</sub>) of compound 6s



**Figure S61.** <sup>1</sup>H NMR (200 MHz, CDCl<sub>3</sub>) of compound **6t**



**Figure S62.** <sup>13</sup>C NMR (50 MHz, CDCl<sub>3</sub>) of compound **6t**

Table S1. ADME prediction for compounds **5**.

	<b>5a</b>	<b>5b</b>	<b>5c</b>	<b>5d</b>	<b>5e</b>	<b>5f</b>
<i>Physicochemical properties</i>						
MW (g/mol)	200.30	184.26	220.29	254.74	254.74	226.32
Fraction Csp <sup>3</sup>	0.78	0.75	0.27	0.27	0.27	0.33
Rotatable bonds	3	2	2	2	2	2
H-bond acceptors	1	1	1	1	1	1
H-bond donors	1	1	1	1	1	1
TPSA <sup>a</sup> (Å <sup>2</sup> )	64.43	64.43	64.43	64.43	64.43	92.67
<i>Lipophilicity</i>						
LogP <sup>b</sup>	1.33	0.52	1.72	2.35	2.35	1.74
<i>Water solubility</i>						
Solubility <sup>c</sup> (mg/ml)	3.8	12.2	0.776	0.229	0.229	0.764
<i>Pharmacokinetics</i>						
GI absorption	High	High	High	High	High	High
BBB permeant	No	No	No	Yes	Yes	No
Pgp substrate	No	No	No	No	No	No
CYP1A2 inhibitor	No	No	Yes	Yes	Yes	Yes
CYP2C19 inhibitor	No	No	No	Yes	Yes	Yes
CYP2C9 inhibitor	No	No	No	No	No	No
CYP2D6 inhibitor	No	No	No	No	No	No
CYP3A4 inhibitor	No	No	No	No	No	No
<i>Druglikeness</i>						
Lipinski violations	0	0	0	0	0	0
<i>Medicinal chemistry</i>						
PAINS alerts	0	0	0	0	0	0
Brenk alerts	1	1	1	1	1	1
Leadlikeness violations	1	1	1	0	0	1

<sup>a</sup> Topological Polar Surface Area. <sup>b</sup> Predicted according to XLOGP3 program. <sup>c</sup> Values predicted by ESOL method [Delaney, J.S. ESOL: Estimating Aqueous Solubility Directly from Molecular Structure. *J. Chem. Inf. Model.* **2004**, *44*, 1000–1005. DOI: 10.1021/ci034243x]

Table S2. ADME prediction for compounds **6**

	<b>6a</b>	<b>6b</b>	<b>6c</b>	<b>6d</b>	<b>6e</b>	<b>6f</b>	<b>6g</b>	<b>6h</b>	<b>6i</b>	<b>6j</b>	<b>6k</b>	<b>6l</b>	<b>6m</b>	<b>6n</b>	<b>6o</b>	<b>6p</b>	<b>6q</b>	<b>6r</b>	<b>6s</b>	<b>6t</b>
<i>Physicochemical.</i>																				
MW (g/mol)	262.33	304.41	338.85	310.43	288.36	322.81	322.81	294.39	350.43	358.84	358.84	358.84	314.36	330.42	393.29	393.29	364.87	393.29	364.87	336.45
Fraction Csp <sup>3</sup>	0.31	0.44	0.44	0.5	0.4	0.4	0.4	0.46	0.15	0.17	0.17	0.17	0.19	0.19	0.17	0.17	0.19	0.17	0.19	0.21
Rotatable bonds	3	5	5	5	4	4	4	4	5	4	4	4	4	4	4	4	4	4	4	4
H-bond acceptors	2	2	2	2	2	2	2	2	2	2	2	2	3	2	2	2	2	2	2	2
H-bond donors	0	0	0	0	0	0	0	0	0	0	0	0	0	0	0	0	0	0	0	0
TPSA <sup>a</sup> (Å <sup>2</sup> )	72.71	72.71	72.71	100.95	72.71	72.71	72.71	100.95	72.71	72.71	72.71	72.71	85.85	100.95	72.71	72.71	100.95	72.71	100.95	129.19
<i>Lipophilicity</i>																				
LogP <sup>b</sup>	1.69	2.95	3.58	2.96	2.14	2.77	2.77	2.16	3.77	3.97	3.97	3.97	2.74	3.36	4.6	4.6	3.99	4.6	3.99	3.37
<i>Water solubility</i>																				
Solubility <sup>c</sup> (mg/ml)	0.69	0.104	0.029	0.102	0.336	0.0944	0.0944	0.325	0.0135	0.00764	0.00764	0.00764	0.0752	0.0256	0.00212	0.00212	0.00718	0.00212	0.00718	0.0245
<i>Pharmacokinetics</i>																				
GI absorption	High	High	High	High	High	High	High	High	High	High	High	High	High	High	High	High	High	High	High	High
BBB permeant	No	Yes	Yes	No	No	Yes	Yes	No	Yes	Yes	Yes	Yes	No	No	Yes	Yes	No	Yes	No	No
Pgp substrate	No	No	No	No	No	No	No	No	No	No	No	No	No	No	No	No	No	No	No	No
CYP1A2 inhibitor	Yes	No	Yes	Yes	Yes	Yes	Yes	Yes	No	No	No	No	No	Yes	No	No	Yes	No	Yes	Yes
CYP2C19 inhibitor.	No	Yes	Yes	Yes	Yes	Yes	Yes	Yes	Yes	Yes	Yes	Yes	Yes	Yes	Yes	Yes	Yes	Yes	Yes	Yes
CYP2C9 inhibitor	No	No	Yes	Yes	No	Yes	Yes	No	Yes	Yes	Yes	Yes	Yes	Yes	Yes	Yes	Yes	Yes	Yes	Yes
CYP2D6 inhibitor	No	No	No	No	No	No	No	No	No	No	No	No	No	No	No	No	No	No	No	No
CYP3A4 inhibitor	No	No	No	No	No	No	No	No	Yes	Yes	No	No	No	Yes	Yes	Yes	Yes	Yes	Yes	Yes
<i>Druglikeness</i>																				
Lipinski violation	0	0	0	0	0	0	0	0	0	0	0	0	0	0	0	0	0	0	0	0
<i>Med. Chem.</i>																				
PAINS alerts	0	0	0	0	0	0	0	0	0	0	0	0	0	0	0	0	0	0	0	0
Brenk alerts	1	1	1	1	1	1	1	1	2	1	1	1	1	1	1	1	1	1	1	1
Leadlikeness viol.	0	0	1	0	0	0	0	0	2	2	2	2	0	0	2	2	2	2	2	0

<sup>a,b,c</sup> see Table S1.



Table S3. Variables used for PCA analysis

<b>Entry</b>	<b>Variable</b>
#1	activity
#2	Fraction Csp3
#3	Number of Rotatable bonds
#4	Number of H-bond acceptors
#5	Number of H-bond donors
#6	TPSA
#7	XLOGP3
#8	ESOL Solubility (mg/ml)
#9	ESOL Class
#10	GI absorption
#11	BBB permeant
#12	Pgp substrate
#13	CYP1A2 inhibitor
#14	CYP2C19 inhibitor
#15	CYP2C9 inhibitor
#16	CYP2D6 inhibitor
#17	CYP3A4 inhibitor